Eddy Current Loss Modeling for Design of PM Generators for Wind Turbines

Proefschrift

ter verkrijging van de graad van doctor
aan de Technische Universiteit Delft,
op gezag van de Rector Magnificus prof. ir. K.C.A.M. Luyben,
voorzitter van het College voor Promoties,
in het openbaar te verdedigen op donderdag 16 oktober 2014 om 10:00 uur
door

Anoop JASSAL

Master of Science in Electrical Engineering

geboren te Hoshiarpur, India

Dit proefschrift is goedgekeurd door de promotor:
Prof.dr.eng. J.A. Ferreira

Copromotor:
Dr.ir. H. Polinder

Samenstelling promotiecommissie:

Rector Magnificus, voorzitter
Prof.dr.eng. J.A.Ferreira, Technische Universiteit Delft, promotor
Dr.ir. H.Polinder, Technische Universiteit Delft, copromotor
Prof.(emer).dr. J. Tapani, Aalto University, Finland
Prof.dr.ir. L. Dupre, Ghent University, Belgium
Prof.dr. A. Neto, Technische Universiteit Delft
Prof.dr. G.J.W. van Bussel, Technische Universiteit Delft
Dr.ir. D.J.P. Lahaye, Technische Universiteit Delft

ISBN: 978-94-6203-677-2

Printed at: CPI - Koninklijke Wöhrmann B.V., The Netherlands

To my family and friends for their love and support

Acknowledgements

"It took time which was running too fast, I thank my lord it has been done at last."

As I am writing this acknowledgement, the two lines above describe my state of mind. It is a milestone in my life and culmination of an effort not only from my side but also from many individuals who have made it possible. I would like to thank and acknowledge their support here.

I would first and foremost like to thank my supervisor Dr. Henk Polinder and promoter Prof. Dr. J.A. Ferreira who have shown immense patience and support for me during this research. I appreciate their zeal, passion and understanding of technical as well as non-technical aspects of a research. A special thanks to Dr. Domenico Lahaye for his support and motivation for both analytical and computational parts of this research.

My research was supported by VWEC B.V. (now XEMC-Darwind) and the team there has been a constant motivation for me. I would take this opportunity to thank Mr. Kees Versteegh and Mr. Hugo Groenman who despite the financial crisis and management changes kept me aloof from the worries about funding. A heartfelt thanks to Mr. A.S. Karanth, Michiel, Robert, Chen, Kejia, Manoj and all those involved in A-90/XV-90 project for technical support, discussions and maintaining a great working environment.

Many thanks to our wonderful, diverse and cooperative EPP group who made me feel at home at TU Delft. Special thanks to Ghanshyam, Deok-Je, Alex, Martin (for helping me with Matlab, FE simulations and Dutch translations), Johan, Zhihui, Marcelo, Dalibor, Ivan, Milos, Ilija, Todor, Rick, Yi Wang, Yeh Ting and all other colleagues whom I have worked with. Many thanks to Ir. Dong Liu for carrying out useful experiments in the lab. Heartfelt thanks to Mr. Rob Schoevaars, Harry, Kasper and all laboratory staff for their prompt help and support during experimental work.

I would also like to acknowledge the support, friendship, encouragement and immeasurable help offered by Nada, Balazs, Kostas, Ivo, Fadiah and Marcela. Thanks guys for standing by my side during thick and thin of life !

I can't thank enough to my family back in India who have been my supporting pillars. It is because of their vision and hard-work that I could even think about doing higher studies. Thanks Mom-Dad and sister Renu for your patience and everything you have given me. Thanks to all my Indian

friends who have supported me throughout my life especially Navdeep, Saurabh, Neeraj, Abhishek, Amarsha, Nitin, Shuchi, Tanu, all GEROH members and many more.
Last but not the least I would thank my loving, bubbly and immensely supportive wife, Harsh, without whom this whole research would have been a dry-grinding task.

- *Anoop Jassal*

Table of Contents

List of Figures

List of Tables

List of Symbols and Abbreviations

Latin Letters

A	Magnetic vector potential	[Wb.m^{-1}]
A	Surface current density	[A. m^{-1}]
A	Area	[m^2]
A	Phase A of 3 phase balanced system	
B	Phase B of 3 phase balanced system	
B	Magnetic flux density	[T]
b	Height of 2d simplified analytical geometry	[m]
b	Width in geometrical dimensions	[m]
C	Phase C of 3 phase balanced system	
E	Electrical field strength	[V.m^{-1}]
f	Electrical frequency	[Hz]
g	Constant for solution of partial diff. equation	
g	Mechanical air gap	[m]
g	Acceleration due to gravity	[m/s^2]
H	Magnetic field intensity	[A.m]
h	Constant for solution of partial diff. equation	
h	Height in machine geometry	[m]
I	Current	[A]
J	Electrical current density	[A.m^{-2}]
j	Operator for imaginary part	
K	Surface current density	[A.m^{-1}]
K	Loss coefficient	
k	Constant for spatial distribution	
k	Constant used in variable separation	
l	Length/thickness in machine geometry	[m]
m	Constant used in variable separation	
m	Mass	[kg]
n	Rotational speed	[rad.sec^{-1}]
n	Number of harmonic	
n	Constant used in variable separation	
P	X coordinate dependent part of partial diff. eqn.	
P	Power loss/Power	[W]
p	Number of poles	

Q	Y coordinate dependent part of partial diff. eqn.	
q	Slots per pole per phase	
R	Electrical resistance	[ohm]
S	Space dependent part of partial diff. equation	
S	Number of slots	
T	Time dependent part of partial diff. equation	
T	Torque	[N]
t	Time	[s]
U	Voltage	[V]
V	Electrical scalar potential/Voltage	[V]
V	Linear speed of harmonic	[m/s]
X	X coordinate in Cartesian system	[m]
Y	Y coordinate in Cartesian system	[m]

Greek Letters

α	Constant used in PDE solution	
β	Constant used in PDE solution	
γ	Constant used in PDE solution	
δ	Skin depth	[m]
θ	Spatial angle	[radians]
λ	Wavelength	[m]
μ	Permeability	[$H.m^{-1}$]
ν	Velocity	[m/s]
π	Constant	
ρ	Electrical resistivity	[Ohm.m]
σ	Electrical conductivity	[$S.m^{-1}$]
τ	Distance/Pitch	[m]
ω	Rotational speed/Electrical frequency	[$Radian.s^{-1}$]

Subscripts

0	Pertaining to free space or initial condition
1,2,3,..	Region of PDE solution in simplified geometry
a,b,c	Electrical Phase A, Phase B and Phase C
h	Harmonic number in rotor reference frame
ext	external
m	Pertaining to magnet
n	Harmonic number
p	Pertaining to pole dimensions
r	Pertaining to rotor
r	Relative
r, rem	Magnetic Remanance
ry	Pertaining to rotor yoke
s	Stator/Slot quantity
sy	Pertaining to stator yoke
t	Pertaining to tooth dimension
x,y,z	Component in x, y or z direction

Subscripts for Power/Power Loss

_	Combines two subscripts
ac	Alternating current
Cus	Stator copper loss
dc	DC quantity
e, eddy	Eddy current loss
Fe	Total iron loss
Fes	Stator iron loss
Fer	Rotor iron loss
gen	Generator power
in	Input power
load	Load
m, mech	Mechanical
out	Output
Pm	Prime mover
r	Static ring region / Rotor region

Superscripts and Accents

s	Stator quantity
2,3,…	Raised to power (square, cube, …)
e	External quantity
ˆ	Peak value
→	Vector Quantity

Abbreviations

DFIG	Doubly Fed Induction Generator
EESG	Electrically Excited Synchronous Generator
FE	Finite Element
GCD	Greatest Common Divisor
LCM	Least Common Multiple
MMF, mmf	Magneto Motive Force
ODE	Ordinary Differential Equation
PDE	Partial Differential Equation
PM	Permanent Magnets
PMDD	Permanent Magnet Direct Drive
PMSG	Permanent Magnet Synchronous Generator
SCIG	Squirrel Cage Induction Generator
SG	Synchronous Generator
WRIG	Wound Rotor Induction Generator

1. Introduction

This chapter presents an introduction to the field of research. The need for such a research justified by recent trends and developments is explained. After a bird's eye view of the whole field, the problem statement is formulated. The chapter culminates in a brief outline of the thesis.

1.1. Wind – A Renewable Energy Source

Our ever increasing energy need is prompting us to look for alternative energy sources. At present most of the energy is generated using fossil fuels which contribute to CO_2 concentration in atmosphere and hence global warming. Moreover, the amount of available fossil fuels is limited. Therefore, to circumvent the problem of global warming and to fulfill the energy demand, renewable energy sources are being targeted as an alternative. It is clear from fig. 1.1(a) that gradually, the composition of energy sources is changing and this change is likely to continue in the near future.

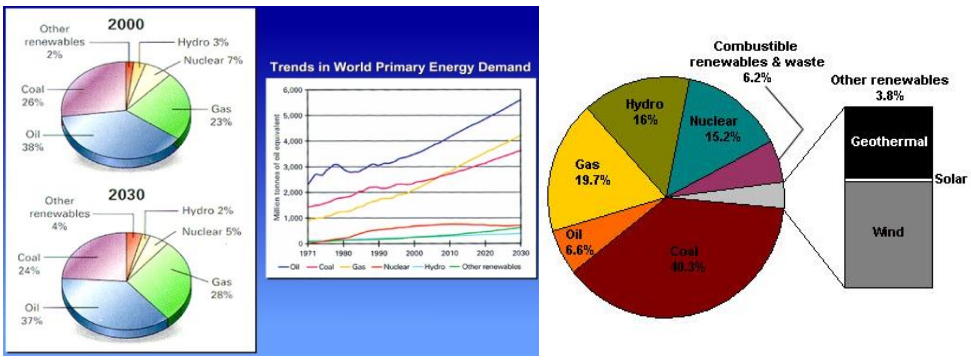

a) b)

Fig.1.1: a) Energy sources trend; b) Breakup of energy sources
Source a): International Energy Agency, 2002; Source b): Earth Trends 2008, using data from IEA 2007

From fig. 1.1(b) it can be easily observed that wind energy is a highly productive source of renewable energy. Wind is abundant, clean and everlasting whereby utilizing it fully to its capacity is imperative. In order to further utilize the potential of this renewable source, there is a trend to go offshore i.e. further from coast towards deeper sea.

1.2. The Offshore Trend: Conditions and Challenges

This recent trend of installing wind turbines further from shore towards deeper sea came into picture because of:

- High availability of wind
- High wind speed
- Low visual impact

The possibility of much more energy yield is a reasonable driver to go offshore. Moreover, experience in offshore installations for example oil rigs, shipping etc. already exists in industry. Nevertheless there are many challenges to be met due to different ambient conditions compared to wind turbines inland/onshore. There are also challenges which can arise due to wind energy injection into the existing system of transport of electricity. These challenges are highlighted below.

- The sea environment is one of the most corrosive environments.
- Maintenance in offshore region is a challenge because of limited accessibility.
- Erection and commissioning of wind turbines in deep sea is difficult.
- The whole concept has to be economical to keep a reasonable price per unit of energy.
- Connection of converted wind energy to existing on-shore power system and to bring it to the end user.
- Technical dynamics i.e. integration of wind energy with existing electrical network.
- Economical dynamics: i.e. electricity unit pricing, commitment and trade between different countries. An understandable challenge is to keep the price of energy from renewable sources competitive with other sources of energy (like hydro, thermal etc.)

From the perspective of wind turbines, the main constraints for an offshore scheme are of high reliability, high efficiency and reasonable cost. At present there is a lot of discussion in industry as well as academia regarding which type of generators are most suitable for offshore conditions? The answer is not straight forward as each type has its pros and cons. Therefore this research becomes even more interesting and reasonable as it is a step towards the answer to this question.

1.3. Wind Energy Conversion

Wind has a lot of energy content as such but this energy is required to be converted into some useful form like mechanical motion or electricity. In order to convert the flow of wind into electrical energy, the following main components are needed:

a) Wind turbine rotor i.e. blades connected to a hub to convert wind flow into rotary motion.

b) Support structure i.e. tower, nacelle, hub etc.
c) Generator to convert rotary motion into electricity.
d) Pitch system for blades to harness the wind energy efficiently.
e) Yaw system to orient the wind turbine rotor in the direction of wind.
f) Foundation on which the whole structure is erected.
g) Power electronic converter to ensure smooth power supply
h) Cabling, lightning protection and grounding.
i) Transformer for grid connection (if required)
j) Cooling mechanism and auxiliaries.

In this thesis, we focus only on the generator part of the wind turbine. The generator part is where the mechanical power is converted into useful electricity. The generator is a very critical part and in some cases (as in a direct-drive topology) most expensive single component of the wind turbine after the rotor blade assembly. However, expensive or not, the generator is the heart of the wind turbine.

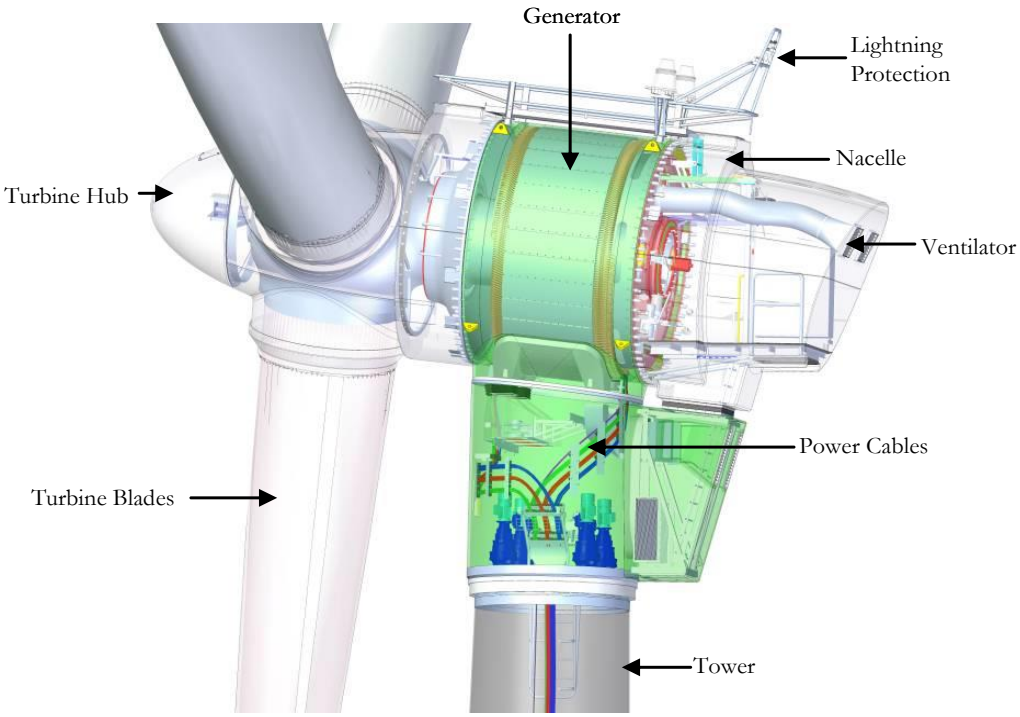

Fig.1.2: Wind turbine components

1.3.1 Types of Generators in Wind Turbines

There are many types of wind turbines in the market these days and many ways to classify them. Interested readers can have a look at [1]-[3] and [5]-[10]. Here we will focus on classification based on generator systems

1.3.1.1 Squirrel Cage Induction Generators (SCIG)

The basic advantage of squirrel cage induction generators is ruggedness due to simplicity in mechanical construction. A gearbox is often used to run the generator at high speeds however a direct driven version has also been investigated [4]. The SCIG are further divided into three types:

A. Fixed speed geared and directly connected to the grid

This concept is one of the oldest, cheapest and simplest concepts for generator system of a wind turbine. The scheme shown in fig. 1.3 was popular in early nineties but new installations are rather rare these days because of poor power quality. There is no converter connection but to compensate for reactive power drawn from the grid, capacitor banks are used. In some configurations, a soft starter is employed to improve power quality.

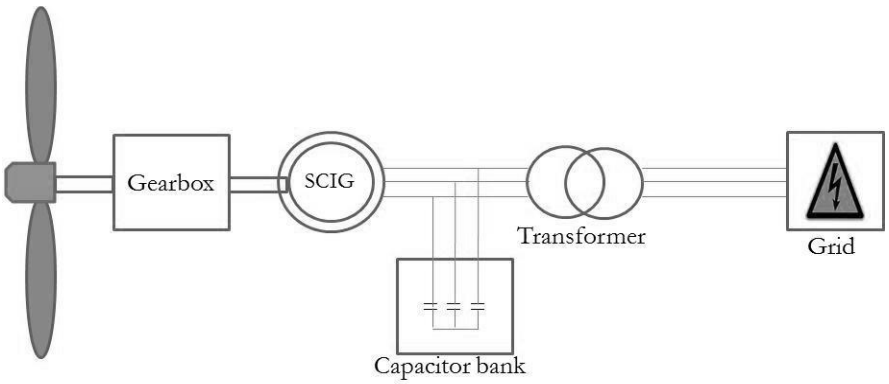

Fig.1.3: Fixed speed geared concept for SCIG

B. Variable speed geared and connected to grid with full converter

The aim of this concept, shown in fig. 1.4 is to utilize ruggedness of SCIG with improvement in power quality. The full converter used in this concept is able to maintain good power quality but adds appreciable cost to the generator system.

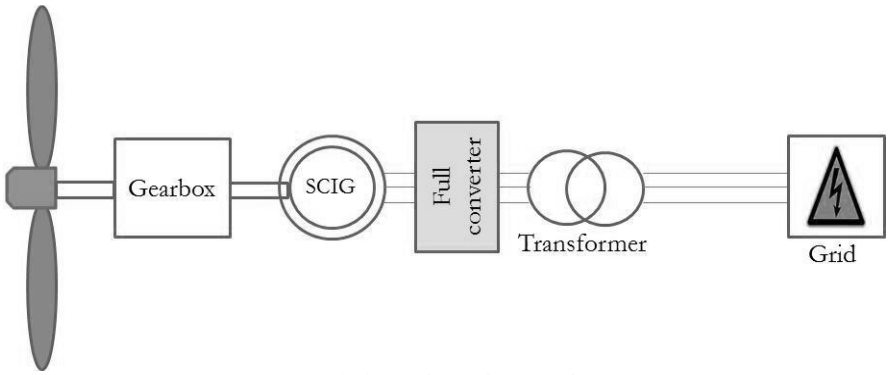

Fig.1.4: Variable speed geared concept for SCIG

C. Variable speed direct driven and connected to grid with full converter

The concept of using SCIG and direct drive topology has been developed keeping offshore scenario into perspective [4]. Due to high reliability of the SCIG, this concept has some advantages but the mass of a direct driven SCIG is very large which limits its utility. This scheme shown in fig. 1.5 has not been applied and hence not in market yet.

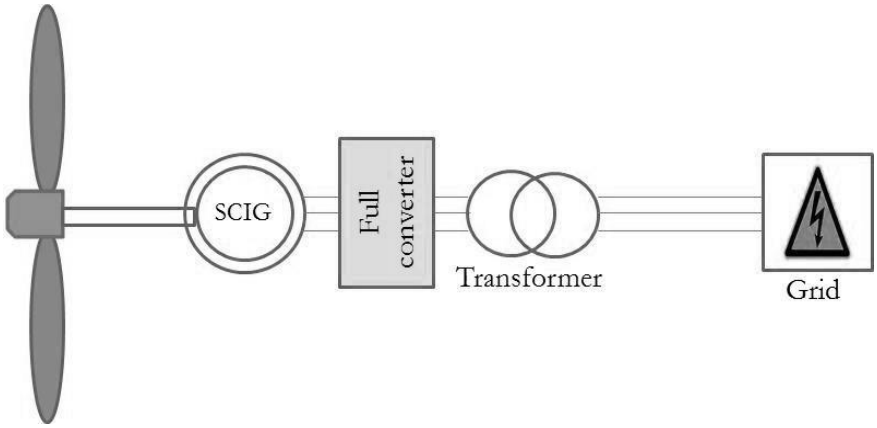

Fig.1.5: Variable speed, direct drive concept for SCIG

1.3.1.2 Wound Rotor Induction Generators (WRIG)

A. Limited variable speed, geared and directly connected to grid

The limited variable speed concept is also known as "OptiSlip" concept depicted in fig. 1.6. This concept has been primarily used by Vestas (V66-1.65 MW) and Suzlon (2 MW) [6].

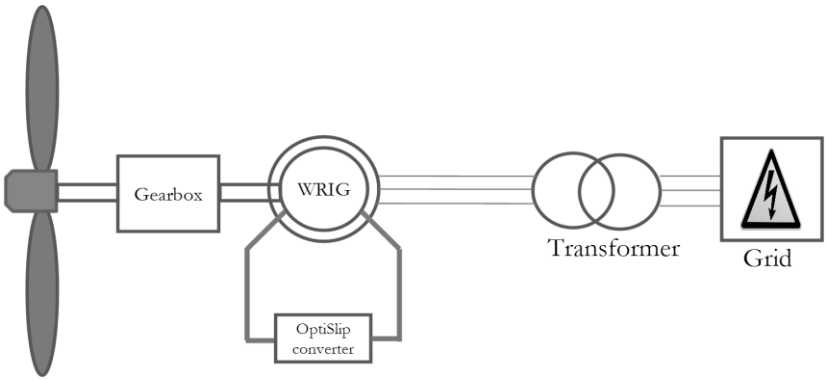

Fig.1.6: Limited variable speed geared concept for WRIG (OptiSlip)

The generator system for this concept is a WRIG and has a variable external rotor resistance. The external resistance is changed via a power electronic converter which is controlled optically and is mounted on the generator rotor (hence the name OptiSlip). Consequently, the output power fluctuations of the generator system can be controlled. This scheme gets rid of brushes and slip-rings, the maintenance issues can be negotiated well. On the downside, the rotational speed can be controlled only upto 10% above the synchronous speed.

B. Variable speed, geared and connected to grid with partial converter (popularly known as DFIG)

The wound rotor induction generators are most popular generator systems in the market till date. A partial converter is utilized to supply magnetizing current at a particular frequency to the wound rotor of the induction generator so as to maintain the output frequency at the stator terminals. Stator can be directly connected to the grid or via a transformer. The configuration is shown in fig. 1.7. Due to double connection with grid these are popularly known as Doubly Fed Induction Generators (DFIG).

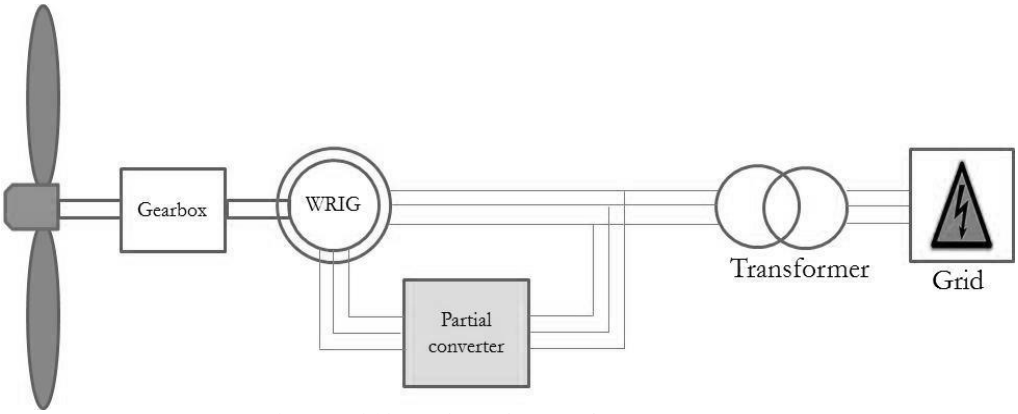

Fig.1.7: Variable speed geared concept for WRIG (DFIG)

The use of partial converter, which is about 20-30% of the rated power of the generator, makes it cost effective and power quality efficient. However complex control system, mechanical gearbox and use of brushes makes the system prone to failures.

1.3.1.3 Synchronous Generator (SG)

Synchronous generators are the conventional power generators. However in order to use these generators for wind energy, they require either mechanical speed control or full converter at their grid interface. According to the method of field excitation, these can be classified into electrically excited and PM excited machines. A system which aims at using advantages of both PMSG and geared systems is also present in the market.

A. Variable speed direct drive, electrically excited and connected to grid with full converter

These generators are the conventional synchronous generators with separately excited field winding on the rotor as shown in fig. 1.8. These machines are well known, rugged and provide high degree of voltage control. However, because of low rotational speed, these machines are very large. Another disadvantage is additional losses in the rotor winding which carries DC current. Currently these machines are well established in the market.

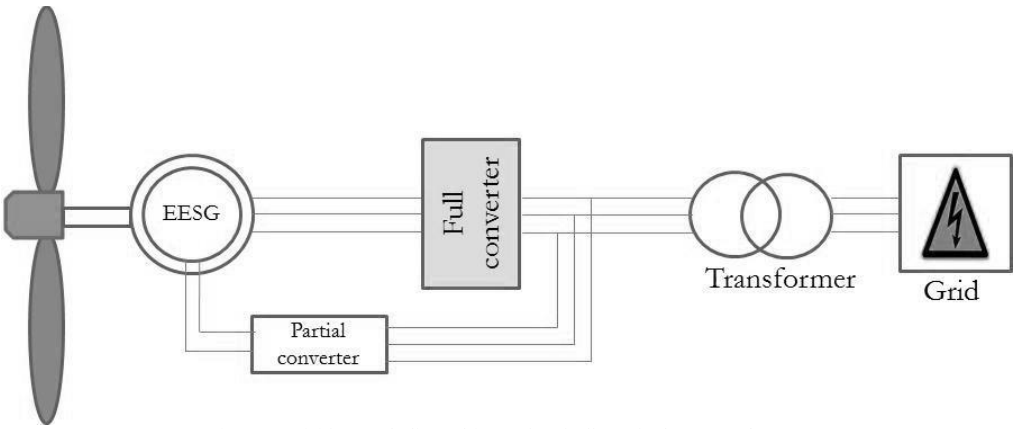

Fig.1.8: Variable speed, direct driven, electrically excited concept for SG

B. Variable speed direct drive, Permanent Magnet (PM) excited and connected to grid with full converter

The variable speed PM excited generator systems offer highest efficiency because of absence of rotor copper losses (as compared to EESG). The PMs ensure that the machine is very rugged and has high power density. The minimal moving parts promise

high reliability which makes these machines a candidate for offshore installations. On the other hand, PMs are expensive and need additional mechanical protection against the environment. As shown in fig. 1.9, Absence of gearbox means that the machine ends up large in size, massive and expensive. Nevertheless these machines are very popular and gaining considerable market share. This thesis deals with PMSG type of machines in detail.

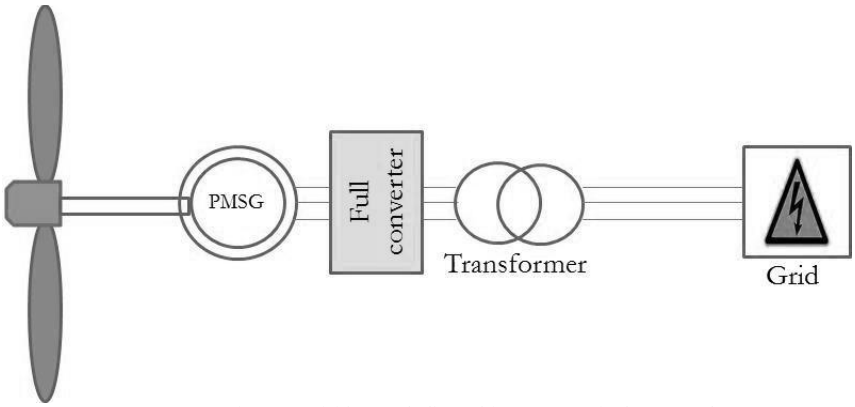

Fig.1.9: Variable speed, direct driven, PM excited concept for SG

C. Variable speed, geared, Permanent Magnet (PM) excited and connected to grid with full converter

In order to overcome the disadvantages of PMSG's large size, weight and cost, an interesting topology has gained attention recently. This topology requires a gearbox in addition to the PMSG system as shown in fig. 1.10. High speed of operation makes the generator smaller and supposedly cost effective. Thus a cheaper generator can be specified by using a 1, 2 or 3 stage gearbox and increasing the speed of rotation of generator. The advantages are the same as in PMSG type system. Addition of gearbox adds some reliability constraints to overall system.

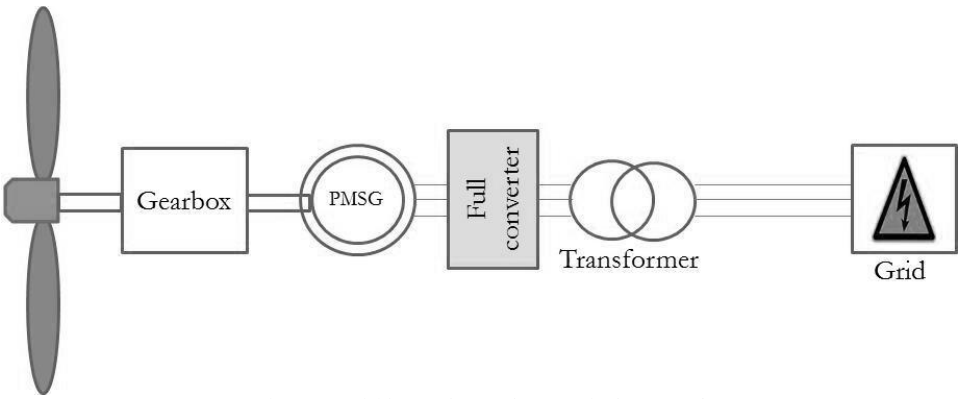

Fig.1.10: Variable speed, geared, PM excited concept for SG

We can summarize the most important types of generator systems used in wind industry as shown in table 1-1.

TABLE 1-1: GENERATOR SYSTEMS IN WIND TURBINES

Generator system		Speed control	Drive train	Converter	C	W	M	E
Squirrel Cage Induction Generator (SCIG)		Fixed	Geared	No	++	++	+/-	--
		Variable	Direct Driven	Full	+	--	++	-
Wound Rotor Induction Generator (WRIG)		Limited Variable	Geared	Partial (optislip)	++	++	-	--
		Variable	Geared	Partial	++	++	--	+/-
Synchronous Generator (SG)	Electrically excited field (EESG)	Variable	Direct Driven	Full	+	--	-	+
		Variable	Geared	Full	+	-	-	+
	PM field (PMSG)	Variable	Direct Driven	Full	--	--	++	++
		Variable	Geared	Full	++	++	-	+

C = Cost; W = Weight; M = Maintenance; E = Efficiency

So far we have seen that each generator type used in the industry has its own advantages and disadvantages. In order to reach a decision regarding offshore wind energy, we must focus on a certain type of generator and see how we can make it more suitable for power generation. PMSG seems to be very promising in terms of reliability and efficiency. The main manufacturers for this technology are Goldwind, Vensys, Scanwind, EWT, STX with General electric (GE) and Siemens also entering the field.

Looking at the generator system, at present, most popular machine technology in this field is distributed winding, radial-flux synchronous machine. If we look at manufacturing cost breakup (see fig. 1.11) of direct-drive wind turbines, the generator cost is substantial [21]. A deeper analysis reveals that apart from PM material cost, an important part of generator cost is stator coil manufacture, its assembly into winding with insulation and impregnation. These costs are high because of excessive manual labor involved in winding the generator. Thus concentrated windings which can substantially reduce the manual labor in winding of generator (due to possibility of automation) have been considered in this thesis.

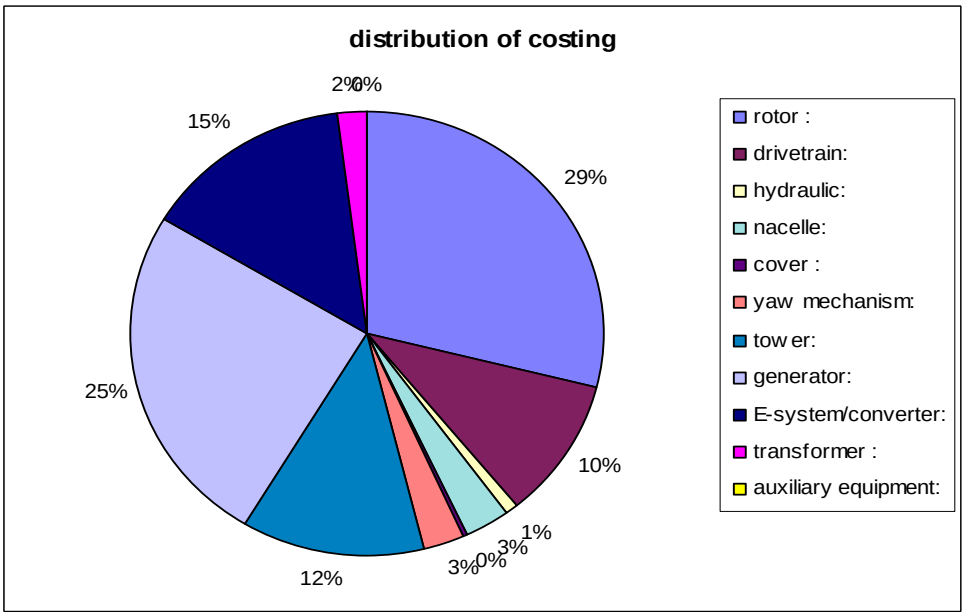

Fig.1.11: PM Generator – cost breakup [21]

1.4. Concentrated windings

In order to overcome the shortcomings of PMDD generators, while still using PM for field excitation, many solutions and concepts have been proposed in literature. PM machines with fractional pitch double layer concentrated windings have been proven successful for low power machines. These windings have a coil mounted on each tooth of the stator rather than being distributed in a number of slots as shown in fig. 1.12. These machines offer smaller sizes, high power densities and high efficiencies [13],[14] and [15]. The concept has already been applied to wind energy generators by many researchers [8],[11],[15] and [19] though for smaller power ratings. We can say that the concept has a lot of potential however much more effort is required to establish this technology in the market. There are some design issues/pitfalls while using concentrated windings which have been brought out by [12]-[20]. The important issues which need attention at design stage are:

- Winding factor can be low compared to the distributed windings.
- Cogging torque can be high due to slots being open type/rectangular.
- Eddy current losses in solid conductive parts due to space harmonics and sub harmonics in the magnetic field of concentrated windings.

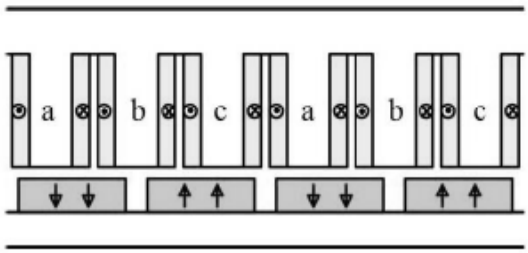

Fig.1.12: Cross section of a concentrated winding topology

A lot of research has been done in order to make concentrated windings a viable option for the goals of cost and weight reduction for wind energy generators. The above mentioned disadvantages have been tackled adequately to facilitate design process. Although still in an early phase, research is proving that concentrated windings can be employed for electrical generators for wind energy applications. The winding factor and cogging torque can be successfully controlled by selection of appropriate slot pole combination. Also the method of calculation of these parameters can be found in [13]-[19].

The Eddy current losses however are still very little known in the field of large direct drive wind turbines. A lot of literature is available for small high speed machines. Large synchronous machines with wound field poles have also been dealt with since early 1940's. The research in the field of large direct drive machines with PMs is relatively new. In [22] analytical and FE methods to calculate eddy current losses in the solid conductive parts of wind turbines are compared. Thus it is evident that concentrated winding topology can be applied to wind turbine generators. The problem remaining is "how to define the slot pole combination such that it leads to low eddy current losses?" Jassal and Polinder [19] have proposed to distribute the coils around the periphery of the machine to reduce the eddy current losses however firm guidelines can't be deduced.

1.5. Research Focus

This thesis exclusively focuses on the electrical generator part of the whole wind turbine system. It is justified because generator is one of the most expensive components of a wind turbine. Out of the many types of wind turbine generators possible, this thesis deals with Permanent Magnet Direct Drive (PMDD) or PMSG type of generators. This type of generator has been chosen because it fits the criteria for offshore applications viz. high energy yield and low number of components (therefore high reliability).

However, these generators are expensive due to distributed windings (high number of coils) as shown in fig. 1.13(a), PM material cost and a full converter. Therefore, it is evident that we need to do some research regarding the cost of these generators. In that respect, an important feature of this whole research is to use fractional pitch concentrated windings (fig. 1.13(b)) instead of distributed windings in stator of PMDD

generator so as to lower manufacturing costs. This is possible because of winding automation in case of concentrated windings. The resulting winding is wound over each tooth resulting in much smaller overhangs compared to a distributed winding.

There is another drawback of this winding scheme in the form of induced losses in solid parts of the machine. The losses are present because of eddy currents induced by the high harmonic content of the winding magneto motive force or mmf as shown in fig. 1.14 (more details are presented in chapter 3, sections 3.1 and 3.2).

Wind turbines are high torque low speed machines which results in solid rotor yoke because it is the torque carrier. A straight forward solution is to laminate the rotor (like stator) but this will lead to additional manufacturing and assembly costs while putting a compromise on strength of torque carrier. Due to this reason, this option has not been considered for analysis.

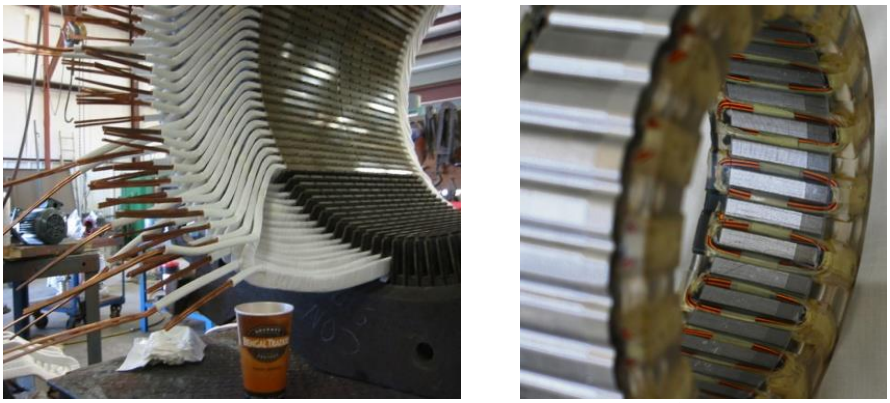

a) b)

Fig.1.13: a) Distributed winding normally used b) Concentrated winding topology

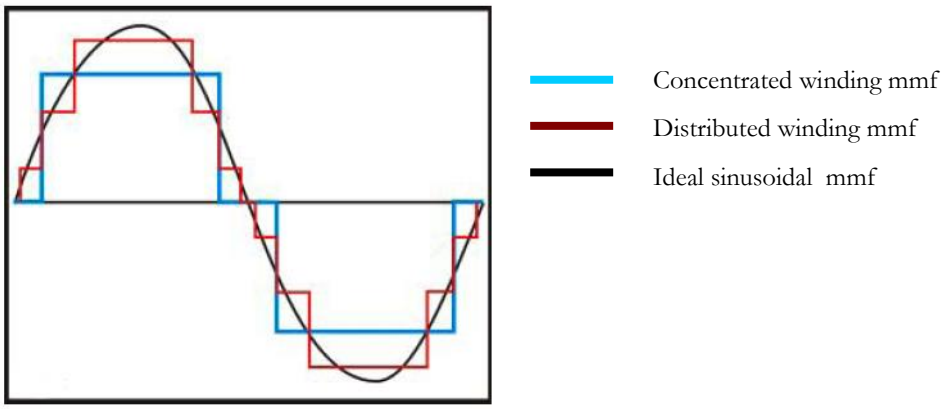

Fig.1.14: Concentrated winding mmf compared with distributed winding mmf

1.6. The Thesis Objective

As mentioned in section 1.4, there are some additional eddy current losses associated with the choice of concentrated windings. Since high performance magnets used in PMDD generators are also conductive, the eddy current losses in the magnets can be so high that the magnets get permanently de-magnetized due to temperature rise. Therefore in order to design a good machine, it is imperative to take these eddy current losses into account. Therefore the main objective of this research can be formulated as:

"Eddy current loss modeling for design of permanent magnet concentrated winding generators for wind turbines"

The subsequent deliverables pertaining to the main objective can be defined as:

- A simple and generic analytical model for predicting eddy current losses.
- Validation of the analytical model using FEM; Validation of analytical and FE models formulation using experiments to bring out effect of simplifications used for models.
- Deduction of trends in eddy current losses for various slot-pole combinations.
- Design guidelines for PMDD generators with respect to eddy current losses.

1.7. Thesis Outline

The thesis has been organized into 8 chapters.

Chapter 1 introduces the field of application and defines the objective of thesis.

Chapter 2 gives an overview of the state of art in manufacturing of PM direct drive generators. This chapter also forms the basis of reason for research.

Chapter 3 gives the background of research done in the field of eddy current loss analysis. An extensive literature survey is conducted on methods and developments in eddy current loss analysis in electrical machines. More details of the problem taken up as the main scientific contribution are presented.

Chapter 4 is dedicated to analytical modeling of electromagnetic field and analysis of eddy current losses in solid parts. For analytical modeling:

- 2d model is formulated because axial length of machine is much larger than the pole-pitch whereby end effects are neglected.
- Rectangular coordinate system is used because diameter of machine is very large and a section of machine is almost rectangular.
- All materials are chosen as linear and isotropic.
- Motion is included in analytical model.

Chapter 5 presents Finite element (FE) modeling for eddy current losses in PMDD generators for wind turbines.

- First a simplified time-harmonic model is presented for validation of analytical model.
- Full transient simulations are performed for analysis of losses with all geometrical effects taken into account.
- The model is applied to a number of possible configurations

Chapter 6 contains experimental analysis and results. These experiments are conducted on 9 kW machines with concentrated windings. The aim of the chapter is to validate the analytical and FE models developed for large direct drive machines.

- Static tests are performed to validate analytical models.
- Rotary tests are performed to validate FE models.

Chapter 7 compares modeling results to generate trends and design guidelines for designing large wind energy generators with concentrated windings.

Chapter 8 summarizes the conclusions and recommendations.

Bibliography

[1] A.Larsson, "The power quality of wind turbines", PhD dissertation, Chalmers University of Technology, Göteborg, Sweden, 2000.

[2] L. H. Hansen, L. Helle, et al. "Conceptual survey of generators and power electronics for wind turbines", Risø-R-1205(EN), 2001.

[3] M. Dubois, "Optimized permanent magnet generator topologies for direct drive wind turbines", Ph.D. dissertation, Delft University of Technology, Delft, The Netherlands, 2004.

[4] M.Henriksen, "Feasibility study of induction generators in direct drive wind turbines", MSc thesis, Technical University of Denmark (DTU), May 2011.

[5] P. Lampola, "Directly driven, low-speed permanent-magnet generators for wind power applications", Ph.D. dissertation, Helsinki University of Technology, Finland, 2000.

[6] D.J.Bang, "Design of transverse flux permanent magnet machines for large direct drive wind turbines", PhD. Dissertation, Delft University of Technology, Delft, The Netherlands, 2010.

[7] H. Polinder, F.F.A. van der Pijl, G.J. de Vilder, P. Tavner, "Comparison of directdrive and geared generator concepts for wind turbines", IEEE Trans. Energy Conversion, Vol. 21, pp. 725-733, September 2006.

[8] S. Widyan, "Design, optimization, construction and test of rare-earth permanent magnet electrical machines with new topology for wind energy applications", Ph.D. dissertation Technische Universität Berlin, Berlin, Germany, 2006.

[9] H. Polinder and J. Morren, "Developments in wind turbine generator systems", Electrimacs 2005, Hammamet, Tunisia.

[10] H. Polinder, S.W.H. de Haan, M.R. Dubois, J.G. Slootweg, 'Basic operation principles and electrical conversion systems of wind turbines'. In EPE Journal, December 2005 (vol. 15, no. 4), pp. 43-50.

[11] Wrobel, R.; Mellor, P.H.; , "Design Considerations of a Direct Drive Brushless Machine With Concentrated Windings," Energy Conversion, IEEE Transactions on , vol.23, no.1, pp.1-8, March 2008.

[12] Wang, J.; Xia, Z. P.; Howe, D.; Long, S.A.; , "Comparative Study of 3-Phase Permanent Magnet Brushless Machines with Concentrated, Distributed and Modular Windings," Power Electronics, Machines and Drives, 2006. The 3rd IET International Conference on , vol., no., pp.489-493, Mar. 2006.

[13] J. Cros, P. Viarouge, "Synthesis of high performance pm motors with concentrated windings", IEEE Transactions on Energy Conversion, vol. 17, pp. 248–253 (2002).

[14] F. Magnussen, C. Sadarangani, **"**Winding factors and Joule losses of permanent magnet machines with concentrated windings," in Proc. of the 2003 IEEE International Electric Machines and Drives Conference**,** 2003, pp. 333 – 339, vol.1.

[15] H. Polinder, M.J. Hoeijmakers, M. Scuotto, "Eddy-current losses in the solid back-iron of permanent-magnet machines with concentrated fractional pitch windings," in Proc. of the 2006 IEE International Conference on Power Electronics, Machines and Drives, Dublin, 4-6 April 2006, pp. 479-483.

[16] Bianchi, N.; Bolognani, S.; Fornasiero, E.; , "An Overview of Rotor Losses Determination in Three-Phase Fractional-Slot PM Machines," Industry Applications, IEEE Transactions on , vol.46, no.6, pp.2338-2345, Nov.-Dec. 2010.

[17] Zhu, Z.Q.; Ng, K.; Schofield, N.; Howe, D.; , "Improved analytical modelling of rotor eddy current loss in brushless machines equipped with surface-mounted permanent magnets," Electric Power Applications, IEE Proceedings - , vol.151, no.6, pp. 641- 650, 7 Nov. 2004

[18] Ishak, D., Zhu, Z.Q., and Howe, D.: "Eddy-current loss in the rotor magnets of permanent-magnet brushless machines having a fractional number of slots per pole," Magnetics, IEEE Transactions on , vol.41, no.9, pp. 2462- 2469, Sept. 2005.

[19] Jassal, A., Polinder, H., Shrestha, G., Versteegh, C., 2008. "Investigation of Slot Pole Combinations and Winding Arrangements for Minimizing Eddy Current Losses in Solid Back-Iron of Rotor for Radial Flux Permanent Magnet Machines", Proceedings of the International Conference on Electric Machines, Sept. 2008, CD-ROM, Paper ID 1292.

[20] El-Refaie, A., Jahns, T., Novotny, D. W., 2006. "Analysis of Surface Permanent Magnet Machines With Fractional-Slot Concentrated Windings", IEEE Transactions on Energy Conversion, Vol. 21, Issue 1, Mar. 2006, pp. 34-43.

[21] C. J. A. Versteegh, "Design of the Zephyros Z72 wind turbine with emphasis on the direct drive PM generator" NORPIE 2004, NTNU Trondheim Norway, 14 – 16 June, 2004.

[22] Jassal, A.; Polinder, H.; Lahaye, D.; Ferreira, J.A.; , "Analytical and FE calculation of eddy-current losses in PM concentrated winding machines for wind turbines," *Electric Machines & Drives Conference (IEMDC), 2011 IEEE International* , vol., no., pp.717-722, 15-18 May 2011

2. State of Art in PM Generator Manufacture

The aim of this chapter is to present the modern methods used in manufacture of PM distributed winding generators for wind turbines. This chapter primarily targets the students/readers who don't have sufficient background of the electrical machine manufacturing technologies. For an expert, these processes are very well known. The chapter highlights the labor intensive aspect of the distributed windings which adds to the cost and manufacturing time of a machine. These aspects establish the reasons for looking into alternate winding topologies such as concentrated windings to lower the cost and manufacturing time. A 2 MW wind turbine generator, designed built and tested forms the basis of description. This generator was developed in the Netherlands and manufactured in Germany whereby the author was involved in the electromagnetic design of the generator.

2.1. Permanent Magnet Direct Drive Generators

Permanent Magnet Direct Drive (PMDD) wind energy generators are gaining popularity amongst manufacturers as they have high energy density and low maintenance. Unfortunately these types of generators are heavy and expensive. A lot of research aimed at weight and cost optimization is going on in the field of PM generators [1]-[4]. PMDD generators have come of age with the invention of high performance magnets, like Samarium Cobalt and Neodymium-boron-iron which has made it possible to design high performance generators. In this chapter, the aim is to highlight the limitations of the distributed winding type PMDD type machines used for wind turbine application.

Developments in electrical machine technology have led to evolution of manufacturing methods of electrical machines as well. Manufacturing methods in principle are old but owing to technology, scale of manufacture and standards, the manufacturing processes have become complex. It is important to know how are these machines manufactured and where can the process be improved further. Starting with the general construction of a PMDD generator, the major parts as shown in fig. 2.1 are:

1. Stator Housing
2. Stator iron - laminates
3. Coils and winding
4. PM assembly
5. Rotor back-iron, shaft and support structure
6. Bearings

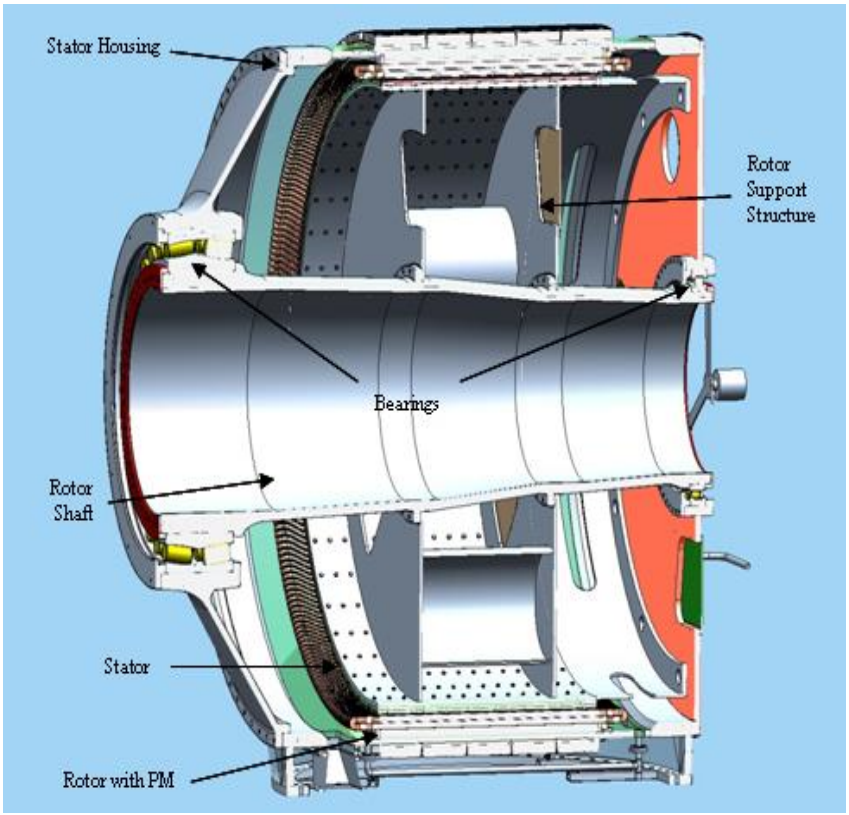

Fig.2.1: Major components of a PMDD generator for wind turbine

2.1.1 Specifications of the 2 MW Generator

The PM direct drive generator was designed to operate in a warm tropical climate which poses the following design constraints:

a) Design wind class: IEC 3A according to IEC 61400
b) Maximum Outer Lamination Diameter: 3.9 m (Transportation constraint)
c) Power output: 2 MW at grid
d) Rotational speed: 18 rpm
e) Voltage output: As per Converter Requirement (Line voltage ~ 540 V)
f) Ambient Temperature: -20^{0}C to 50^{0}C for partial loading
40^{0}C for full load
g) The heat dissipation should be ~ 7 kW/m^2 (for an area of ~ 18m^2)

TABLE 2-1: GENERATOR PARAMETERS

Nominal power at grid	2 MW
Nominal voltage	537 V
Nominal current	2450 A
Outer diameter	3.9 m
Axial length	1.5 m
Nominal Speed	18 rpm
Input Torque	1.18 MNm
Cooling air gap	Forced air
Cooling outside	Natural air
Surface heat dissipation	~7 kW/m^2
Bearing configuration	Double bearing
Winding	Distributed

2.2. Stator Construction

This section deals with the stator or stationary part of the generator only. Various sub-parts of the stator and their construction is explained further.

2.2.1 Stator Housing

The stator housing is the outermost covering of the electrical machine which holds all the electromagnetically active parts [9]-[10]. In most general terms, stator housing is an inactive part and plays the role of keeping all assemblies in place. The size of large machines and the requirement of a high mechanical strength normally mean that the housing is casted as one part. However in very large machines generally housing is casted in large sections which are welded together (fig. 2.2). The material normally used for housing is cast steel.

The inner size of the housing is machined thereafter to house the stator laminates. The housing also carries the mechanism of fixing the laminated steel (for construction of stator yoke) to itself thereby maintaining the air gap radius.

In natural air cooled systems, such as the one employed in the presented generator, housing also aids in cooling the machine. External cooling fins were mounted on the outside of the housing. In case generator is water cooled or force air cooled, this cooling function of the stator housing is limited. Nevertheless it can be seen that generator housing is one of the critical components of the generator assembly because of multiple roles it play and the required mechanical precision.

Fig.2.2: Stator housing for the 2 MW generator for wind turbine

2.2.2 Stator Yoke - Laminates

The stator yoke is in form of thin sheets of magnetic steel called "steel laminates" shown in fig. 2.3. The laminates are available in form of rolled thin sheets (~1mm). The sheets are electrically insulated to prevent flow of eddy currents. The shape of stator teeth/slots including stator back iron are either laser-cut (for small amount) or punched out (for large amounts) from this sheet. The maximum width of this electrical sheet steel is about 1.25m. This presents a limit on the maximum length of a section of stator yoke obtainable from the sheet. Consequently, a number of smaller segments are arranged within the generator housing to form the complete round stator. The stator yoke is built (axially) as a stack of these sheets cut into the shape of the sections of the machine as shown in fig. 2.4. These sheets are placed along the supports mounted on the stator housing. The stacked sheets are then pressed together (see fig. 2.5) to form the axial length of the machine. These individual segments are interleaved to maintain

equal pressure during laminate pressing whereby the sheets are equally strained and breakage can be avoided.

Fig.2.3: Insulated sheet-steel strips

Fig.2.4: Generator Housing laminate assembly

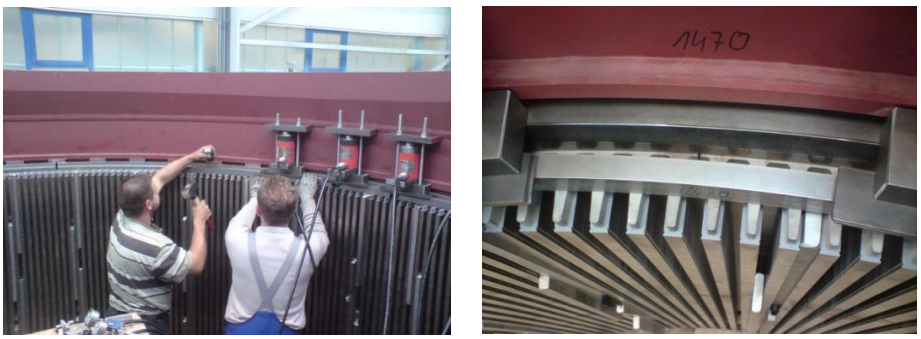

a) b)

Fig.2.5: Stator yoke manufacture - a) Lamination pressing with hydraulic cylinders for compression b) Pressed stack to form stator teeth and yoke

2.2.3 Coils and Winding

The following sections give a brief overview of the winding types used in machine manufacture followed by a detailed description of the lap winding manufacture.

2.2.3.1 Common Winding Types in Large Electrical Machines

The electrical machine winding can be done in many ways and there are several different methods to classify them. Detailed winding overviews can be found in literature and interested readers are referred to [6]-[13]. The purpose of this section is to introduce only the main winding types commonly used in large electrical machines and bring out their advantages and disadvantages. The common winding types can be classified as:

A) Distributed type: In this winding, the coils of same phase are distributed in a number of slots and then interconnected to produce the required MMF. The distributed type can be further classified as single layer and double layer. There are many other types of windings which can fall under this category such as wave winding, mush winding, hair pin windings etc. [7] and [8] but we will restrict ourselves to the single layer concentric and double layer lap windings. This is because these winding types are most commonly used for large machines such as wind turbine generators.

Single Layer Concentric Winding

The single layer concentric winding has only one coil side in each slot and therefore only one *layer* of conductors in a slot as shown in fig. 2.6.

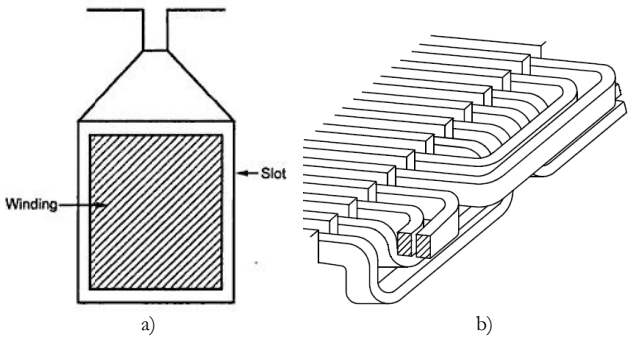

Fig.2.6: Single layer concentric winding: a) Cross section b) Isometric View [14]

The advantages of this type of winding are:

a) High fill factor i.e. more copper conductor area in a slot.
b) No half-filled slots after finishing the winding

The main limitations of this type of winding are

a) Complex end windings as different shapes are needed for coil crossover.
b) Winding short-pitching for harmonic elimination not possible.

Double Layer Lap Winding

The double layer lap winding is the most commonly used distributed winding type for large machines. This type of winding has two coil sides in each slot and therefore two *layers* of conductors in a slot as shown in fig. 2.7.

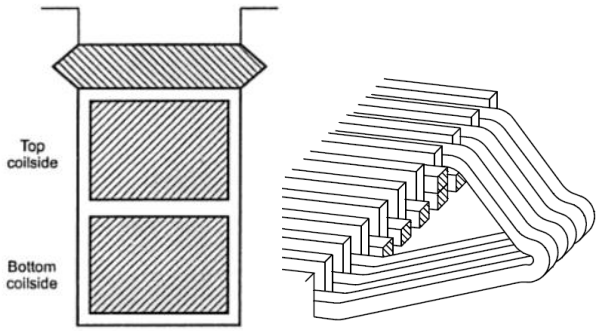

Fig.2.7: Double layer lap winding: a) Cross section b) Isometric View [14]

The advantages of this type of winding are:

a) Symmetric end windings and only one shape of coil is needed.
b) Coils can be short pitched to eliminate harmonics.

The main limitations of this type of winding are

a) Lower fill factor (compared to single layer winding) because of inter-layer insulation within top and bottom coil-side.
b) Half-filled slots obtained after completion of winding.

B) Concentrated type: This winding is also known as tooth-wound winding and fractional slot winding (slots/pole/phase is a fraction). In this winding each coil of a phase is wound around a tooth. These windings are not very popular design option in large machines because of the harmonic rich mmf content they produce as discussed in sections 1.4 and 1.5. These windings can also be single or double layer [11]-[13] but in the context of thesis, we will elaborate only on the double layer type as shown in fig. 2.8

In smaller machine size (~ few kW) this type of winding has been very successful [11] and [12]. The main reason is that for smaller machine sizes, the labor intensive winding process can be automated while utilizing semi-closed slots. For larger machines,

the logical choice for winding automation is by using pre-formed coils. This invariably requires open slots which in turn contribute to mmf harmonics and therefore eddy current losses in solid conductive parts.

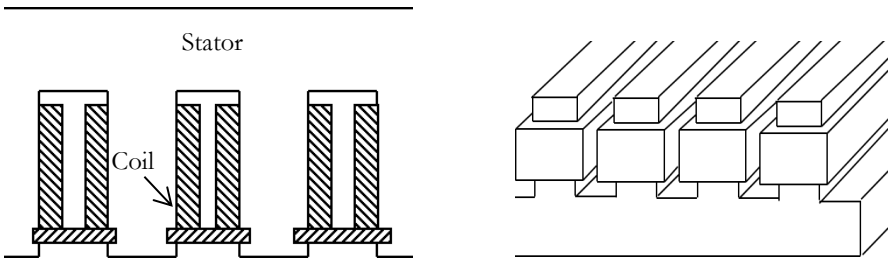

Fig.2.8: Concentrated coil winding: a) Cross section b) Isometric View

The advantages of this type of winding are:

a) Short and symmetric end windings and only one shape of coil is needed.
b) Coil winding can be automated whereby labor, cost and time for production can be reduced.

The main limitations of this type of winding are

a) Lower fill factor* due to necessity of workable mechanical gap between coil sides in same slot.
b) Presence of slot harmonics in flux which can lead to eddy current losses.

**Note: Single layer concentrated windings can have high fill factor but since they are known to have higher eddy current losses [13] these are not considered in this thesis.*

2.2.3.2 Winding of Reference Machine: 2 Layer Lap Type

The method of distributed lap winding with preformed coils used in this machine is well established [6]-[10]. In general the text-books dealing with the design of electrical machines gives details of mmf production from the distributed winding as well as some schematics of how a distributed lap winding is laid into slots. However, the description given in text books is usually not sufficient to form clear picture of the manufacturing process. This makes it difficult to foresee the problems of manufacture of such windings. Therefore this section has been included in this thesis.

The coils and winding arrangement is the most difficult and labor intensive part of an electric machine. The need for special skill-set and workmanship restricts the assembly process of the machine.

As shown in fig. 2.9, the whole process of machine winding starts with insulated copper conductors on spools. First of all, the strands from various spools are tightly

wrapped to form a simple loop. Thereafter, the loop is insulated with an insulating cotton tape to prepare the loop for coil formation. This step can be done automatically or manually depending on the coil size. Once the loop has been insulated, it is stretched hydraulically to form the coil shape for a distributed winding. The shape is such that one side of coil can be placed in top side of the slot and another coil can be placed in the bottom side of the slot.

a)

b)

c)

d)

Fig.2.9: Coil manufacturing precedure - a) Individual wires joined together to form conductor b) Looping of conductor to form rough shape on a winding-jig c) Finished spool held together with tape d) The spool stretched to create the diamond coil shape

The next step is placement of coils in slots and interconnection to form the machine winding. This step (fig. 2.10) is also very labor intensive because of distributed windings and hence large number of coils to be interconnected.

a) b)

Fig.2.10: Machine winding a) Loose coil ends after coil layout in slots b) Brazing of the end connectors for coil interconnection

The interconnection is done by brazing the coil ends. The brazed coil ends are then insulated manually and cable connections for terminals are prepared. This process is shown in fig. 2.11. Finally the machine winding is checked for insulation strength according to various standard tests and sent for insulation impregnation.

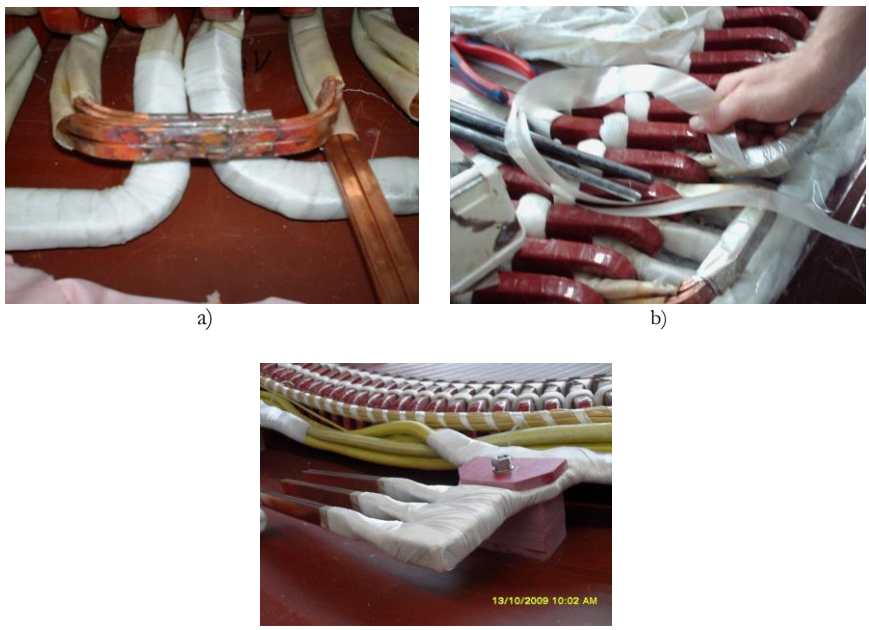

a) b)

c)

Fig.2.11: Machine winding a) Coil end connections brazed b) Insulation of end connection manually c) terminal preparation

The most popular impregnation method is vacuum pressure impregnation where the whole machine after winding is placed in a steel chamber which creates vacuum inside.

Then the insulating material is allowed to flow and due to negative pressure, the insulating material goes on to the surface of generator. After a sufficiently thin and uniform layer of insulating material is deposited on the stator, the machine is taken out heated in an oven to harden the insulating material.

Another method is resin impregnation where viscous resin is allowed to flow through the stator at a slow pace, whereby the coil insulation absorbs the resin. The machine is then heated in an oven to dry and harden the resin. This method was used for the machine under discussion due to unavailability of a vacuum impregnation tank which was large enough to accommodate the machine. The steps of resin pumping and resin baking are shown in fig. 2.12 and fig. 2.13 respectively.

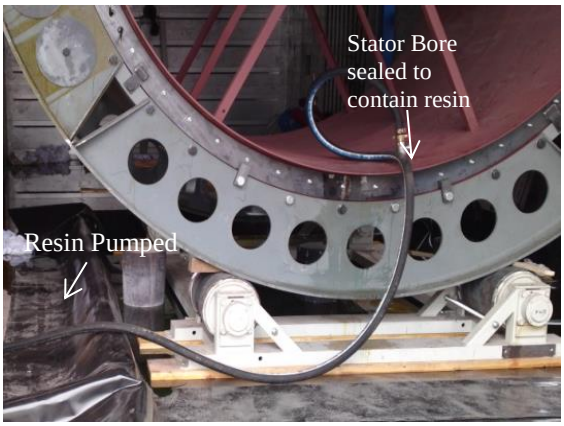

Fig.2.12: Machine impregnation – Resin being pumped into the stator assembly

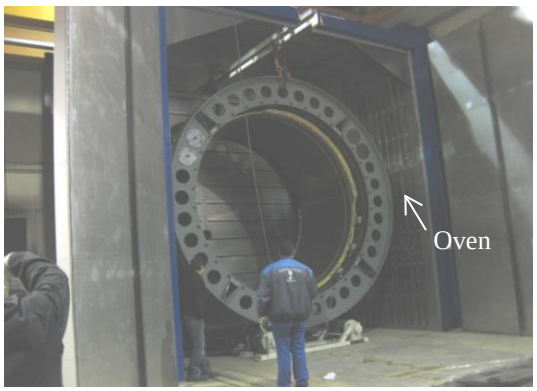

Fig.2.13: Machine impregnation –Baking for resin hardening in a large oven

2.3. Rotor Construction

Different manufacturers use different generator rotor topologies (having different consequences). Since the main objective of the thesis is to calculate eddy current losses due to concentrated windings, this topic is a side-track. This section has been nevertheless included to keep the completeness in this overview of state of the art PM generators manufacture. Consequently, the section is very short and general.

2.3.1 PM Assembly on Rotor

A very challenging task in assembly of the whole generator is assembling active magnets on to the rotor. In one case, the whole rotor can be assembled with un-magnetized magnets and then the magnets can be magnetized later. This method poses important challenges in maintaining the quality of magnetization and requirement of special equipment to magnetize the magnets. In context of the machine in discussion, we focus on assembly of already magnetized magnets (as these were used). There are basically two ways to achieve this. First method is to pre-assemble the whole rotor and magnets then lower the assembly into stator bore as shown in fig. 2.14.

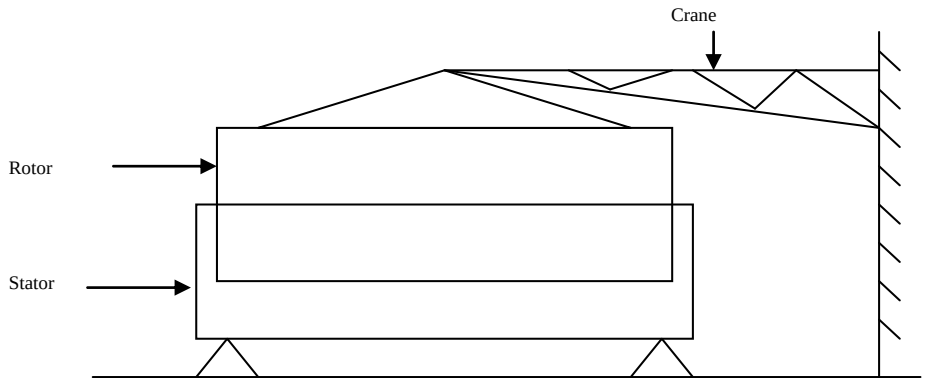

Fig.2.14: Generator assembly – pre assembled rotor with magnets inserted into stator bore

Second method is to insert and align rotor back iron in stator bore and insert magnets on the rotor surface thereafter. Both these methods require negotiation of attractive magnetic forces between stator yoke and the magnets. The second method i.e. magnets insertion on to the rotor was chosen to avoid risks during assembly. This method is depicted in fig. 2.15.

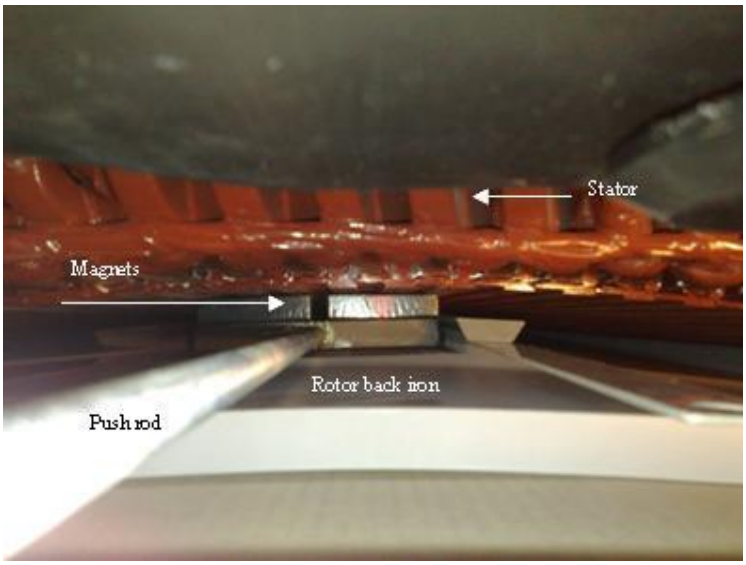

Fig.2.15: Rotor assembly – magnet insertion on to rotor

2.3.2 Rotor Back-iron, Shaft and Support Structure

The rotor back-iron is cast steel machined to the dimensions of the rotor. The tolerance on manufacture of this part is very high because this part ensures that the mechanical air gap between PMs and stator yoke is maintained under all conditions. Such high accuracy demands strong support structure which adds to weight and cost of the machine. The shaft is also casted and machined accurately to fit bearings and rotor structure.

2.3.3 Bearings

The choice and placement of bearings has major consequences on overall size, weight and mechanical design of the machine. The bearings are often custom made. In general, for large PMDD machines, there is a choice of single or double bearing system however some triple bearing systems are also reported [5]. In the present design double bearings were used because of long axial length. Fig. 2.16 and 2.17 show important bearing placement concepts and types used in wind turbines.

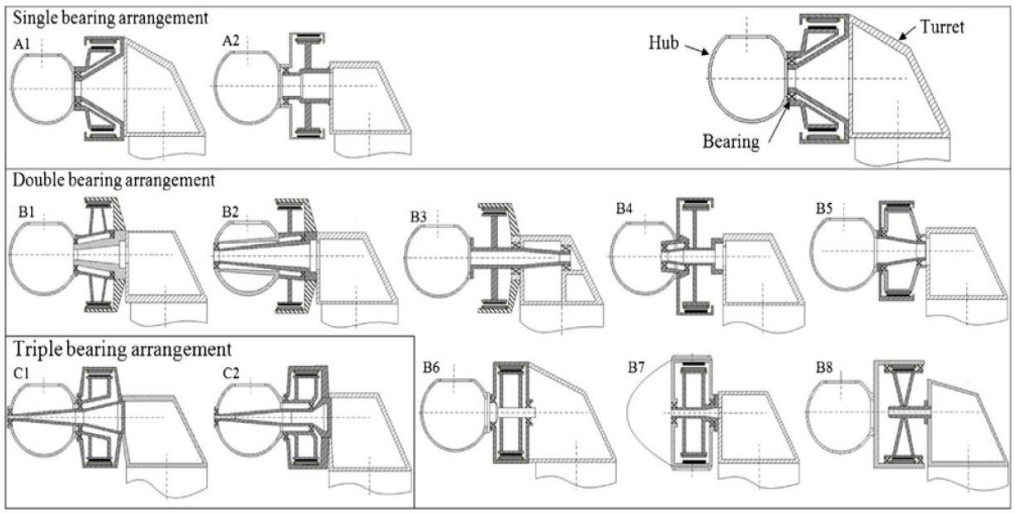

Fig.2.16: Bearings used in wind turbines: single, double and triple bearing [5]

a) b)

Fig.2.17: Bearings used in wind turbines: a) Single layer tapered bearing b) Double layer tapered bearing [5]

2.4. Limitations Posed by PMDD Generators

A conventional PMDD generator is heavy, large and costly. The reasons for this are emanating from the following properties of the machine.

- In direct drive topology, rotational speed of the generator rotor is low whereas torque is high. Therefore a large diameter and higher number of pole pairs is required resulting in a large machine.
- It uses Permanent magnets for creating excitation field. These magnets are still costly as a material, adding to the overall cost.
- Depending on the design, fixation of PM on rotor might require innovative techniques to negotiate magnetic force between the iron and PM.
- A small air gap has to be maintained to maximize air gap flux due to which rotor support structure becomes very heavy.

- A large and heavy machine increases logistics costs (costs of transport, hoists and cranes etc.)
- PM have a danger of demagnetization due to high temperature. Cooling of these generators is a major issue especially at sites which have high ambient temperatures. This necessitates margins to be taken in design, for example, lowering the current density, over-sizing the magnets, increasing surface area of machine etc.
- Permanent Magnets are also prone to corrosion and special protection is needed to ensure their long life.

It is with this background that new methods of machine manufacture are being considered. We will restrict our scope of interest to PM direct drive machines for wind energy applications.

2.5. Summary

In this chapter, the manufacturing methods for large PM machines used in the industry today have been explained. Manufacturing experience and some design details for an actual 2 MW PM generator are shared. The procedure and therefore the difficulties in manufacture of the labor intensive distributed windings are explained. The limitations posed by such PM direct drive generators have been documented based on the experience.

Bibliography

[1] E. Spooner, P. Gordon, C.D. French, "Lightweight, Ironless-Stator, PM Generators for Direct-Drive Wind Turbines" Electric Power Applications, IEE Proceedings, Volume 152, Issue 1, pp. 17 – 26, 7 Jan. 2005.

[2] McDonald A.S., Mueller M.A., Polinder H., "Comparison of generator topologies for direct-drive wind turbines including structural mass" Proc. Int. Conf. Electrical Machines (ICEM),Crete, Greece, September 2006.

[3] McDonald A.S., "Structural analysis of low-speed, high torque electrical generators for direct drive renewable energy converters", PhD Thesis, School of Engineering & Electronics, University of Edinburgh, UK, 2008.

[4] S.Engström, B.Hernnäs, C.Parkegre, S. Waernulf , "Development of NewGen - a new type of direct-drive generator", proceedings of EWEC, London, UK, 2004

[5] J.N.Stander, G.Venter, M.J. Kamper, "Review of direct-drive radial flux wind turbine generator mechanical design", Research article, Wind Energy magazine pp. 459–472, July 2011, DOI:10.1002/we.484.

[6] M.Kostenko and L.Piotrovsky, "Electrical Machines – II: Alternating current machines", 3rd edition 1974, pp. 51-102.

[7] A.K.Sawhney, "A course in Electrical Machine Design", 5th edition, Dhanpat Rai and Co. Publishers, pp.230, 289-295.

[8] M.G. Say, "The performance and design of alternating current machines" 3rd edition, CBS Publishers, pp. 196-224.

[9] P.C.Sen, "Principles of Electrical machines and power electronics", 2nd edition, Wiley Publishers, pp. 132-136 and pp. 569-578.

[10] A.E.Fitzgerald, C.Kingsley and S.D.Umans, "Electric Machinery", 6th edition, Tata McGraw-Hill publishers, pp.173-212 and pp.644-656.

[11] J. Cros, P. Viarouge, "Synthesis of high performance pm motors with concentrated windings", IEEE Transactions on Energy Conversion, vol. 17, pp. 248–253 (2002).

[12] F. Magnussen, C. Sadarangani, **"**Winding factors and Joule losses of permanent magnet machines with concentrated windings," in Proc. of the 2003 IEEE International Electric Machines and Drives Conference**,** 2003, pp. 333 – 339, vol.1.

[13] H. Polinder, M.J. Hoeijmakers, M. Scuotto, "Eddy-current losses in the solid back-iron of permanent-magnet machines with concentrated fractional pitch windings," in Proc. of the 2006 IEE International Conference on Power Electronics, Machines and Drives, Dublin, 4-6 April 2006, pp. 479-483.

[14] H.Polinder "Lecture Notes for the course AC Machines", TU Delft, 2008.

3. Eddy Current Losses

This chapter gives an overview of the research done in the field of eddy current losses in permanent magnet machines and details of the problem taken up as the main scientific contribution i.e. eddy current loss modeling of large direct drive wind turbines with concentrated windings. The contents of this chapter have been published in electrical power applications journal, IET [115].

3.1. Eddy Current Loss – Physics

Eddy currents or Foucault currents were discovered by French physicist Léon Foucault in 1851[114]. The name eddy current comes from the fact that the circulation of currents resembles vortices caused in fluids by turbulence of flow. The physics of eddy currents follows from Lenz's law which states that:

"An induced current is always in such a direction as to oppose its cause"

Eddy current is induced in a conductor to oppose the change in flux that generates it. The eddy currents are caused when a conductor is exposed to a changing magnetic field due to relative motion of the magnetic field source and conductor or due to variations of the field with time.

This can cause a circulating flow of electrons, or a current, within the body of the conductor. These "eddies" of current create induced magnetic fields that oppose the change of the original magnetic field due to Lenz's Law. The phenomenon of eddy currents has many physical effects some of which are undesirable while some can be used. The two major effects of eddy currents are:

a) Magnetic field opposition: The eddy currents generate their own field so that they counteract the primary field that produced them. This property is used in eddy current braking, crack testing etc.
b) Heating: The circulation of eddy currents leads to ohmic heating of the conductor they are induced in. This can be a desirable property in heating applications while it is a drawback in electrical machines.

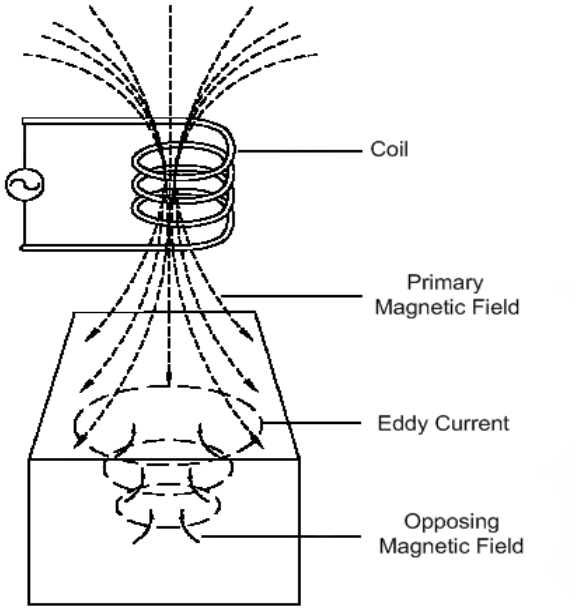

Fig.3.1: Eddy currents induced in a conductor
Source http://www.spacialenergy.com/images/etfield.gif

3.2. Eddy Current Losses in Concentrated Windings

It is known thus far that eddy current losses are induced in solid conductive parts of machines when concentrated windings are used. The main reason for induction of eddy currents is the space harmonic content in mmf produced by the concentrated windings. Time harmonics due to converter operation also induce eddy current losses but in this thesis attention has been focused on space harmonics as they are inherent to the generator while time harmonics are external to the generator. In a machine with concentrated windings, each winding is wound around a tooth of machine.

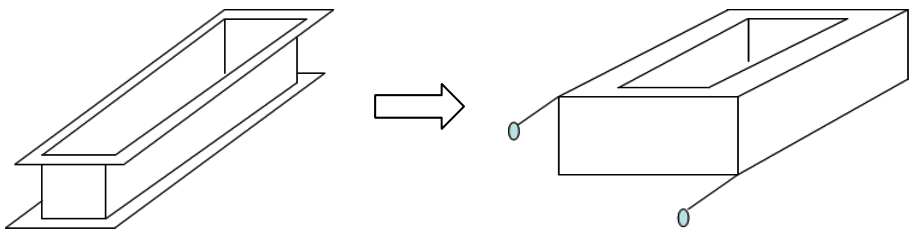

Fig.3.2: A concentrated winding former and after winding the coil around the former

The mmf produced by concentrated windings is not sinusoidal but trapezoidal. In many cases it can be treated as rectangular wave. These waveforms can be decomposed into a number of harmonics using Fourier series. Some of these harmonic fields rotate at same speed as rotor and these are called the torque producing harmonics. However there can be significant harmonic fields which rotate at a speed different than the rotor giving rise to a relative motion between a conductive surface and a magnetic field. These conditions are responsible for induction of eddy currents in the conductive body.

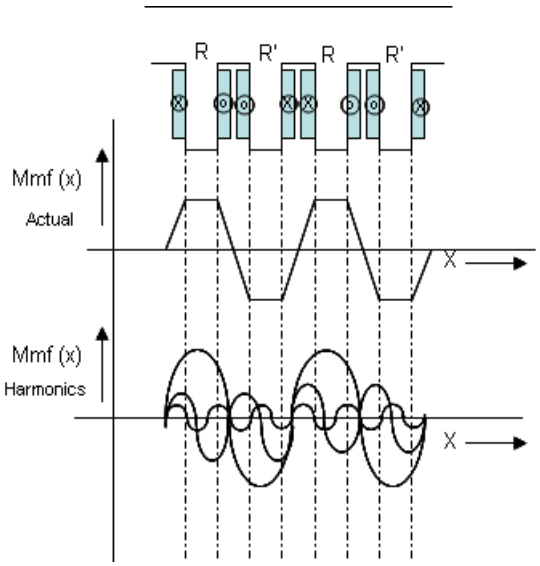

Fig.3.3: Harmonic content of concentrated winding mmf for an arbitrary phase distribution

The dissociation of these fields into their harmonic components depends strongly on the winding distribution and slot-pole combination used in a concentrated winding machine.

The problem of eddy current losses in electrical machines with concentrated windings is not new. However, in the field of large low speed electrical machines such as wind turbine generators, it is relatively new. Amongst wind turbines also we are focussing on large direct drive machines with PM excitation. Though PM machines have all the advantages regarding force density and efficiency, the PM themselves are very sensitive to temperature. If due to any reason, temperature increases to a certain value, the magnets can be permanently de-magnetized.

Another problem associated with high performance PMs is that they are electrically conductive. Eddy currents can be induced within the PMs and the heating effect of these induced eddy currents can raise the magnet temperature. It is imperative to study the effect of induced eddy current losses in case of concentrated winding machines. PM

machines can't be exposed to high temperatures due to risk of demagnetization. To limit the temperature rise, what has been done in the past is to reduce current density, increase surface area, add fins to the machine housing etc. The additional cooling fans form an obvious choice. This subject of machine cooling still has some scope wherein it might be useful to try to inculcate machine cooling in the concentrated winding topology.

With respect to cooling also, this topology has potential because we can have more surfaces exposed for cooling (for example if we blow air in between the two coils mounted on stator teeth).

3.3. Eddy Current Losses in Electrical Machines – A Survey

Electrical machines are one of the prime inventions of mankind. Their utility and importance need no introduction. Like many engineering utilities, electrical machines have been evolving over time. In the past 150 odd years, we have been able to develop a whole branch of electrical engineering dealing specifically with electrical machines. One of the most important subjects falling under the category of electrical machine design is iron losses in the electrical machines. The complex geometry, material properties, presence of time varying electromagnetic fields amidst electrically conducting parts have made the study of iron losses rather challenging and interesting. There are many general iron loss formulations which are used to estimate and group the iron losses in electrical machines. According to most accepted view, the Iron losses in electrical machines can be broadly classified into three categories:

a) Eddy current losses: The resistive losses caused due to induced electric currents which are produced due to change in flux density.
b) Hysteresis Losses: The losses within the structure of magnetic material (at domain level) due to changes in flux density.
c) Excess Losses: The excess losses arise because of internal correlation fields between magnetic domains. These fields, together with other effects such as eddy currents, act as a damping field opposing any changes in the external magnetizing field hence the excess loss is produced.

Triggered by experiments and empirical relations, the early research focused on first two types of losses i.e. eddy current and hysteresis losses. Steinmetz classified that energy lost in iron losses is composed of two components [1].

$$E = \eta \hat{B}^{1.6} + \varepsilon N \hat{B}^2 \tag{3-1}$$

Where,
E = Energy Lost per cycle; η = the coefficient of hysteresis; ε = the coefficient of eddy currents; N= frequency; $\hat{B}$ is the peak flux density.

The first part of this expression is the hysteresis loss contribution and the second part presents eddy current loss contribution. Jordan proposed a similar formulation but with different exponents [2].

$$P_{fe} = C_{hyst} f\hat{B}^2 + \eta_{exc} C_{ec} f^2 \hat{B}^2 \tag{3-2}$$

Here, P_{fe} = Iron losses; f is electrical frequency; $\hat{B}$ is the peak flux density; C_{hyst} and C_{ec} are coefficients of hysteresis and eddy current losses; η_{exc} is the excess or anomalous loss factor.
With further experience, another loss term called "excess losses" was added to account for discrepancies in measurements and calculations [3].

$$P_{fe} = C_{hyst} f\hat{B}^2 + C_{ec} f^2 \hat{B}^2 + C_{ex} f^{1.5} \hat{B}^{1.5} \tag{3-3}$$

Another formulation for total iron losses is by dissociating losses caused by linear magnetization, rotational magnetization and losses cause by higher harmonics [4]. This development has its roots in increased use of power electronics and hence increased harmonic content in power supply or generated voltage.

$$P_{fe} = C_1 P_{lin} + C_2 P_{rot} + C_3 P_h \tag{3-4}$$

Here, C_1, C_2 and C_3 are empirical coefficients and P_{lin}, P_{rot} and P_h denote power loss due to linear magnetization, rotation magnetization and higher harmonics respectively.
However, in this particular research we are going to focus on eddy current loss analysis in electrical machines. Eddy current or Foucault current is a well-known phenomenon in electromagnetics. There are numerous eminent people who contributed to this field of research and it is not possible to name them all here. In order to limit the scope, only rotating machinery and journal publications were considered in the survey. This is because the trends in the field of development of eddy current loss analysis can be projected easily even with this restricted scope. The research on this subject can be divided into three stages based on the most used/popular method of analysis.

a) Stage I: Early phase 1892~1950
b) Stage II: Middle phase 1951~1990
c) Stage III: Modern phase 1990 onwards

This demarcation in stages is porous and has been done to arrange the evolution of this research systematically. It is important to note that in many cases more than one method is employed to reach a conclusion. There is a primary analysis which is a

contribution and a secondary analysis which is used to validate the model or experiments. The phases and their segregation according to the methods are based on the primary method of analysis used by the authors.

The chapter starts with a general introduction to iron losses in electrical machines and then a fundamental description of eddy current loss phenomenon are presented. After that, the three stages of development are described. Some formulations used during the development stage have been summarized. The formulations are chosen to represent a variety of effects which scientists/engineers were trying to capture for example, popular formulations with 2d/3d analysis, linear/non-linear materials, scalar/vector potential etc. are chosen. It might be pointed out that the problem formulations are not limited to those mentioned in the survey but it is not possible to include all formulations. Based on the literature material studied in this research, certain trends have been brought out.

3.3.1 Stage 1: 1892~ 1950 – Experiments and Formulas

Like many physical discoveries, the eddy currents were "observed" first and then the science able to describe the phenomenon was built around those observations. Therefore, initial studies were done on giving a theoretical basis for the phenomenon. The scientists of those times were trying to understand the effects produced by these intriguing currents. From the perspective of electrical machines, the losses due to eddy currents were first studied seriously in 1892 by J.J.Thomson [5] where he analyzed heating effects of eddy currents in an iron plate.

Amongst the rotating machines, DC machines were the most popular machines until the invention of AC machines by Tesla and Ferraris almost simultaneously around 1888 [6] and [7]. In DC machines, eddy current losses were studied in conductors and armature iron especially due to slotting of armature [8]-[12]. However, eddy current losses were not given that much importance before late 1800s. The invention of AC current, induction machines and transformers triggered a lot of interest in analysis of eddy current losses. It was quickly understood that these losses depend on material conductivity and surface area where current could flow. Consequently, sheet steel laminations were being used to restrict eddy current losses in cores of machines since (atleast) as early as 1900 [13]. Thereafter, the research on materials and methods to reduce such losses was carried out. Meanwhile, electromagnetic field modeling was also getting more elaborate and accurate. Following these developments, M.B.Field wrote one of the first analytical papers on eddy current losses in solid and laminated conducting materials [14].

From about 1904 onwards, research in induction machines picked up but it saturated soon [15]-[17]. This could be because induction machines reached an optimum performance level suitable enough for applications of that time. The same trend can be seen in eddy current loss analysis in the field of power transformers. From the study of methodology employed by most authors of this time, it can be said that initial research (late 1800's to early 1900's) was done to observe the effects of the eddy currents. Therefore, most of the research was based on performing experiments and deriving

empirical formulas to calculate eddy current losses. This practice continued for almost three decades. During this period, some publications on induction machines and transformers can be seen as in [13], [14] and [18]. Considerable interest was also shown in material characterization [19]-[24]. Around 1937, engineers and scientists started analyzing losses in cores of synchronous machines analytically [24] and [25]. This work was one of the first scientific works on eddy current losses in AC machines.

TABLE 3-1: SOME FORMULAE USED FOR EDDY CURRENT LOSSES CALCULATIONS

First Author	Formula	Methodology
F.W.Carter [28]	$P_e = kv^{1.5}\hat{B}^2\sqrt{\lambda}$ $\hat{B} = Flux-density(peak); \lambda = tooth-pitch$ $v = velocity$	Theoretical
	$P_e = k_e m^2 \hat{B}^2 \left(\frac{v}{\lambda}\right)^{1.5}$ here, $m = thickness(lam.)$;	Theoretical
M.B. Field [14]	$P_e = 0.315\rho m\hat{H}_s^2\left(\frac{\sinh mh - \sin mh}{\cosh mh - \cos mh}\right)$ $\rho = resisivity; \hat{H}_s = Field-strength : surface$ $m = 2\pi 10^{-4}\sqrt{\frac{f\mu}{10\rho}}; h = thickness; \mu = permeability$	Analytical
C.A.Adams [9]	$P_e = \frac{2.65}{10^4}\left(\frac{B}{10^3}\right)^{2.5}\left(\frac{v}{10^3}\right)^{1.55} q^{1.88}\sqrt{\lambda}$ $q = \frac{slot-opening}{airgap}(cm); v = velocity(cm/s)$ $\lambda = tooth-pitch(cm); B = Flux-density$	Experimental
K.Aston [26]	$P_e = k_e B^x v^{1.75}(g+0.05)\frac{s^3}{\lambda^{4.9}}$	Experimental
	$P_e = k_e B^x v^{1.7}\left(1-\frac{0.0207}{g}\right)\frac{s^3}{\lambda^{3.1}}$ $v = speed(ft/\min); s, \lambda, g, k_e$ are constants	Experimental
T.Spooner [17]	$P_e = k\hat{B}^{2.6}\frac{v^{1.6}}{\lambda^{0.3}}\left(\frac{s}{g}\right)^{2.2}$	Experimental

Till that time linear formulation (in Cartesian coordinates) of machines was popular [26] and [27]. This was followed by some more experimental work in 1941 by Rao and Aston who summarized previously used formulas in literature of the time. Readers interested in knowing about these formulas can refer to [26]. The formulas thus developed were used for refining the design of machines.

A loss calculation comparison using different formulae has been presented by Aston and Rao in fig. 20 of [26]. This type of loss comparison however is not very scientific. This is because of complexity of problem we can't determine a common reference for all the formulae. Different scientists at different times have different correlations within their findings. Hence details on this quantitative comparison of losses have been omitted. It may also be highlighted here that the above table doesn't list all the available formulations for calculation of eddy current losses which is virtually impossible to include in a single paper. However, the purpose here is to show the empirical nature of the results. It was the lack of consistency in expressions and measurements that led to further improvement in the eddy current loss formulation in stage II. At this stage analytical, semi-empirical and empirical analysis' availability was a trigger for other applications for eddy currents as well. Heating, braking and crack detection are just a few to name. In short, we can say that this period presents observation of phenomenon of eddy currents followed by keen pursuit of understanding it according to the means available at that time. This laid ground for the next period which dealt extensively with the scientific development of methods for analysis of eddy current and losses thereof especially in rotating electrical machines.

3.3.2 Stage II: 1951-1990- Analytical Methods

The 2d analytical methods for determination of electro-magnetic fields had already developed during stage I of the research on eddy current losses. B.Hague wrote a book on the electromagnetic field modeling in engineering applications as early as 1929 [29]. Till the end of stage I, rectangular coordinates, linear materials and harmonic formulations were popular. In stage II, as we will see later in this section, material non-linearity, effects of curvature and 3d effects were taken into account in analytical modeling.

The most popular machines of stage II were the conventional synchronous machines. This can be directly linked to development of many hydro-power and thermal-power plants erected during this period especially 1965-90. This resulted in an increased use of synchronous machines for generation of electricity. In this period significant research was done on sheet steel used in electrical machines and eddy current loss analysis thereof [30]-[32]. It is already known and acknowledged that an appreciable amount of research was done in Germany and France related to electrical machines, materials and electromagnetic field modeling. The utility of these works is somewhat restricted due to the language and hence not considered for formulating trends in this survey.

A. General Formulation for Eddy Current Losses

The general formulation which almost all the authors followed consisted of magnetic field solution starting from Maxwell's equations. This type of analysis existed in stage I and scientists were building upon that knowledge to include more complex geometries, material properties and 3d effects. Here in this section, we briefly explain the general formulation of eddy current based problems. The initial formulations of eddy current losses in this stage were in 2 dimensions. The following assumptions were used to setup the problem.

- Cartesian coordinates were used in 2d analysis
- Materials were assumed linear wherein B-H curve was a straight line.
- The end effects were neglected.
- The stator was assumed slotless and the winding was replaced by a current sheet placed at an effective air gap. Fourier series was commonly used to take into account space harmonics.

Using these assumptions, the analytical models could then be solved by employing boundary conditions. The problem was solved for magnetic potential. Both scalar and vector magnetic potential were used but vector magnetic potential seemed more popular. The solution of magnetic potential leads to calculation of an induced current density and then material resistivity is used to calculated eddy current losses. This analysis is very common and therefore details of analysis are not presented here. Interested readers can refer to [110] and [111] for details. Some important formulations are presented in table 3-2.

B. Developments in eddy current loss analysis- Stage II

H.Bondi and K.C.Mukherji presented a thorough analytical model for tooth ripple losses in pole shoes of synchronous generators in 1957 [33]. Following this, P.D.Agarwal wrote a benchmark paper on eddy current losses in solid and laminated iron in 1959 [34]. Apart from that, A.J.Wood and C.Concordia wrote a series of four papers on machines with solid rotors in 1958-1960 [35]-[38]. These papers were completely analytical with rigorous mathematical theory. Effects of curvature, 3d effects and material non-linearities were explored analytically. This was also one of the first detailed analytical works in polar coordinates. Although these papers were focusing more on field modeling but eddy current losses could be analyzed from these results.

From 1961-1970 we can see a steep rise in analytical work done on magnetic field modeling and eddy current losses in electrical machines. In 1962, P.Hammond and N.Kesavamurthy wrote on eddy current losses in solid conductive slabs followed by research on eddy current losses in thin sheets [39] and [40]. This analysis was taken a step further by SubbaRao by including effect of saturation analytically in 1964 [30] and

[31]. Effect of eddy current reaction field in analytical eddy current loss calculation was aptly done in the same period by Mukherji [32].

Although technically possible, the analytical modeling started becoming very complex at this stage. The results thus obtained were also not very accurate (compared to measured experimental results) owing to a number of assumptions required to solve such complex problems analytically. The engineers and scientists were looking for somewhat better methods to formulate and solve eddy current loss problems. One of the approaches used at that time was the circuit approach linked to analytical modeling [41]. R.L.Stoll and P.Hammond generalized the theory of loss modeling due to eddy currents in 1965-66 [42] followed by the first attempt of using numerical methods for analyzing eddy current losses in 1967 [43]. K.Oberretl while working on pole losses in synchronous generators presented an innovative analog circuit methodology for inculcating the effect of variable permeability (saturation) in loss calculation [44]. This method received some attention but never became main-stream. From 1967-1970, pioneers like P.J.lawrenson, C.J. Carpenter and R.A.Jamieson worked extensively on theory of eddy current losses in conductive media including 3d effects [45]-[48]. In 1970, K.K.Lim and P.Hammond developed universal loss charts for eddy current losses in thick conductive plates serving as a guide to machine designers [49]. They used analytical as well as experimental results to derive those charts. The 1970's also saw the first major deviation from analytical to numerical methods for electrical machines. R.L.Stoll presented general solution method for eddy current losses numerically in 1970[50] followed by a power series method together with J.Muhlhaus [51] in the same year. Soon after that, Finite Element (FE) method appeared on the scene. In the field of electrical machines, M.V.K.Chari, P.Reece and C.J.Carpenter were the first proponents of this method and it gained immediate popularity [52]-[54]. The reason for this deviation was the capability of FE method to model difficult geometries and inclusion of material properties [55]. The popularity of FE and numerical methods is evident from a steep decline in the usage of analytical modeling (see fig. 3.4). There were also attempts to include circuital analysis along-with numerical methods to simulate eddy current losses in a more physical sense [56].

A sharp decline in research on eddy current losses in rotating machines in 1980's was noticed. One reason could be that most commonly used machines already reached somewhat optimal performance levels by iterating on design and experience. There was hardly any new research focusing on eddy current loss analysis on induction machines or synchronous machines in 1980's. However, modeling of magnetic fields was still going on [57]-[61]. The FE method for eddy current loss calculation did get some attention [60]-[62].

We can term this period as a period of analysis and formulation of new tools for problems related to eddy currents in rotating electrical machines. The analytical methods matured and the FE methods came into existence during this period. By the late 1980's, FE methods were still limited by the computing capabilities and numerical algorithms available at that time. This shortcoming was soon overcome assisted by a revolution in computing in the early 1990's.

TABLE 3-2: SOME ANALYTICAL FORMULATIONS USED FOR EDDY CURRENT LOSS CALCULATION

First Author	Problem Formulation	Loss Calculation
H.Bondi [33]	- 2d Cartesian coordinates. - Scalar potential - Linear - End effects neglected	$P_e = \frac{\rho\omega}{2\pi}\int_0^{2\pi/\omega}\int_s [\Re(J \times H).ds].dt$ P_e = eddy current losses; J = current density; H = magnetic field intensity
N.Kesavamurthy [40]	- 2d Cartesian coordinates. - Vector potential - Linear - end effects neglected	$P_e = \frac{1}{4}\sum(\hat{E}_{x0r}\hat{H}_{y0r}\cos\psi_{10r} - \hat{E}_{y0r}\hat{H}_{x0r}\cos\psi_{20r})$ P_e = eddy current losses; $\hat{E}_{x0r}, \hat{E}_{y0r}$ = Electric field peak x,y comp.; $\hat{H}_{x0r}, \hat{H}_{y0r}$ = Magnetic field intensity x,y comp. ψ_{10r}, ψ_{20r} = Respective phase angles
V.Subbarao [31]	- 2d Cartesian coordinates. - Vector potential - non-linear material - end effects neglected	$P_e = \frac{4}{\pi^2}\omega ab\mu_m H_m^2 \Phi_2$ ω = electrical frequency a, b = dimensions in m μ_m = normalized permeability H_m = normalized field intensity Φ_2 = normalized flux (complex)
R.L.Stoll [42]	- 2d Cartesian coordinates. - Vector magnetic potential - linear material - end effects neglected	$P_e = \frac{1}{2}\mathrm{Re}\left[\frac{j\rho qp^2(\hat{K}_z e^{-qb})^2(\zeta - j\eta)}{\{(\mu_r + \zeta)^2 + \eta^2\}}\right]$ $\zeta = \sqrt{\frac{\{1+\sqrt{(1+p^4)}\}}{2}}; \eta = \sqrt{\frac{\{-1+\sqrt{(1+p^4)}\}}{2}}$ $p = \sqrt{\frac{\mu_0\mu_r\omega}{q^2\rho}}; q = \pi / g;$ g = pole pitch; Other symbols have usual meanings
P.J.Lawrenson [47]	- 3d polar coordinates. - Vector mag. potential - linear material	$P_e = \frac{a\omega}{2\pi}\int_0^{2\pi/\omega}\int_0^{2\pi}\left(\int_0^a \{[S_z]_{z=0} - [S_z]_{z=L}\}.dr - \int_0^L [S_r]_{r=a}.dz\right)d\theta dt$ a = radius of cylinder S_r, S_z = radial and axial component of poynting vector L = Length of cylinder Other symbols have usual meanings

3.3.3 Stage III: 1991 Onwards-FE, Numerical and Analytical Methods

The 1990's saw regenerated interest in eddy current losses owing to developments in Permanent Magnet (PM) machines, power electronics and concentrated windings. A significant increase in utility of PM machines and combination of power electronic converters with Induction machines brought a second wind to eddy current loss analysis. G.R.Slemon and X.Liu proposed an approximate modeling of eddy current losses based on analytical flux variation calculation in 1990[63]. Z.Liu et al. presented a rather useful analytical model to predict eddy current losses analytically [64]. This was the outcome of past developments on analytical methods and ready verification available in form of FE analysis. Some research on materials and geometrical research is reflected in [65] and [66]. The analytical methods developed thus far are still being used today with minor improvements. The most important developments during this stage came from numerical and FE methods for eddy current loss calculations.

In 1992-1993, B.C.Mecrow and A.G. Jack showed improved possibilities with non-linearity and 3d FE modeling [67]. Further, electro-thermal coupling for eddy current loss calculation using analytical and numerical methods was proposed [68].

The later part of 90's saw 3d FE modeling techniques being developed as importance of end-effects in PM machines was being realized [69]. Japanese had been working steadily on material properties of PM material, laminations and steel during the 90's but much of useful results from Japanese research started appearing in early 2000's probably because of extensive use of 3d FE analysis which was better equipped to deal with eddy current problems now. Many PM machines were used with power electronic converters which added to eddy current losses as well. F.deng, T,Nehl and H.Polinder have analyzed these effects in detail [70]-[74].

A. Numerical Methods and FE Formulation for Eddy Current Losses

There are many numerical methods which have been used to solve electrical engineering problems. Power series or successive approximation method and finite difference method were the first major numerical methods to be used for eddy current loss problems [111]. The power series method however failed to take into account the reaction field of eddy current losses properly which led to its decline [112]. On the other hand the finite difference method, based on Taylor's series was very popular before the advent of FE method. The finite difference method was limited because of large number of simultaneous equations required to be solved. Unavailability of computing power available at that time (stage I) led to gradual decline in popularity of this method. Interested readers can refer to [111] for details of this method. However, from the literature survey, the primary and most popular numerical method used in the field of electrical machines is Finite Element method which we will discuss here briefly. FE method uses numerical techniques to solve partial differential equations but the problem is divided into a "finite number of elements" and requires minimization of energy

functional solved locally for each element. For eddy current problems the energy functional can take the form [60]:

$$F = \int_V \left[\left(\frac{|\bar{B}|^2}{2\mu} \right) - \bar{J}.\bar{A} + i\pi f \sigma \bar{A}^2 \right] dv$$

$\bar{B}$= magnetic field; $\bar{A}$= mag. vector potential; μ= permeability; v = volume; (3-5)
σ= electrical conductivity; $\bar{J}$= applied current density; f= frequency

The mathematical problem to be solved is then minimization of energy functional F i.e.

$$\frac{\partial F}{\partial \bar{A}} = 0 \tag{3-6}$$

The theory of finite elements is well known and since the paper is focused on literature survey of eddy current losses, the solution methods are not explained here. After solution of $\bar{A}$, the induced eddy current density can be found from

$$\bar{J}_{ind}(x, y, z) = -i.2\pi f \sigma(x, y, z)\bar{A}(x, y, z) \tag{3-7}$$

Eddy current losses can be calculated easily by integrating this current density over an area

$$P_e = \iiint_V \frac{\bar{J}_{ind}^2(x, y, z)}{\sigma} dV \tag{3-8}$$

P_e is the eddy current loss ; $\bar{J}_{ind}$ is the induced current density; V is volume; σ is conductivity

The overall solution is compiled and can be easily displayed for a chosen quantity as well as some other derivable quantities from the original variable solved for. It may be mentioned that because of discretization of the domain in FE method, complex geometries and material non-linearities can be easily handled. FE method has developed a lot since its inception into electrical engineering. Various new algorithms, mathematical techniques have been implemented to improve the modeling and post-processing of FE method. Description of various innovations in numerical methods is out of scope for this survey.

TABLE 3-3: SOME NUMERICAL FORMULATIONS USED FOR EDDY CURRENT LOSS CALCULATION

First Author	Problem Formulation	Loss Calculation	Method
R.Stoll [51]	- 2d Cartesian - Vector potential	$A_{kl}^{(1)} = (K_{k0} + K_{k1}y + K_{k2}y^2 + ... + K_{kk}y^k) \times e^{\pi y/g} e^{-j\pi x/g}$ A_k = kth order term in power series for A (mag. vector potential); K_k = coefficient g = pole pitch; *Eddy current losses are then calculated from solution of A	Power Series
B.C.Mecrow [67]	- 3d Cartesian - Scalar mag. potential - End effects included - Linear Material	$\nabla \times \frac{1}{\sigma} \nabla \times T_A = \nabla \times \frac{1}{\sigma} \nabla \times T_B = -\frac{d}{dt}\left[\frac{\mu}{2}(T_A + T_B) - \nabla\Omega\right]$ T_A, T_B = Potential functions in adjacent bodies Ω = Scalar magnetic potential σ = Electrical conductivity μ = Permeability T_A, T_B and Ω are solved to get eddy current density and losses	FE
W.N.Fu [113]	- 2d Cartesian - Vector mag. potential - linear material - end effects neglected	$\nabla \times (v\nabla \times A) + \sigma \frac{\partial A}{\partial t} - \frac{\sigma}{l_M} u_{mn} = \nabla \times (vB_r)$ $P_e = \sum_{n=1}^{N} \left[\sum_{m=1}^{M} \sigma l_M \iint_{\Omega_{mn}} \left(\frac{\partial A}{\partial t} + \frac{u_{mn}}{l_M} \right)^2 d\Omega + i_{1n}^2 R_{kn} + (i_{1n}^2 + i_{Mn}^2) R_{kn} \right]$ P_e = Eddy current losses in magnets A = magnetic vector potential axial component v = reluctivity of the material M, N = slices and bars cut out of the domain u_{mn} = voltage between nodes of the nth bar and mth slice l_M = Axial length per slice of magnet R_{kn} = Terminal resistance between adjacent bars	Circuit element coupled with FE

K.Yamazaki [97]	- 3d cartesian - Vector mag. potential - linear material	$\nabla \times \left(\frac{1}{\mu} \nabla \times A \right) = J_a - \sigma \left(\frac{\partial A}{\partial t} + \nabla \varphi \right) + \frac{1}{\mu_0} \nabla \times M$ $\nabla \cdot \left\{ \sigma \left(\frac{\partial A}{\partial t} + \nabla \varphi \right) \right\} = 0$ $v_a = v_{oa} + R_a i_a = \frac{d\Phi}{dt} + R_a i_a$ $P_e = \frac{2d}{\sigma} \int_0^b \int_0^a \left(\left\| J_x(x,y) \right\|^2 + \left\| J_y(x,y) \right\|^2 \right) dxdy$ $A, \varphi =$ magnetic vector and electric scalar potential resp. $\mu, \sigma =$ permeability and conductivity resp. $J_a =$ Armature current density; $M =$ Magnetization of PM $v_a, R_a, i_a =$ Armature voltage, resistance and current resp. $\Phi =$ Flux linkage of armature coil $a, b =$ Dimensions; $J_x(x,y),\ J_y(x,y) =$ x,y comp. of induced current density calculated analytically	FE + Analytical

B. Developments in eddy current loss analysis- Stage III

Just as we observed a rapid increase in analytical methods in 1960's, another phenomenon that virtually exploded in research during 2000-2010 was the PM machines. Almost 70% of the research of eddy current losses was done on PM machines of one type or another. The Neodymium magnets were available for cheaper prices and it led to a great impetus on development of PM machines. However, this time around the tools i.e. methods to deal with eddy current loss problems were at hand. Therefore, in this period we see extensive use of analytical methods and FE methods to reach good machine designs [75]-[81]. Z.Q.Zhu, D.Ishak and D.Howe wrote many papers related to modeling of magnetic fields and eddy current losses in PM machines [82]-[85]. Although the techniques used were not new but the application was rather new. It led to tremendous interest in PM machines for large power applications especially in the field of renewable energy like Archimedes Wave Swing (AWS), PM Direct drive generators for wind turbines etc. [86].

Many new applications were identified with the advent of PM machines. High speed machines without slots, fault tolerant machines and switched reluctance machines etc indicated a new breed of application where eddy current loss analysis was deemed necessary [87]-[90]. At the same time a lot of research on investigating the eddy current losses in conductive Neodymium magnets themselves was gathering momentum. 3d FE is the favorite tool when it comes to material characterization because of difficulty in modeling material anisotropy and end effects analytically. PMs are conductive and therefore modeling eddy current losses in magnets was imperative [91]-[93]. K.Yamazaki and Y.Fukushima et al. have done a lot of work on eddy current loss analysis in PMs

[94]-[97]. In Europe also, significant amount of work on material characterization for steel laminations solid iron samples etc. has been done [98]-[101].

With all these advancements, modeling of machines for new applications benefitted and we can see a lot of publications on analysis of these special machines. M.Markovic and Y.Perriard have presented generalized models for slotless PM machines in 2007-09 respectively [102] and [103]. The low power machines (fractional kW – few kW) can be made cheaper using concentrated windings with fractional pitch because of winding automation possibility. However, these types of windings also have eddy current losses associated with them [104]-[108]. There is a good literature survey on analytical machine modeling mentioned in [109]. A very thorough literature survey on practical design aspects of concentrated winding machines can be found in [110].

Therefore, any development in the sector of fractional pitch concentrated winding machines led to analysis of eddy current losses associated with them. The latest additions in such machines are the ultra-high speed machines (~10^5 rpm or more) and PM direct drive wind turbines. These machines utilize concentrated windings for cost benefits, and high power densities. For some applications where 3d effects play a major role, analytical methods are rather limited whereby it becomes necessary to resort to the 3d FE calculations. It is important to note that in this period, both the analytical and FE methods have been used extensively. The probable reason could be that analytical methods give a quick insight into dependence of design on various parameters which is good for optimization. FE methods are more accurate however they take longer time to solve. Thus a combination of these methods is the preferred way at present.

3.4. Results and Trends

From literature survey, it is clear that the main methodologies used in analysis of eddy current losses are:

a) Experimental: The analysis is done by experimental observations and empirical formulas derived for eddy current losses thereof.
b) Analytical: Starting from Maxwell's equations magnetic and electric field quantities are derived and used for evaluating eddy current losses.
c) Numerical: This method is basically same as analytical method with the exception that instead of a mathematical expression, the derived partial differential equations are solved numerically.
d) Finite Element (FE): This is an advancement of numerical methods where the whole space is divided into very fine mesh and the quantities are derived by solving for each region numerically. A big advantage is that any geometry, motion and non-linearity can be incorporated at the same time whereas a probable disadvantage is long time taken to solve and requirement of specialized software which is rather expensive.
e) Equivalent Circuits: The machine is modeled in terms of lumped elements arranged in an equivalent circuit depending on machine geometry. The eddy current losses are then derived from this equivalent circuit.

Each of these methods has played an important part in development of theory of eddy current loss analysis. However the popularity and utility of methods have been changing over time. These trends have been deduced based on this extensive literature survey. The utility percentage shown in fig.3.4 is based on the number of papers used for this survey. It is not an exact number however the trend projected by these numbers is indicative of the actual utility.

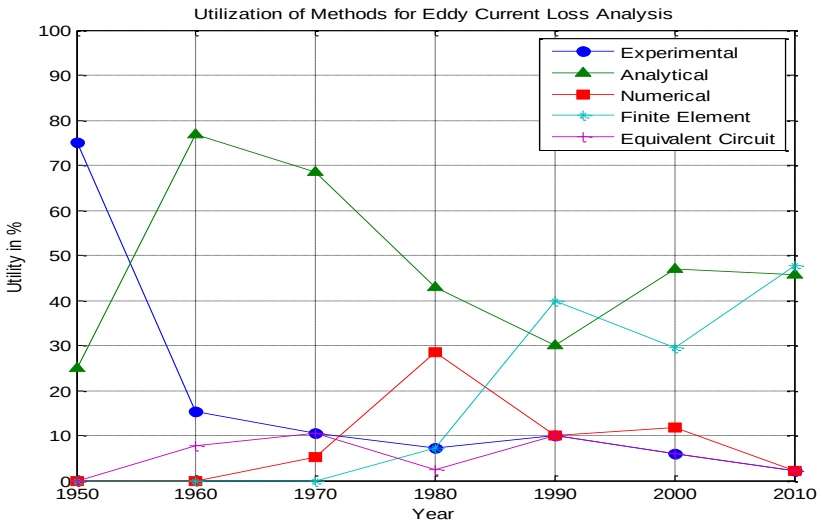

Fig.3.4: Eddy currents loss analysis methods in Electrical machines

Further, it can be seen from the literature survey that the research focus on eddy current losses in the field of electrical machines shifted in different time periods. The main trend of research and the types of machines studied can be grouped as:

a) General: This means development of methodology and analysis tools related to eddy current loss analysis.
b) Materials: This indicates the research which didn't focus on any particular type of machine but on the materials which can be used in the machines. For example, research on eddy current losses in sheet steel laminations and solid iron.
c) Conventional DC machines: These machines need no introduction but in this survey, these machines refer to electrically excited DC machines with rotating armatures and commutator.
d) Conventional Induction machines: These include squirrel cage and wound rotor type of induction machines and with or without power electronic drive connected to them.
e) Conventional Synchronous machines: This term refers to the synchronous machines with electrically excited field winding on the rotor and distributed stator windings in the stator.

f) PM machines: This is a general term and there can be many different types of PM machines. In this survey this refers to general class of PM machines which use PM as the field excitation.

g) Special: These machines appeared in late 1990's and switched reluctance motors, single phase motors, printed circuit board motors, flux switching machines etc. falls under this category.

It may also be mentioned here that the percentage of focus on research is relative and based on the number of papers used in this survey only. The purpose here is to present trends rather than numbers. Figure 3.5 shown below projects the focus of research during a given time period relative to other machine types in question.

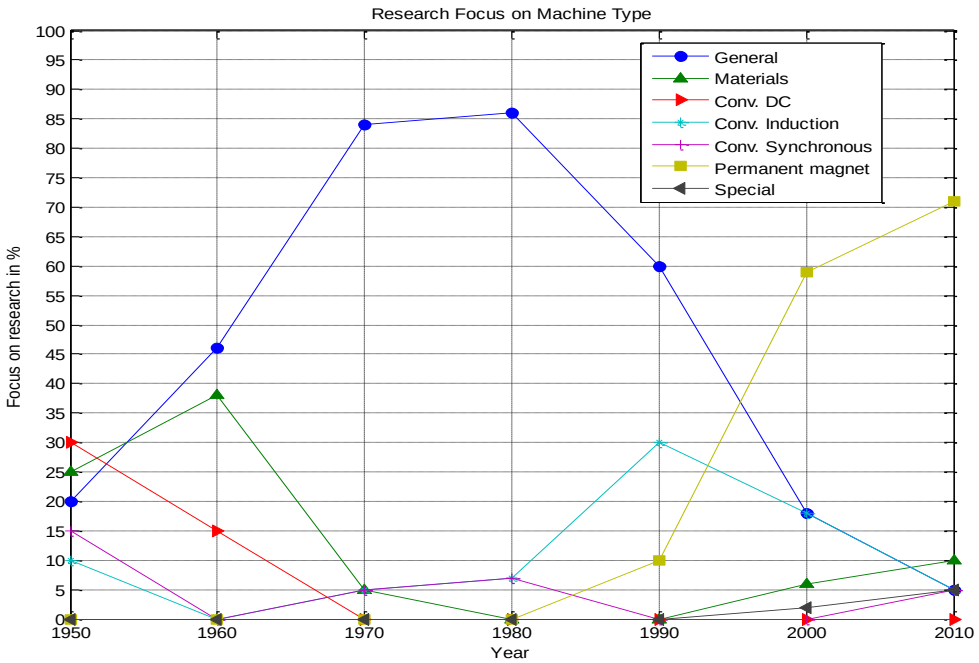

Fig.3.5: Eddy currents loss analysis – Focus on type of machine

3.5. Summary

The basic physics behind Eddy current losses is briefly explained, followed by details of eddy current loss generation in concentrated windings. The historical development of the Eddy current loss analysis in rotating electrical machines has been documented. Trends in development of Eddy current loss analysis are derived based on an extensive literature survey.

Bibliography

[1] Steinmetz, C.P.; "On the law of hysteresis (originally from 1892)," Proceedings of the IEEE , vol.72, no.2, pp. 197- 221, Feb. 1984.

[2] Pry, R.H. and Bean, C.P.; "Calculation of the energy loss in magnetic sheet materials using a domain model," Journal of Applied Physics vol. 29, no.3, pp. 532-533, Mar. 1958.

[3] Bertotti, G.; "General properties of power losses in soft ferromagnetic materials ," Magnetics, IEEE Transactions on , vol.24, no.1, pp.621-630, Jan 1988.

[4] Jacobs, S., Hectors,D. et al.; , "Magnetic material optimization for hybrid vehicle PMSM drives," EVS24 – International Battery Hybrid and Fuel Cell Electric Vehicle Symposium, Stavanger, Norway, 2009

[5] Thomson J.J.: "On the heat produced by eddy currents in an iron plate exposed to alternating magnetic field", The electrician, vol. 28, 1892.

[6] Tesla N.: "Electro Magnetic Motor", US Patent Number: 0381968, May1888.

[7] Bowers, B.; "Scanning our past from London: Galileo Ferraris and alternating current," Proceedings of the IEEE , vol.89, no.5, pp.790-792, May 2001.

[8] Field, A. B.: "Eddy Currents in Large Slot-Wound Conductors," American Institute of Electrical Engineers, Transactions of the , vol.XXIV, no., pp.761-788, Jan. 1905.

[9] Adams, Comfort A., Lanier, A. C., Pope, C. C., and Schooley, C. O.: "Pole-Face Losses," American Institute of Electrical Engineers, Transactions of the , vol.XXVIII, no.2, pp.1133-1156, June 1909.

[10] Press, A.: "Incremental armature copper losses at no-load and armature teeth eddy-current losses," Electrical Engineers, Journal of the Institution of , vol.53, no.250, pp.820-823, June 15 1915.

[11] Hughes, E.: "Iron losses in d.c. machines," Electrical Engineers, Journal of the Institution of , vol.63, no.336, pp.35-50, December 1924.

[12] Gilman, R. E.: "Eddy Current Losses in Armature Conductors," American Institute of Electrical Engineers, Transactions of the , vol.XLIII, no., pp.246-251, Jan. 1924.

[13] Townsend, F.: "Eddy Current Losses in Transformers," American Institute of Electrical Engineers, Transactions of the , vol.XVII, no., pp.319-334, Jan. 1900.

[14] Field, M.B.: "Eddy currents in solid and laminated masses," Electrical Engineers, Journal of the Institution of , vol.33, no.169, pp.1125-1143, September 1904.

[15] Hanssen, I. E.: "Calculation of Iron Losses in Dynamo Electric Machinery," American Institute of Electrical Engineers, Transactions of the , vol.XXVIII, no.2, pp.993-1001, June 1909.

[16] Taylor, H.W.: "Eddy currents in stator windings," Electrical Engineers, Journal of the Institution of , vol.58, no.290, pp.279-298, April 1920.

[17] Spooner, T.: "Squirrel-Cage Induction-Motor Core Losses," American Institute of Electrical Engineers, Transactions of the , vol.XLIV, no., pp.155-163, Jan. 1925.

[18] Lloyd, M. G., and Fisher, J. V. S.: "The Testing of Transformer Steel," American Institute of Electrical Engineers, Transactions of the , vol.XXVIII, no.1, pp.439-467, Jan. 1909.

[19] Scott, K.L.: "Variation of the Inductance of Coils due to the Magnetic Shielding Effect of Eddy Currents in the Cores," Proceedings of the Institute of Radio Engineers , vol.18, no.10, pp. 1750- 1764, Oct. 1930.

[20] Peterson, E. and Wrathall, L.R.: "Eddy Currents in Composite Laminations," Proceedings of the Institute of Radio Engineers , vol.24, no.2, pp. 275- 286, Feb. 1936.

[21] Reed, M.: "An experimental investigation of the theory of eddy currents in laminated cores of rectangular section," Wireless Section, Institution of Electrical Engineers - Proceedings of the , vol.12, no.35, pp.167-178, June 1937.

[22] Blake, L.R.: "The eddy-current anomaly in ferromagnetic laminae at high rates of change of flux," Proceedings of the IEE - Part II: Power Engineering , vol.96, no.53, pp.705-718, October 1949.

[23] Stewart, K.H.: "Losses in electrical sheet steel," Proceedings of the IEE - Part II: Power Engineering , vol.97, no.56, pp.121-125, April 1950.

[24] Bewley, L. V., and Poritsky, Hillel: "Intersheet Eddy-Current Loss in Laminated Cores," American Institute of Electrical Engineers, Transactions of the , vol.56, no.3, pp.344-346, March 1937.

[25] Concordia, C., and Poritsky, H.: "Synchronous Machine With Solid Cylindrical Rotor," American Institute of Electrical Engineers, Transactions of the , vol.56, no.1, pp.49-179, Jan. 1937.

[26] Aston, K., and Kesava Rao, M.V.: "Pole-face losses due to open slots," Electrical Engineers - Part I: General, Journal of the Institution of , vol.88, no.8, pp.308-312, August 1941.

[27] Gibbs, W.J.: "Tooth-ripple losses in unwound pole-shoes," Electrical Engineers - Part II: Power Engineering, Journal of the Institution of, vol.94, no.37, pp.2, February 1947.

[28] Carter, F.W.: "Pole-face losses," Electrical Engineers, Journal of the Institution of , vol.54, no.253, pp.168-170, January 1 1916.

[29] Hague, B.: "Electromagnetic problems in Electrical Engineering , Chapter IV, Oxford University Press, 1929.

[30] Subba Rao, V.: "Losses in ferromagnetic laminations due to saturation," Electrical Engineers, Proceedings of the Institution of , vol.111, no.12, pp.2111-2117, December 1964.

[31] Subba Rao, V.: "Eddy-current losses in finite sections of solid iron under saturation," Electrical Engineers, Proceedings of the Institution of , vol.111, no.2, pp.343-348, February 1964.

[32] Mukherji, K.C.: "Reaction of eddy currents induced in a ferromagnetic medium on the inducing field," Electrical Engineers, Proceedings of the Institution of, vol.112, no.2, pp.444-445, February 1965.

[33] Bondi, H., and Mukherji, K.C.: "An Analysis of Tooth-Ripple Phenomena in Smooth Laminated Pole-Shoes," Proceedings of the IEE - Part C: Monographs , vol.104, no.6, pp.349-356, September 1957.

[34] Agarwal, P.D.: "Eddy-Current Losses in Solid and Laminated Iron", AIEE Transactions, vol. 78, p.169 , 1959.

[35] Wood, A. J.: "An Analysis of Solid Rotor Machines Part I. Operational Impedances and Equivalent Circuits," Power Apparatus and Systems, Part III. Transactions of the American Institute of Electrical Engineers, vol.78, no.4, pp.1657-1665, Dec. 1959.

[36] Wood, A. J., and Concordia, C.: "An Analysis of Solid Rotor Machines Part II. The Effects of Curvature," Power Apparatus and Systems, Part III. Transactions of the American Institute of Electrical Engineers, vol.78, no.4, pp.1666-1672, Dec. 1959.

[37] Wood, A. J. and Concordia, C.: "An Analysis of Solid Rotor Machines Part III. Finite Length Effects," Power Apparatus and Systems, Part III. Transactions of the American Institute of Electrical Engineers, vol.79, no.3, pp.21-26, April 1960.

[38] Wood, A. J., and Concordia, C.: "An Analysis of Solid Rotor Machines Part IV. An Approximate Nonlinear Analysis," Power Apparatus and Systems, Part III. Transactions of the American Institute of Electrical Engineers , vol.79, no.3, pp.26-31, April 1960.

[39] Hammond, P.: "The calculation of the magnetic field of rotating machines. Part 3: Eddy currents induced in a solid slab by a circular current loop," Proceedings of the IEE - Part C: Monographs, vol.109, no.16, pp.508-515, September 1962.

[40] Kesavamurthy, N., and Rajagopalan, P.K.: "An analytical method taking account of saturation and hysteresis for evaluating the iron loss in solid-iron cores subjected to an alternating field," Proceedings of the IEE - Part C: Monographs , vol.109, no.15, pp.237-243, March 1962.

[41] Jones, D.A. and Leung, W.S.: "A theoretical and analogue approach to stray eddy-current loss in laminated magnetic cores," Proceedings of the IEE - Part C: Monographs , vol.108, no.14, pp.509-515, September 1961.

[42] Stoll, R.L., and Hammond, P.: "Calculation of the magnetic field of rotating machines. Part 4: Approximate determination of the field and the losses associated with eddy currents in conducting surfaces," Electrical Engineers, Proceedings of the Institution of , vol.112, no.11, pp.2083-2094, November 1965

[43] Stoll, R.L.: "Numerical method of calculating eddy currents in nonmagnetic conductors," Electrical Engineers, Proceedings of the Institution of , vol.114, no.6, pp.775-780, June 1967.

[44] Oberretl, K.: "Magnetic Fields, Eddy Currents, and Losses, Taking the Variable Permeability into Account," Power Apparatus and Systems, IEEE Transactions on , vol.PAS-88, no.11, pp.1646-1657, Nov. 1969.

[45] Lawrenson, P.J., Reece, P., and Ralph, M.C.: "Tooth-ripple losses in solid poles," Electrical Engineers, Proceedings of the Institution of , vol.113, no.4, pp.657-662, April 1966.

[46] Jamieson, R.A.: "Eddy-current effects in solid unslotted iron rotors," Electrical Engineers, Proceedings of the Institution of , vol.116, no.4, pp.612-613, April 1969.

[47] Lawrenson, P.J., and Ralph, M.C.: "General 3dimensional solution of eddy-current and laplacian fields in cylindrical structures," Electrical Engineers, Proceedings of the Institution of , vol.117, no.2, pp.467-472, February 1970.

[48] Carpenter, C.J., and Djurovic, M.: "Three-dimensional numerical solution of eddy currents in thin plates," Electrical Engineers, Proceedings of the Institution of , vol.122, no.6, pp.681-688, June 1975.

[49] Lim, K.K., and Hammond, P.: "Universal loss chart for the calculation of eddy-current losses in thick steel plates," Electrical Engineers, Proceedings of the Institution of , vol.117, no.4, pp.857-864, April 1970.

[50] Stoll, R.L.: "Solution of linear steady-state eddy-current problems by complex successive overrelaxation," Electrical Engineers, Proceedings of the Institution of , vol.117, no.7, pp.1317-1323, July 1970.

[51] Stoll, R.L., and Muhlhaus, J.: "Power-series method of calculating eddy currents in nonmagnetic conductors," Electrical Engineers, Proceedings of the Institution of , vol.119, no.11, pp.1616-1620, November 1972.

[52] Chari, M.V.K.: "Finite-Element Solution of the Eddy-Current Problem in Magnetic Structures," Power Apparatus and Systems, IEEE Transactions on , vol.PAS-93, no.1, pp.62-72, Jan. 1974.

[53] Chari, M.V.K., and Reece, P.: "Magnetic Field Distribution in Solid Metallic Structures in the Vicinity of Current Carrying Conductors, and Associated Eddy-Current Losses," Power Apparatus and Systems, IEEE Transactions on , vol.PAS-93, no.1, pp.45-56, Jan. 1974.

[54] Carpenter, C.J.: "Finite-element network models and their application to eddy-current problems," Electrical Engineers, Proceedings of the Institution of , vol.122, no.4, pp.455-462, April 1975.

[55] Stoll, R.L., and Hindmarsh, R.: "Reduction of local eddy-current losses in turbogenerator stator windings using composite subconductors," Electrical Engineers, Proceedings of the Institution of , vol.123, no.11, pp.1217-1222, November 1976.

[56] Carpenter, C.: "A network approach to the numerical solution of Eddy-current problems," Magnetics, IEEE Transactions on , vol.11, no.5, pp. 1517- 1522, Sep 1975.

[57] Sironi, G., and Van Hulse, J.: "Eddy loss calculation in solid magnetic pieces of electrical machines," Magnetics, IEEE Transactions on , vol.11, no.5, pp. 1523- 1525, Sep 1975.

[58] Yannopoulos-Lascaratos, P.P., and Tegopoulos, J.A.: "Eddy-current distribution in cylindrical structures caused by rotating magnetic fields," Electric Power Applications, IEE Proceedings B , vol.129, no.2, pp.64-74, March 1982.

[59] Demerdash, N.A., Nehl, T.W., Mohammed, O.A., Miller, R.H., and Fouad, F.A.: "Solution of Eddy Current Problems Using Three Dimensional Finite Element Complex Magnetic Vector Potential," Power Apparatus and Systems, IEEE Transactions on , vol.PAS-101, no.11, pp.4222-4229, Nov. 1982.

[60] Brauer, J.: "Finite element calculation of eddy currents and skin effects," Magnetics, IEEE Transactions on, vol.18, no.2, pp. 504- 509, Mar 1982.

[61] Ferrari, R., and Pinchuk, A.: "Complementary variational finite-element solution of Eddy current problems using the field variables," Magnetics, IEEE Transactions on , vol.21, no.6, pp. 2242- 2245, Nov 1985.

[62] Jack, A.G., and Mecrow, B.C.: "Methods for magnetically nonlinear problems involving significant hysteresis and eddy currents," Magnetics, IEEE Transactions on, vol.26, no.2, pp.424-429, Mar 1990.

[63] Slemon, G.R. and Liu, X.: "Core losses in permanent magnet motors," Magnetics, IEEE Transactions on , vol.26, no.5, pp.1653-1655, Sep 1990 .

[64] Liu, Z.J., Vourdas, A., and Binns, K.J.: "Magnetic field and eddy current losses in linear and rotating permanent magnet machines with a large number of poles," Science, Measurement and Technology, IEE Proceedings A , vol.138, no.6, pp. 289- 294, Nov 1991.

[65] Rabinovici, R.: "Nonlinear eddy current effects in ferromagnetic materials in the presence of DC magnetic fields," Magnetics, IEEE Transactions on , vol.27, no.4, pp. 3704- 3709, Jul 1991.

[66] Arkadan, A.A., Vyas, R., Vaidya, J.G., and Shah, M.J.: "Effect of toothless stator design and core and stator conductors eddy current losses in permanent magnet generators," Energy Conversion, IEEE Transactions on , vol.7, no.1, pp.231-237, Mar 1992.

[67] Mecrow, B.C., and Jack, A.G.: "The modelling of segmented laminations in three dimensional eddy current calculations," Magnetics, IEEE Transactions on , vol.28, no.2, pp.1122-1125, Mar 1992.

[68] Liu, Z.J., Binns, K.J., and Low, T.S.: "Analysis of eddy current and thermal problems in permanent magnet machines with radial-field topologies," Magnetics, IEEE Transactions on , vol.31, no.3, pp.1912-1915, May 1995.

[69] Bobbio, S., Del Pizzo, A., Marignetti, F., and Pagano, E.: "Eddy current iron losses in axially laminated brushless motors," Electric Power Applications, IEE Proceedings - , vol.142, no.3, pp.183-190, May 1995.

[70] Fang Deng: "Commutation-caused eddy-current losses in permanent-magnet brushless DC motors," Magnetics, IEEE Transactions on , vol.33, no.5, pp.4310-4318, Sep 1997.

[71] Polinder, H.: "On the losses in a high-speed permanent-magnet generator with rectifier with special attention to the effect of damper cylinder", PhD Dissertation, TU Delft, The Netherlands, 1998.

[72] Fang Deng, and Nehl, T.W.: "Analytical modeling of eddy-current losses caused by pulse-width-modulation switching in permanent-magnet brushless direct-current motors," Magnetics, IEEE Transactions on , vol.34, no.5, pp.3728-3736, Sep 1998.

[73] Ruifang Liu, Mi, C.C., and Gao, D.W.: "Modeling of Eddy-Current Loss of Electrical Machines and Transformers Operated by Pulsewidth-Modulated Inverters," Magnetics, IEEE Transactions on , vol.44, no.8, pp.2021-2028, Aug. 2008.

[74] Okitsu, T., Matsuhashi, D., and Muramatsu, K.: "Method for Evaluating the Eddy Current Loss of a Permanent Magnet in a PM Motor Driven by an Inverter Power Supply Using Coupled 2d and 3d Finite Element Analyses," Magnetics, IEEE Transactions on , vol.45, no.10, pp.4574-4577, Oct. 2009.

[75] Polinder, H., and Hoeijmakers, M.J.: "Eddy-current losses in the segmented surface-mounted magnets of a PM machine," Electric Power Applications, IEE Proceedings - , vol.146, no.3, pp.261-266, May 1999.

[76] Kawase, Y., Ota, T., and Fukunaga, H.: "3d eddy current analysis in permanent magnet of interior permanent magnet motors," Magnetics, IEEE Transactions on , vol.36, no.4, pp.1863-1866, Jul 2000.

[77] Atallah, K., Howe, D., Mellor, P.H., and Stone, D.A.: "Rotor loss in permanent-magnet brushless AC machines," Industry Applications, IEEE Transactions on , vol.36, no.6, pp. 1612- 1618, Nov/Dec 2000.

[78] Drubel, O., and Stoll, R.L.: "Comparison between analytical and numerical methods of calculating tooth ripple losses in salient pole synchronous machines," Energy Conversion, IEEE Transactions on , vol.16, no.1, pp.61-67, Mar 2001.

[79] Nerg, J., Niemela, M., Pyrhonen, J., and Partanen, J.: "FEM calculation of rotor losses in a medium speed direct torque controlled PM synchronous motor at different load conditions," Magnetics, IEEE Transactions on , vol.38, no.5, pp. 3255- 3257, Sep 2002.

[80] Chunting Mi, Slemon, G.R., and Bonert, R.: "Modeling of iron losses of permanent-magnet synchronous motors," Industry Applications, IEEE Transactions on , vol.39, no.3, pp. 734-742, May-June 2003.

[81] Bottauscio, O., Pellegrino, G., Guglielmi, P., Chiampi, M., and Vagati, A.: "Rotor loss estimation in permanent magnet machines with concentrated windings," Magnetics, IEEE Transactions on , vol.41, no.10, pp. 3913- 3915, Oct. 2005.

[82] Toda, H., Zhenping Xia, Jiabin Wang, Atallah, K., and Howe, D.: "Rotor eddy-current loss in permanent magnet brushless machines," Magnetics, IEEE Transactions on , vol.40, no.4, pp. 2104- 2106, July 2004.

[83] Zhu, Z.Q., Ng, K., Schofield, N., and Howe, D.: "Improved analytical modelling of rotor eddy current loss in brushless machines equipped with surface-mounted permanent magnets," Electric Power Applications, IEE Proceedings - , vol.151, no.6, pp. 641- 650, 7 Nov. 2004.

[84] Ishak, D., Zhu, Z.Q., and Howe, D.: "Eddy-current loss in the rotor magnets of permanent-magnet brushless machines having a fractional number of slots per pole," Magnetics, IEEE Transactions on , vol.41, no.9, pp. 2462- 2469, Sept. 2005.

[85] Amara, Y., Jiabin Wang, and Howe, D.: "Analytical prediction of eddy-current loss in modular tubular permanent-magnet machines," Energy Conversion, IEEE Transactions on, vol.20, no.4, pp. 761- 770, Dec. 2005.

[86] Polinder, H., Mecrow, B.C., Jack, A.G., Dickinson, P.G., and Mueller, M.A.: "Conventional and TFPM linear generators for direct-drive wave energy conversion," Energy Conversion, IEEE Transactions on , vol.20, no.2, pp. 260- 267, June 2005.

[87] Mecrow, B.C., Jack, A.G., Haylock, J.A., and Coles, J.: "Fault-tolerant permanent magnet machine drives," Electric Power Applications, IEE Proceedings - , vol.143, no.6, pp.437-442, Nov 1996.

[88] Hor, P.J., Zhu, Z.Q., Howe, D., and Rees-Jones, J.: "Eddy current loss in a moving-coil linear tubular permanent magnet brushless motor," Magnetics, IEEE Transactions on , vol35,no.5, pp.3601-3603, Sep 1999.

[89] Atkinson, G.J., Mecrow, B.C., Jack, A.G., Atkinson, D.J., Sangha, P., and Benarous, M.: "The Analysis of Losses in High-Power Fault-Tolerant Machines for Aerospace

Applications," Industry Applications, IEEE Transactions on , vol.42, no.5, pp.1162-1170, Sept.-Oct. 2006.

[90] Klauz, M., and Dorrell, D.G.: "Eddy Current Effects in a Switched Reluctance Motor," Magnetics, IEEE Transactions on , vol.42, no.10, pp.3437-3439, Oct. 2006.

[91] Kawase, Y., Yamaguchi, T., Sano, S., Igata, M., Ida, K., and Yamagiwa, A.: "3d eddy current analysis in a silicon steel sheet of an interior permanent magnet motor," Magnetics, IEEE Transactions on , vol.39, no.3, pp. 1448- 1451, May 2003.

[92] Aoyama, Y., Miyata, K., and Ohashi, K.: "Simulations and experiments on eddy current in Nd-Fe-B magnet," Magnetics, IEEE Transactions on , vol.41, no.10, pp. 3790- 3792, Oct. 2005.

[93] Yamazaki, K., Shina, M., Miwa, M., and Hagiwara, J.: "Investigation of Eddy Current Loss in Divided Nd–Fe–B Sintered Magnets for Synchronous Motors Due to Insulation Resistance and Frequency," Magnetics, IEEE Transactions on , vol.44, no.11, pp.4269-4272, Nov. 2008.

[94] Yamazaki, K., and Abe, A.: "Loss Investigation of Interior Permanent-Magnet Motors Considering Carrier Harmonics and Magnet Eddy Currents," Industry Applications, IEEE Transactions on , vol.45, no.2, pp.659-665, March-april 2009.

[95] Yamazaki, K., Fukushima, Y., and Sato, M.: "Loss Analysis of Permanent-Magnet Motors With Concentrated Windings—Variation of Magnet Eddy-Current Loss Due to Stator and Rotor Shapes," Industry Applications, IEEE Transactions on , vol.45, no.4, pp.1334-1342, July-aug. 2009.

[96] Yamazaki, K.; Ishigami, H.; "Rotor-Shape Optimization of Interior-Permanent-Magnet Motors to Reduce Harmonic Iron Losses," Industrial Electronics, IEEE Transactions on , vol.57, no.1, pp.61-69, Jan. 2010.

[97] Yamazaki, K., Kanou, Y., Fukushima, Yu., Ohki, S., Nezu, A., Ikemi, T., and Mizokami, R.: "Reduction of Magnet Eddy-Current Loss in Interior Permanent-Magnet Motors With Concentrated Windings," Industry Applications, IEEE Transactions on , vol.46, no.6, pp.2434-2441, Nov.-Dec. 2010.

[98] Sergeant, P., and Van den Bossche, A.: "Segmentation of Magnets to Reduce Losses in Permanent-Magnet Synchronous Machines," Magnetics, IEEE Transactions on , vol.44, no.11, pp.4409-4412, Nov. 2008.

[99] Chebak, A., Viarouge, P., and Cros, J.: "Analytical Computation of the Full Load Magnetic Losses in the Soft Magnetic Composite Stator of High-Speed Slotless Permanent Magnet Machines," Magnetics, IEEE Transactions on , vol.45, no.3, pp.952-955, March 2009.

[100] Shah, M.R, and EL-Refaie, A.M.: "Eddy-Current Loss Minimization in Conducting Sleeves of Surface PM Machine Rotors With Fractional-Slot Concentrated Armature Windings by Optimal Axial Segmentation and Copper Cladding," Industry Applications, IEEE Transactions on , vol.45, no.2, pp.720-728, March-april 2009.

[101] Ruoho, S., Santa-Nokki, T., Kolehmainen, J., and Arkkio, A.: "Modeling Magnet Length In 2d Finite-Element Analysis of Electric Machines," Magnetics, IEEE Transactions on , vol.45, no.8, pp.3114-3120, Aug. 2009.

[102] Markovic, M., and Perriard, Y.: "Analytical Solution for Rotor Eddy-Current Losses in a Slotless Permanent-Magnet Motor: The Case of Current Sheet Excitation," Magnetics, IEEE Transactions on , vol.44, no.3, pp.386-393, March 2008.

[103] Markovic, M., and Perriard, Y.: "An Analytical Determination of Eddy-Current Losses in a Configuration with a Rotating Permanent Magnet," Magnetics, IEEE Transactions on, vol.43, no.8, pp.3380-3386, Aug. 2007.

[104] Nakano, M., Kometani, H., and Kawamura, M.: "A study on eddy-current losses in rotors of surface permanent-magnet synchronous machines," Industry Applications, IEEE Transactions on , vol.42, no.2, pp. 429- 435, March-April 2006.

[105] Jiabin Wang, Atallah, K., Chin, R., Arshad, W.M., and Lendenmann, H.: "Rotor Eddy-Current Loss in Permanent-Magnet Brushless AC Machines," Magnetics, IEEE Transactions on , vol.46, no.7, pp.2701-2707, July 2010.

[106] Seok-Hee Han, Jahns, T.M., and Zhu, Z.Q.: "Analysis of Rotor Core Eddy-Current Losses in Interior Permanent-Magnet Synchronous Machines," Industry Applications, IEEE Transactions on , vol.46, no.1, pp.196-205, Jan.-feb. 2010.

[107] Amara, Y., Reghem, P., and Barakat, G.: "Analytical Prediction of Eddy-Current Loss in Armature Windings of Permanent Magnet Brushless AC Machines," Magnetics, IEEE Transactions on , vol.46, no.8, pp.3481-3484, Aug. 2010.

[108] Yamazaki, K., and Fukushima, Y.: "Effect of Eddy-Current Loss Reduction by Magnet Segmentation in Synchronous Motors With Concentrated Windings," Industry Applications, IEEE Transactions on , vol.47, no.2, pp.779-788, March-April 2011.

[109] Pfister, P.D., and Perriard, Y.: "Slotless Permanent-Magnet Machines: General Analytical Magnetic Field Calculation," Magnetics, IEEE Transactions on , vol.47, no.6, pp.1739-1752, June 2011.

[110] Bianchi, N., Bolognani, S., and Fornasiero, E.: "An Overview of Rotor Losses Determination in Three-Phase Fractional-Slot PM Machines," Industry Applications, IEEE Transactions on , vol.46, no.6, pp.2338-2345, Nov.-Dec. 2010.

[111] Binns, K.J. and Lawrenson P.J.; "Analysis and computation of electric and magnetic field problems", Pergamon Press 1963, pp. 7-36, 251-302.

[112] Stoll. R.L. ; "The analysis of eddy currents", Oxford University Press, 1974, pp. 73-91.

[113] Fu, W.N.; Liu, Z.J.; , "Estimation of eddy-current loss in permanent magnets of electric motors using network-field coupled multislice time-stepping finite-element method," Magnetics, IEEE Transactions on , vol.38, no.2, pp.1225-1228, Mar 2002.

[114] Pryor, R. , "Multiphysics modeling using COMSOL: A first principles approach", Chapter 6, pp. 392., Jones and Bartlett Publishers 2011 edition.

[115] Jassal, A; Polinder, H; Ferreira, J.A., "Literature survey of eddy current loss analysis in rotating electrical machines", Electric Power Applications, IET, vol.6,no.9.pp. 743-752, Nov. 2012.

4. Analytical Modeling

This chapter presents the analytical model used for calculation of eddy current losses in the solid conductive parts of the PMDD machines. Analytical models are very useful for quick comparative studies on various topologies. The accuracy of such models is rather limited but the process of developing such models gives great insight into physics of the problem. Besides, this chapter also sets up ground for further research in terms of quantifying effects of various assumptions.

4.1. Analytical Models

Analytical models are not new in the field of eddy current loss analysis. A lot of research on developments of analytical models specifically for eddy current loss calculation was done in the 1960-70 [2] and [4]. Readers interested in knowing more about historical development of the analytical methods can refer to [5] and [7]. The strengths of analytical methods are speed of solution, insight into physics of the problem and their generic nature. The limitations of these methods are the assumptions and resulting inaccuracies. Another drawback is long time taken to formulate the model. However, once formulated it takes very short time for solution.

From this thesis' point of view it may be mentioned that this research is not entirely based on analytical modeling but utilizes FE method for calculation of eddy current losses as well. This is because electrical machines have a complex geometry and the analytical methods are limited in capturing the geometrical effects such as slotting of stator and magnets. As mentioned in chapter 3 (see fig. 3.4), the analytical methods still remain very popular because of the insight into problems they offer. This means that the problem features can be easily linked to the design outputs whereby quick comparative studies can be easily performed. Moreover the analytical models don't require very specific and expensive software to perform FE calculations. This is the motivation for doing analytical modeling for this research as well.

4.2. Modeling Approach for PMDD machines

The field of large PMDD machines is rather new and very interesting from research point of view. When starting with such a detailed analysis on PMDD machines, there are

many options and methodologies which can be applied. This section gives a brief motivation behind the choices made for analysis.

Analytical or Finite Element Method?

This is a prime choice which has to be made but for this research both approaches were used. The reason is that both the methods have their own advantages and limitations. The idea is to use analytical models to select the promising topologies and then use FE models to calculate eddy current losses more accurately. In the process, effects of various assumptions made in analytical models can be brought out.

2d or 3d analysis ?

The choice between 2d or 3d is rather easy to make in case of large PMDD machines. 2d analysis was chosen in this case because the axial length of such machines is much larger than the air gap whereby 3d effects can be neglected.

Polar or Cartesian/Rectangular coordinate system ?

For this analysis, Cartesian coordinates were chosen because the radius of large PMDD machines is very large whereby a small section of the machine can be treated as linear. This also makes the mathematics simpler. Later it has been shown that curvature doesn't have substantial effect on the eddy current loss calculation.

Scalar or Vector magnetic Potential ?

The choice between these formulations was made based on some advantages of the use of vector magnetic potential. The flux lines can be directly visualized as lines of constant magnetic vector potential. Many useful quantities such as flux density, electric field, induced current density and other useful quantities can be directly computed from vector magnetic potential. Therefore, magnetic vector potential was chosen. It may be mentioned that either choice will anyways lead to good results.

Linear or non-linear iron ?

Linear formulation for rotor and stator parts was chosen to avoid mathematical complications. Later on it is shown that the effect of material non-linearity is not that prominent on the calculation of eddy current losses. Another reason for such a choice was that there are two fields active in the machine. One is the field due to armature current and the other is the field of PMs. The resultant field is the sum of the two fields if the materials are linear.

4.3. Assumptions

It is not easy to include all the geometrical details in an analytical model. Some simplifications are needed in order to follow the analytical procedure as mentioned in [1],[3] and [4]-[6]. The difficulty is to form and solve the partial differential equations

(valid Maxwell's Equations) for each region of the machine including its geometry effects. The assumptions used are:

1. The stator is slot less, placed at effective air gap from the rotor surface and incurs no losses due to eddy currents.
2. Windings are replaced by an equivalent current sheet travelling along the stator bore surface and varying in time.
3. The relative permeability of stator iron is infinite.
4. The relative permeability of rotor back iron is realistic.
5. All materials are linear and isotropic.
6. The magnets are adjacent to each other so that they occupy the whole surface of rotor and have electrical conductivity so that eddy currents can be induced.
7. 2d modeling in Cartesian coordinates is selected with the assumption that everything remains constant in the z-direction.
8. The end effects are neglected.

Fig.4.1 shows a real PM machine main dimensions and Fig.4.2 shows the simplified model

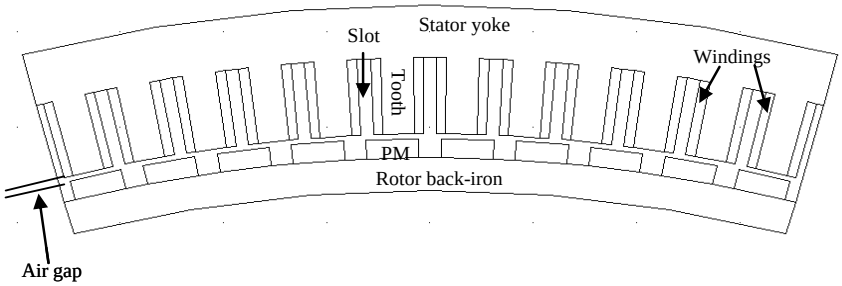

Fig.4.1: Actual geometry of a PM machine

The simplified analytical model of machine consists of four layers and some boundaries.

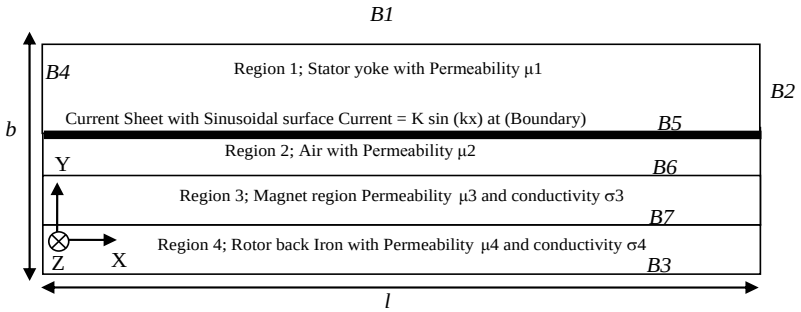

Fig.4.2: Simplified geometry for analytical model

Here B1 – B7 are the boundaries where boundary conditions will be applied.
On B1 and B3, magnetic insulation condition is applied.

On all other boundaries, flux continuity and equivalence of tangential component of magnetic field intensity (H-field) boundary condition is applied. These boundary conditions are explained further in section 4.5.

4.4. Derivation of Partial Differential Equation (PDE)

The primary aim is to compute losses in the back-iron and the magnet region (regions 3 and 4). Starting from Maxwell's equations for quasistatic fields:

$$\nabla \times \vec{H} = \vec{J} + \vec{J}_{ext} \tag{4-1}$$

$\vec{H}$ is the magnetic field strength (A/m);

$\vec{J}$ and $\vec{J}_{ext}$ are induced and external current density respectively (A/m^2)

$$\nabla \times \vec{E} + \frac{\partial \vec{B}}{\partial t} = 0 \tag{4-2}$$

$\vec{E}$ is the electric field (V/m); $\vec{B}$ is the magnetic flux density (T)

$$\nabla \cdot \vec{J}_{ext} = 0 \tag{4-3}$$

$$\nabla \cdot \vec{B} = 0 \tag{4-4}$$

The constitutive relations for the material (assumed isotropic) are:

$$\vec{J} = \sigma \vec{E} \tag{4-5}$$

$$\vec{B} = \mu \vec{H} + \vec{B}_{rem} \tag{4-6}$$

Here σ is the electrical conductivity; μ is the magnetic permeability

$\vec{B}_{rem}$ is the remanent flux density of the magnet.

$\vec{H}$ is the magnetic field strength.

From (4-6), we can write for $\vec{H}$ as:

$$\vec{H} = \frac{1}{\mu}(\vec{B} - \vec{B}_{rem}) \tag{4-7}$$

Substituting this value of $\vec{H}$ in (4-1) we get

$$\nabla \times \left[\frac{1}{\mu} (\vec{B} - \vec{B}_{rem}) \right] = \vec{J} + \vec{J}_{ext}$$
$$\nabla \times \vec{B} = \mu(\vec{J} + \vec{J}_{ext}) + \nabla \times \vec{B}_{rem} \quad (4\text{-}8)$$

Since the permeability is different for different materials, this equation holds true for each region having a constant permeability and not for all regions in general.

From vector calculus we know that $\nabla \cdot (\nabla \times \vec{F}) = 0$ for any vector $\vec{F}$. Also from (4-4) we see that $\nabla \cdot \vec{B} = 0$ and it may be written as:

$$\vec{B} = \nabla \times \vec{A} \quad (4\text{-}9)$$

Here $\vec{A}$ is called the vector potential. Substituting for $\vec{B}$ from (4-9) in (4-8), we get

$$\nabla \times (\nabla \times \vec{A}) = \mu(\vec{J} + \vec{J}_{ext}) + \nabla \times \vec{B}_{rem}$$
and (4-10)
$$\nabla \times (\nabla \times \vec{A}) = \nabla(\nabla \cdot \vec{A}) - \nabla^2 \vec{A}$$

Further, using $\nabla \cdot \vec{A} = 0$ for a Gaussian surface, the left hand side of (4-10) can be written as:

$$-\nabla^2 \vec{A} = \mu \vec{J} + \mu \vec{J}_{ext} + \nabla \times \vec{B}_{rem} \quad (4\text{-}11)$$

Using constitutive relations of (4-5) and (4-6) we can write

$$\vec{J} = \sigma \vec{E}$$
$$\vec{E} = -\frac{\partial \vec{A}}{\partial t} \text{ or } \vec{J} = -\sigma \frac{\partial \vec{A}}{\partial t} \quad (4\text{-}12)$$

Substituting for $\vec{J}$ in (4-11) and re-arranging terms we arrive at the following equation:

$$-\nabla^2 \vec{A} + \mu\sigma \frac{\partial \vec{A}}{\partial t} = \mu \vec{J}_{ext} + \nabla \times \vec{B}_{rem} \quad (4\text{-}13)$$

This equation is Poisson's equation and will be the main equation to be used in evaluating eddy current losses. This equation represents a general case and holds true for vectors in 3 dimensions. However, we made a few assumptions to simplify the field calculation and using the assumptions, we can reason:

a) The stator currents flow only in z direction (perpendicular to plane of reference)
b) $\vec{B}_{rem}$ has only y component and its curl is in z direction only.
c) Only z component of vector potential i.e. A_z is present. We assume 2d geometry and everything is constant in z direction thus A_z depends only on x and y space coordinates (because nothing changes in z direction)

We can rewrite (4-13) in its component form (using our assumptions) as below:

$$-\left(\frac{\partial^2 A_z}{\partial x^2}+\frac{\partial^2 A_z}{\partial y^2}\right)+\mu\sigma\frac{\partial A_z}{\partial t}=\mu J_{zext}+\frac{\partial B_{y,rem}}{\partial x}\hat{z} \tag{4-14}$$

$\vec{J}_{zext}$ is the z component of the external current density, $B_{y,rem}$ is the y component of remanent flux density such that its curl points in z direction. Here $\hat{x},\hat{y},\hat{z}$ are unit vectors for x, y, z coordinates. We have assumed that nothing varies in z direction and that $\vec{B}_{rem}$ has only a y component. Therefore when we take curl of $\vec{B}_{rem}$ there is a variation along x direction signifying the change of polarity of magnet (from North to South and vice-versa) and the direction of curl is along z axis.

Further, there are two magnetic fields interacting with each other. One is the field produced by the permanent magnets and the other is the field produced by the current sheet (representing effect of a winding). The approach is to calculate corresponding vector magnetic potential (for current sheet and permanent magnets) and add together to get the net result. The magnets are considered inactive (but conductive) for calculating the eddy current losses.

The other quantities can be derived further from the vector magnetic potential. For each region of the machine the Poisson's equation (4-13) can be simplified depending on which excitations are present in a particular region. We define the next steps for the case only current sheet is present and magnets are "inactive". However due to current sheet, there is an eddy current loss in the magnets owing to their conductivity. Equations for each region of Fig.4.2 can be written as:

Stator and air gap: $$-\nabla^2 A_z=0 \tag{4-15}$$

Magnets and rotor back iron: $$\nabla^2 A_z=\mu\sigma\frac{\partial A_z}{\partial t} \tag{4-16}$$

4.5. Boundary Conditions

There are two types of boundary conditions applied for modeling. The arrangement of the machine geometry for application of analytical model results in the geometry as shown in fig. 4.2.

4.5.1 Boundary Condition 1

The first boundary condition is implied by Ampere's Law and states that the tangential component of the magnetic field intensity on one side of the boundary is equal to that of the other side with a surface current density added to it. Mathematically, this translates to:

$$\hat{n} \times (\vec{H}_1 - \vec{H}_2) = \vec{K} \tag{4-17}$$

$\vec{H}_1$ is the magnetic field intensity in region 1 on one side of boundary

$\vec{H}_2$ is the magnetic field intensity in region 2 on other side of boundary

$\vec{K}$ is the surface current density at the boundary.

$\hat{n}$ is the unit normal vector to the boundary pointing outwards for each region.

In our coordinate system normal translates to *y* component and tangential translates to x component of the quantity.

Equation (4-17) can be written as $\vec{H}_{x1} - \vec{H}_{x2} = \vec{K}$ and using $\vec{B} = \mu\vec{H}$ we can write:

$$\frac{1}{\mu_1} B_{x1} - \frac{1}{\mu_2} B_{x2} = K \tag{4-18}$$

Using $\vec{B} = \nabla \times \vec{A}$, we can write

$$\frac{1}{\mu_1} \frac{\partial A_{z1}}{\partial y} - \frac{1}{\mu_2} \frac{\partial A_{z2}}{\partial y} = K \tag{4-19}$$

Here, A_{z1} is the z component of magnetic vector potential in region 1,

A_{z2} is the z component of magnetic vector potential in region 2.

4.5.2 Boundary Condition 2

The other boundary condition is implied by conservation of magnetic flux. The boundary condition states that the normal component of the flux density on one side of boundary interface is equal to that on the other side. Mathematically,

$$\hat{n} \cdot (\vec{B}_1 - \vec{B}_2) = 0 \tag{4-20}$$

This means that $B_{y1} = B_{y2}$ .Using $\vec{B} = \nabla \times \vec{A}$, we can write for B_{y1} and B_{y2}

$$\frac{\partial A_{z1}}{\partial x} = \frac{\partial A_{z2}}{\partial x} \tag{4-21}$$

4.6. General Solution of the Partial Differential Equation (PDE)

The stator and air gap have been assumed non-conductive whereby the equation to be solved is Laplace's equation. Due to eddy currents induced in the conductive rotor back-iron and magnets, the equation to be solved gets modified to Poisson's equation.

4.6.1 The General Solution for Laplace's equation

In Cartesian coordinates Laplace's equation can be written as

$$-\left(\frac{\partial^2 A_z}{\partial x^2} + \frac{\partial^2 A_z}{\partial y^2} \right) = 0 \tag{4-22}$$

Assuming the solution to be of the form $A_z(x, y) = P(x)Q(y)$, where P is a function of x only and Q is a function of y only. For simplicity, we can say

$$A_z = PQ \tag{4-23}$$

Calculating derivatives and putting in (4-22), we get

$$\left(Q\frac{\partial^2 P}{\partial x^2} + P\frac{\partial^2 Q}{\partial y^2} \right) = 0 \tag{4-24}$$

Dividing both sides by PQ , we can write

$$\left(\frac{1}{P}\frac{\partial^2 P}{\partial x^2}+\frac{1}{Q}\frac{\partial^2 Q}{\partial y^2}\right)=0$$

or (4-25)

$$\frac{1}{P}\frac{\partial^2 P}{\partial x^2}=-\frac{1}{Q}\frac{\partial^2 Q}{\partial y^2}=\alpha$$

The constant α is the separation constant as we have obtained P as a function of x only and Q as a function of y only. Partial derivatives can be treated as actual derivatives and we get two Ordinary Differential Equations (ODEs) which can be solved as shown below.

We will solve for P only as the solution for Q would be similar. Before actual solution we will consider the three cases that arise for different values of α.

Case 1: If $\alpha = 0$

The Laplace's equation becomes

$$\frac{d^2 P}{dx^2}=0 \tag{4-26}$$

Thus $P = Ax + B$ (on integrating twice)

Case 2: If $\alpha > 0$

Let $P = e^{rx}$ then putting the values of P and its double derivative in

$$\frac{1}{e^{rx}}r^2 e^{rx}=\alpha \tag{4-27}$$

$$\Rightarrow r=\pm\sqrt{\alpha}$$

If $\sqrt{\alpha}$ and $-\sqrt{\alpha}$ are both solutions, then their sum is also a solution. This can be written as:

$$P = m'e^{\sqrt{\alpha}x}+n'e^{-\sqrt{\alpha}x} \tag{4-28}$$

Similarly, we can write for Q,

$$Q = g'e^{\sqrt{-\alpha}y}+h'e^{-\sqrt{-\alpha}y}=g'e^{j\sqrt{\alpha}y}+h'e^{-j\sqrt{\alpha}y} \tag{4-29}$$

Here m', n', g', h' are arbitrary constants.

Putting $\alpha=k^2$ where k is a real number, we can re-write (4-28) and (4-29) as:

$$P = m'e^{kx} + n'e^{-kx} \tag{4-30}$$

$$Q = g'e^{jky} + h'e^{-jky} \tag{4-31}$$

Using the identities

$$\begin{aligned} e^{\theta} &= \cosh\theta + \sinh\theta \\ e^{-\theta} &= \cosh\theta - \sinh\theta \\ e^{j\theta} &= \cos\theta + j\sin\theta \\ e^{-j\theta} &= \cos\theta - j\sin\theta \end{aligned} \tag{4-32}$$

We can also write the solution in hyperbolic sine and cosine terms as

$$P = m\cosh kx + n\sinh kx \tag{4-33}$$

$$Q = g\cos ky + h\sin ky \tag{4-34}$$

Here m, n, g and h are arbitrary constants.

From (4-23) , (4-30) and (4-31) we get the complete solution as:

$$A_z(x,y) = (me^{jkx} + ne^{-jkx})(ge^{ky} + he^{-ky}) \tag{4-35}$$

Case 3: If $\alpha < 0$

In this case, we can write $\alpha = -k^2$. We will get a similar result like (4-35) but P will contain the real exponent terms whereas Q will contain imaginary exponent terms. The complete solution can then be written as:

$$A_z(x,y) = (me^{kx} + ne^{-kx})(ge^{jky} + he^{-jky}) \tag{4-36}$$

We are using a periodic boundary condition on left and right side of our domain i.e. periodicity along x axis, (see fig 4.2) we proceed with the solution where P is having cosine and sine terms. This selection is made owing to known periodicity of sine and cosine terms.

Therefore we choose $\alpha < 0$ and equation (4-36) as the general solution

4.6.2 General Solution of Poisson's Equation and Treatment of Time

Since the Poisson's equation we formulated has time dependent terms, we will first show how periodic time variation is treated in analytical models. Therefore to start with, A_z is a function of space in 2 dimensions (x, y) and time t. Since the field is spatially dependent on x and y coordinates and in addition on time t, we can write the solution of A_z to consist of a part 'T' dependent on time t and a part 'S' dependent on space (x,y) only [4].

$$A_z(x,y,t) = S(x,y).T(t) \tag{4-37}$$

Substituting this result in (4-16) leads to:

$$\begin{aligned} &\nabla^2(ST) = \sigma\mu\frac{\partial}{\partial t}(ST) \\ &\Rightarrow T(\nabla^2 S) = \sigma\mu S\frac{\partial T}{\partial t} \\ &\Rightarrow \frac{\nabla^2 S}{S} = \frac{\sigma\mu}{T}\frac{\partial T}{\partial t} = k^2 \end{aligned} \tag{4-38}$$

Here, k^2 is constant of separation. It must be independent of variations in both time and space. Thus from (4-37), we can separate the time dependent part as:

$$\begin{aligned} &\frac{1}{T}\frac{\partial T}{\partial t} = \frac{k^2}{\sigma\mu} \\ &\Rightarrow \frac{\partial T}{\partial t} - \frac{k^2}{\sigma\mu}T = 0 \\ &T = Ke^{\frac{k^2}{\sigma\mu}t} \end{aligned} \tag{4-39}$$

Here, K is a constant depending upon a particular field.
Similarly, for the space dependent part, from (4-38), we can write

$$\nabla^2 S - k^2 S = 0 \tag{4-40}$$

This equation is known as Helmholtz's equation. Helmholtz's equation needs a more rigorous solution compared to Laplace's equation. However, there is a possible simplification for the case when:

- All field quantities in steady state have amplitudes which are constant and have the time variations which are at same frequency as the excitation
- The media under observation is linear.

If we call the frequency of excitation as ω, then (4-16) can be written as:

$$A_z(x,y,t) = S(x,y)e^{j\omega t} \tag{4-41}$$

Now if we substitute (4-41) into (4-16) we can write:

$$\begin{aligned} & e^{j\omega t}\nabla^2 S = j\omega\sigma\mu S e^{j\omega t} \\ & \Rightarrow \nabla^2 S = j\omega\sigma\mu S \end{aligned} \tag{4-42}$$

Thus the explicit appearance of time can be eliminated and the solution reduces to solution of (4-42) where if:

$$\beta^2 = \omega\sigma\mu \tag{4-43}$$

Helmholtz equation (4-40) can be solved by separation of variables. Expanding in Cartesian coordinates, we can write:

$$\frac{\partial^2 S}{\partial x^2} + \frac{\partial^2 S}{\partial y^2} - j\beta^2 S = 0 \tag{4-44}$$

Then we can write the solution as two parts, $P(x)$ dependent on x only and $Q(y)$ dependent on y only.

$$\begin{aligned} & S = P(x)Q(y) \\ & \therefore \frac{1}{P}\frac{\partial^2 P}{\partial x^2} + \frac{1}{Q}\frac{\partial^2 Q}{\partial y^2} = j\beta^2 \end{aligned} \tag{4-45}$$

Since the right hand side of (4-45) is a constant, we can say that each of the terms on left hand side of (4-45) is a constant as well. Now, assuming

$$\frac{1}{P}\frac{\partial^2 P}{\partial x^2} = -\alpha^2 \tag{4-46}$$

We know that solution to such an equation is:

$$P = m\sin\alpha x + n\cos\alpha x$$

Further, we can write from

$$\frac{1}{Q}\frac{\partial^2 Q}{\partial y^2} = j\beta^2 + \alpha^2 \tag{4-47}$$

The solution to this equation is:

$$Q = g\sinh\left(\sqrt{\alpha^2 + j\beta^2}\right)y + h\cosh\left(\sqrt{\alpha^2 + j\beta^2}\right)y \tag{4-48}$$

Therefore the general solution can be written as:

$$A_z = (m\sin\alpha x + n\cos\alpha x).(ge^{\left(\sqrt{\alpha^2+j\beta^2}\right)y} + he^{-\left(\sqrt{\alpha^2+j\beta^2}\right)y}) \tag{4-49}$$

Here $\beta = \sqrt{\omega\sigma\mu}$ and α is a constant defining variation along x-axis
m,n, g and $h$are constants to be found by using boundary conditions
σ is the conductivity; μ is the permeability and ω is the electrical frequency

This solution is basically a snapshot of the entire picture because there is no mention of time. If we want to know the solution at any time instant t then we should multiply the solution with $e^{j\omega t}$.

4.7. Field Due to Stator Currents Only

As mentioned before, there are two fields present in a PMDD machine. In this section we deal with the field existing due to stator currents only.

4.7.1 Excitation for the field

The machine in question is a concentrated winding machine as shown in fig. 4.1. The mmf produced by concentrated windings comprises of a number of harmonics and is far from sinusoidal. However, the problem setup and general solution we have developed consists of sine and cosine functions or their harmonic form. Therefore, the stator current density has to be expressed a sum of sine and/or cosine functions i.e. as a Fourier series. Thus, in order to apply any arbitrary excitation, we have to decompose the excitation into sine and cosine components. The excitation of the model is deduced using the following steps:

a) First of all, the surface current density waveform is determined as shown in fig. 4.3. The tall rectangular blocks represent the magnitude of current.
b) The amplitudes for various harmonics are deduced from Fourier decomposition of this waveform for one phase. Then the net effect of 3-phases is taken into account by summing the individual phase waveforms.
c) Each of the resultant amplitudes is applied separately as excitation of the current sheet and losses are evaluated.
d) The total losses are then sum of losses computed by individual harmonic excitation.

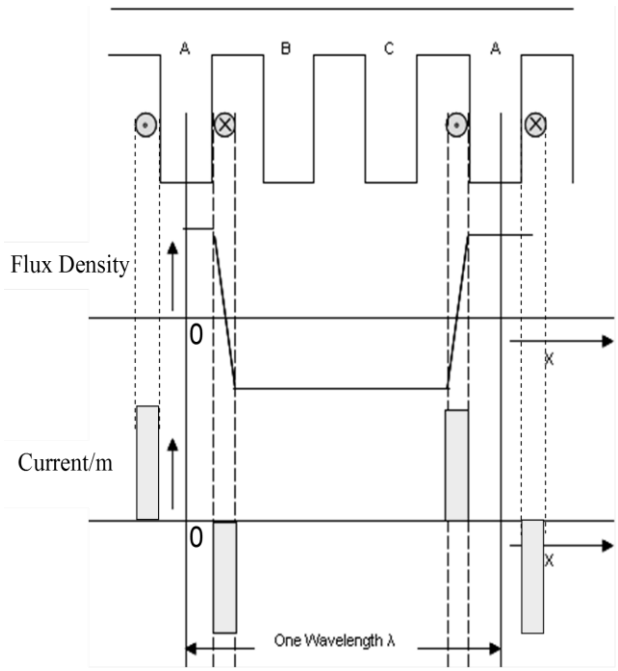

Fig.4.3: Flux density waveform and current/m length for a concentrated winding machine

Each harmonic found after Fourier decomposition of phase A alone, is also present in other phases but displaced and forms a complete set of 3-phase sinusoidal system. Thus for each phase, the surface current density can be written as a sum of harmonics. We can write an expression of the form:

$$K_A = \sum_{n=1}^{\infty} \hat{K}_n \cos(nkx)\cos(\omega t)$$

$$K_B = \sum_{n=1}^{\infty} \hat{K}_n \cos(nkx - \frac{2\pi}{3})\cos(\omega t - \frac{2\pi}{3}) \quad (4\text{-}50)$$

$$K_c = \sum_{n=1}^{\infty} \hat{K}_n \cos(nkx - \frac{4\pi}{3})\cos(\omega t - \frac{4\pi}{3})$$

Here,

K_A, K_B, K_C are surface current densities of phase A,B and C respectively (A/m)

$\hat{K}_n$ is amplitude of nth harmonic's surface current density (A/m)

ω is the electrical frequency(rad/s); t is time (s)
k is a constant for space distribution ; x is a space coordinate

The net effect is summation of the three separate phase contributions. It can be easily verified that after summation, the current sheet for nth harmonic can be written as:

$$K_n = \frac{3}{2}\hat{K}_n \cos(nkx - \omega t) \qquad \text{for } n = 1,4,7,\ldots \quad (4\text{-}51)$$

$$K_n = \frac{3}{2}\hat{K}_n \cos(nkx + \omega t) \qquad \text{for } n = 2,5,8,\ldots \quad (4\text{-}52)$$

$$K_n = 0 \qquad \text{for } n = 3,6,9,\ldots \quad (4\text{-}53)$$

This represents the actual excitation in the form of a travelling wave which is both function of space and time. Fig.4.4 shows an example of decomposition of surface current density. Each harmonic forms an excitation for the analytical model.

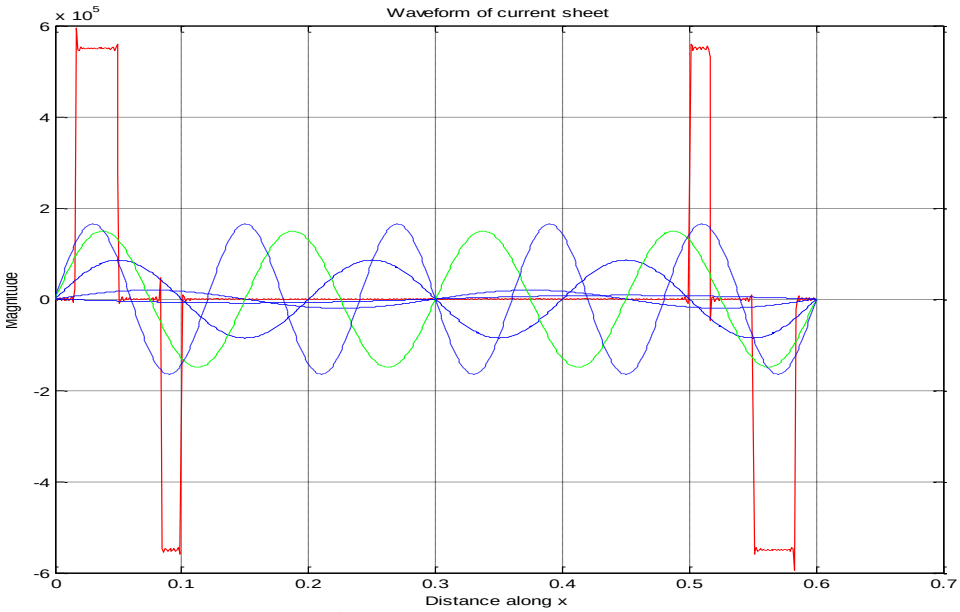

Fig.4.4: Surface current density (A/m) decomposition for 9-8 combination concentrated winding machine

4.7.2 Effect of motion

The excitation for the magnetic field in the model is a travelling wave of current density. The rotor of a machine moves at constant speed but each harmonic field (produced by stator mmf decomposition) except the torque producing harmonic, rotates at a different speed w.r.t rotor. Furthermore, the direction of rotation is also different for different space harmonics.

This relative difference in speed of harmonics and rotor is responsible for inducing eddy current losses in the solid conductive parts of the machine. The effect of motion results in a modification of the frequency induced by a harmonic. The speed of n^{th} harmonic can be calculated as:

$$v_n = \frac{\lambda_1 f}{n} \tag{4-54}$$

v_n is travelling velocity of n^{th} harmonic.

λ_1 is fundamental wavelength.

f is the fundamental electrical frequency.

The relative speed of the harmonic w.r.t. the moving part can be calculated as

$$v_h = v_n \pm v_r \tag{4-55}$$

Here,

v_h is the relative speed of harmonic

v_r is the speed of rotor

$\pm$ is a + if the harmonic moves in opposite direction to the rotor and – if the harmonic moves in same direction as rotor.

The equivalent change of frequency can be calculated from (4-54) by replacing v_n with v_h and calculating the frequency as:

$$f_h = \frac{nv_h}{\lambda_1} \text{ and } \omega_h = 2\pi f_h \tag{4-56}$$

Consequently, the excitation in (4-51) and (4-52) can now be expressed as

$$\begin{aligned} K_n &= \frac{3}{2}\hat{K}_n(\cos nkx \cos \omega_h t \pm \sin nkx \sin \omega_h t) \\ K_n &= \frac{3\hat{K}_n}{4}\left[(\cos nkx - j\sin nkx).e^{j\omega_h t} \pm (\cos nkx + j\sin nkx).e^{-j\omega_h t}\right] \end{aligned} \tag{4-57}$$

It must be noted that the frequency ω in (4-57) has been modified to ω_h .

Equation (4-57) also indicates that there is a space dependent part and a time dependent part defining *K*. Since we know that variation in time is sinusoidal, we can solve for space part alone. Further, (4-57) shows that there are two excitations possible, one with $+\omega$ i.e. $(\cos kx - j\sin kx)$ and another with negative $-\omega$ i.e. $(\cos kx + j\sin kx)$. Therefore if we apply either of these excitations actual losses will then be twice the losses calculated due to such an excitation.

4.7.3 Some Important Observations – Current Sheet Excitation

The reference figure for general solution is fig. 4.2 which has been reproduced here for ease of reference

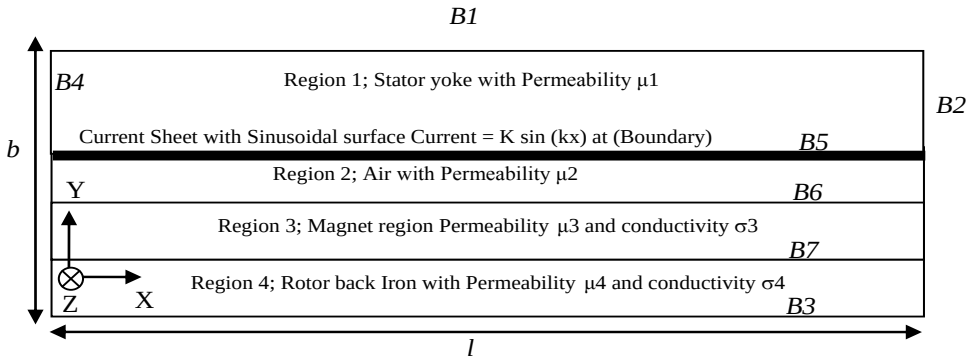

Fig.4.5: Simplified geometry for analytical model

a) The solution for each harmonic in the regions without conductivity and eddy current losses is given by (4-36) which is reproduced here.

$$A_z(x,y) = (me^{kx} + ne^{-kx})(ge^{jky} + he^{-jky}) \tag{4-36}$$

b) The general solution for regions with conductivity and eddy current losses has been derived in (4-49) which is reproduced here.

$$A_z = (m\sin\alpha x + n\cos\alpha x).(ge^{\left(\sqrt{\alpha^2+j\beta^2}\right)y} + he^{-\left(\sqrt{\alpha^2+j\beta^2}\right)y}) \tag{4-49}$$

c) Since we can choose the origin of excitation in fig. 4.4 for excitation, we can get either an even or an odd function whereby we know that variation along x-axis is either a sine or a cosine. Therefore, knowing the excitation, we get rid of either m or n of the general solution.

d) The excitation for the model is taken into account in the boundary condition 1, applied on boundary *B5*.

Afterwards we can apply boundary conditions to all other boundaries and solve for find particular solution in this configuration. The details of solution are presented in the appendix in form of a sample problem.

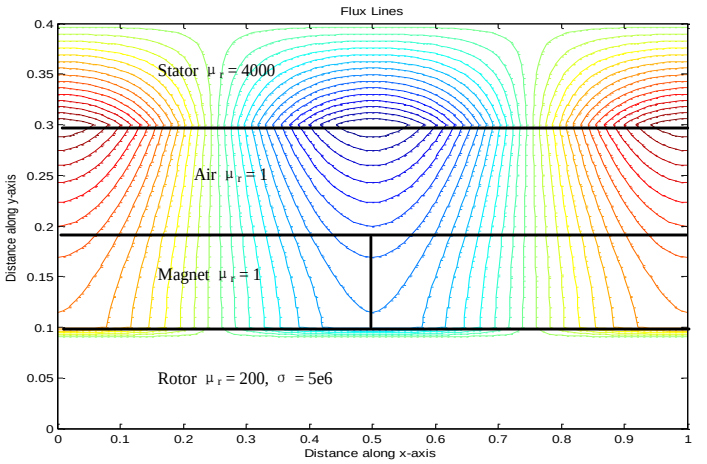

a)

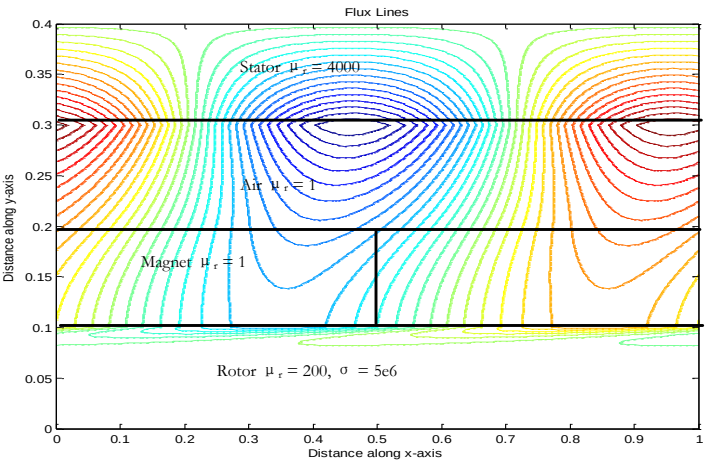

b)

Fig.4.6: Effect of motion (arbitrary model) a) Flux lines without motion b) Flux lines with motion

4.8. Field Due to Magnets Only

In this section, the field due to presence of PM alone has been presented. The analytical calculation is based on the assumptions resulting in the geometry of fig. 4.7 shown below.

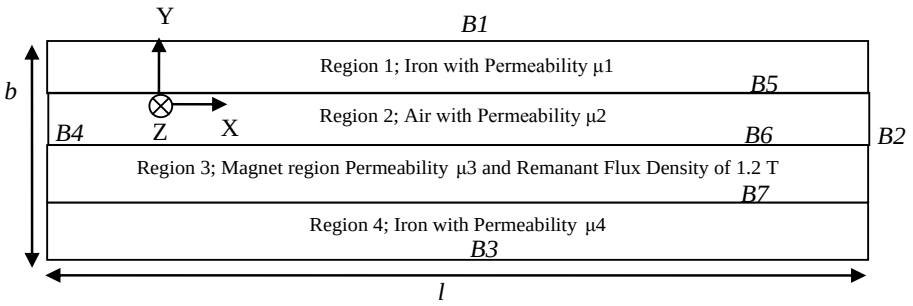

Fig.4.7: Geometry for field due to magnets only

Region 1 is iron having permeability $\mu 1$Region 2 is air, having permeability $\mu 2$
Region 3 is iron, having permeability $\mu 3$ and conductivity $\sigma 3$
Region 4 is iron, having permeability $\mu 4$ and conductivity $\sigma 4$
Subscripts 1, 2, 3 and 4 define the region where the quantity is present.

4.8.1 Excitation for the field of PMs

The Flux density due to the magnets (in region 3) is defined as a square wave. The expression for this wave is represented by a summation of Fourier series expansion. The summation of harmonics leads to a flux density waveform as shown in fig. 4.8.

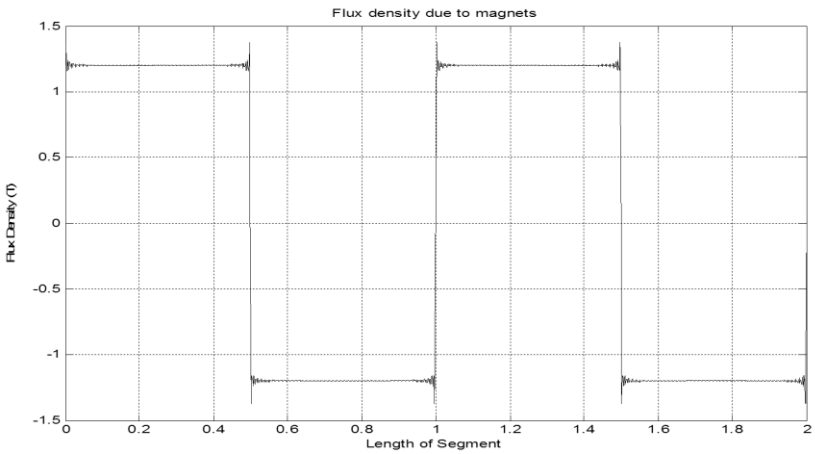

Fig.4.8: Excitation for field due to magnets only

$$\sum_{n=1,3,5...}^{\infty} \frac{4B_r}{n\pi} \sin(nkx) \tag{4-58}$$

Here, $k = \frac{2\pi}{l}$

4.8.2 Some Important Observations – Field of PM

a) Since the waveform is an odd function, a sum of sine components only exists. Therefore, we know that variation along x-axis is sinusoidal.
b) There is no excitation source in regions 1,2 and 4. Therefore, we have to solve Laplace equation in these regions.
c) In region 3 we have a flux density of 1.2 T as shown in fig. 4.8. This is given as a sum of harmonics. In this region we solve the equation

$$-\nabla^2 \vec{A} = \nabla \times \vec{B}_{rem} \tag{4-59}$$

d) For regions 1,2 and 4 the general solution will be of the form:

$$\sum_{n=1,3,5,\ldots}^{\infty} \sin(nkx)(g_m e^{jnky} + h_m e^{-jnky}) \tag{4-60}$$

$k = 2\pi$
m = 1,2,3 or 4 denote the region of interest

e) For region 3, the general solution is obtained by adding a particular integral of to the general solution of Laplace equation as explained in [4]. This particular integral can be easily found out to be

$$-\frac{(2n\pi)4B_r}{n^3k^2\pi}\sin(nkx) \tag{4-61}$$

Thus the general solution of (4-29) in region 3 is given by:

$$\sum_{n=1,3,5,\ldots}^{\infty} \sin(nkx)\left[g_m e^{jnky} + h_m e^{-jnky} - \frac{(2n\pi)4B_r}{n^3k^2\pi} \right] \tag{4-62}$$

$k = 2\pi$
m = 1,2,3 or 4 denote the region of interest

After that we can apply boundary conditions to find particular solution in this configuration. The flux lines are shown in fig. 4.9.

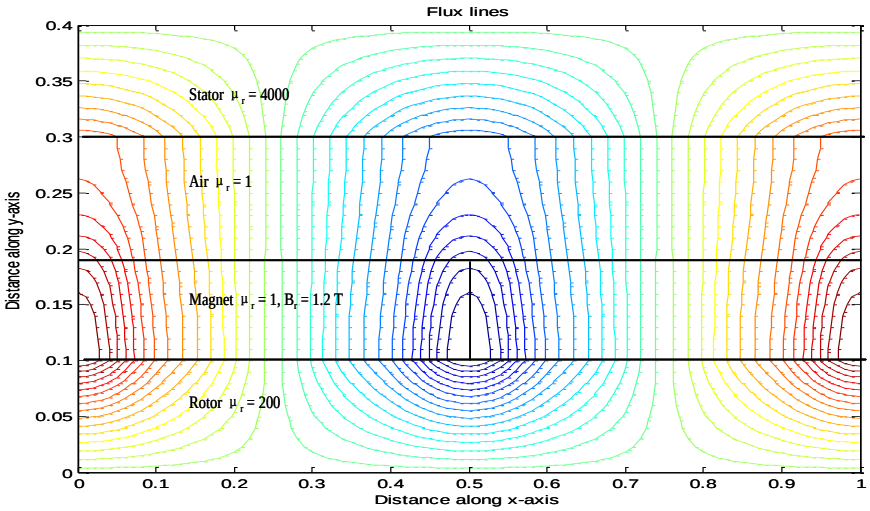

Fig.4.9: Flux lines due to permanent magnets only

4.9. The Combined Magnetic Field

The combined magnetic field is found by superposition i.e. the summation of the field produced by the stator currents and the field produced by the permanent magnets. This summation is valid because the materials have been assumed to be linear. As shown in fig. 4.10, the effect of high frequency stator currents can be seen as some skin effect in the back-iron region belonging to the rotor of the machine.

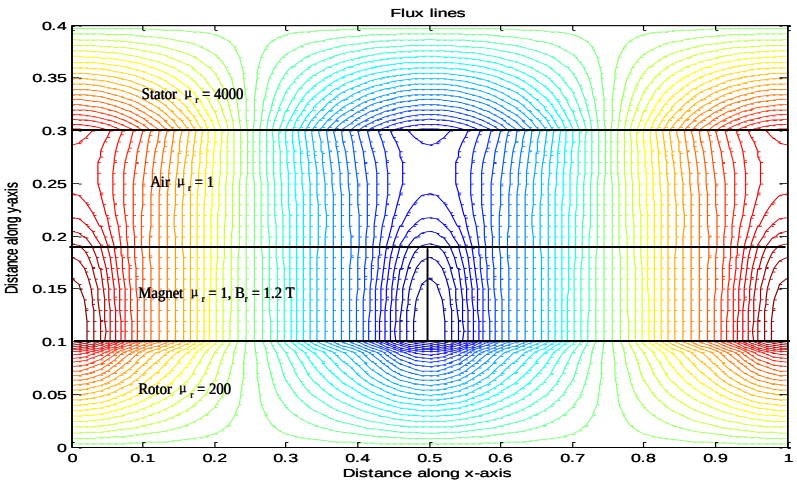

Fig.4.10: Flux lines due to both current sheet and magnets

4.10. Derived Quantities from A_z

There are many quantities which can be easily derived from magnetic vector potential. From this research's point of view, the most important derived quantities are:

1. Magnetic flux density B: Serves as a visual aid to analyze the results.
2. Induced current density J: The induced current density is used to compute the eddy current losses in solid conductive parts of the machine.

4.10.1 Magnetic Flux Density from A_z

The magnetic flux density can be derived by taking curl of Az. Basically we use (4-9) and since $\vec{A}$ has only a z-component, $\vec{B}$ can have only x and y components. Therefore, using rectangular coordinates, we can write (4-9) as:

$$\vec{B} = \frac{\partial A_z}{\partial y}\hat{x} - \frac{\partial A_z}{\partial x}\hat{y} \tag{4-63}$$

The flux densities of the PM and stator field are shown in fig. 4.11 and 4.12 respectively.

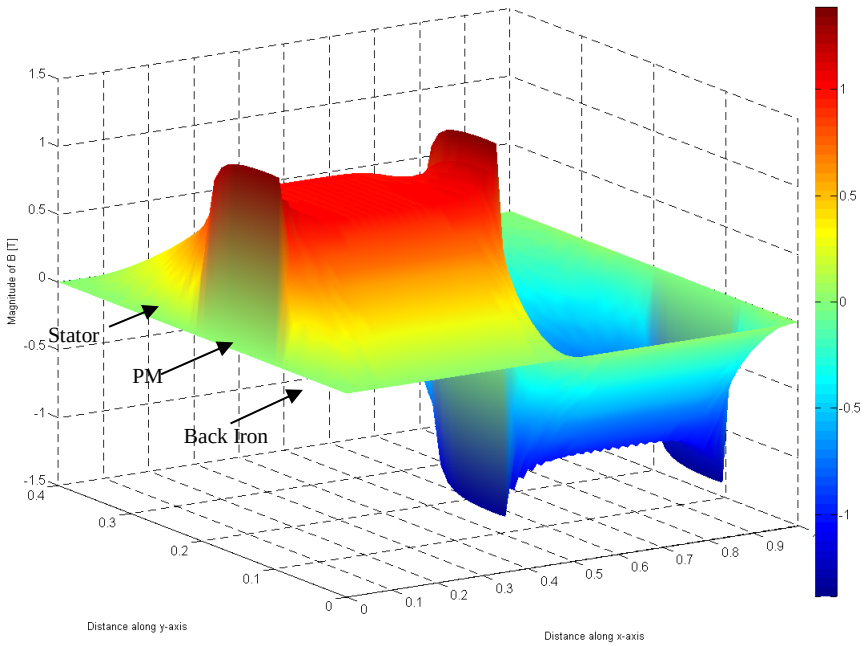

Fig.4.11: Flux density due to magnets for the case of PM excitation, Br = 1.2 T

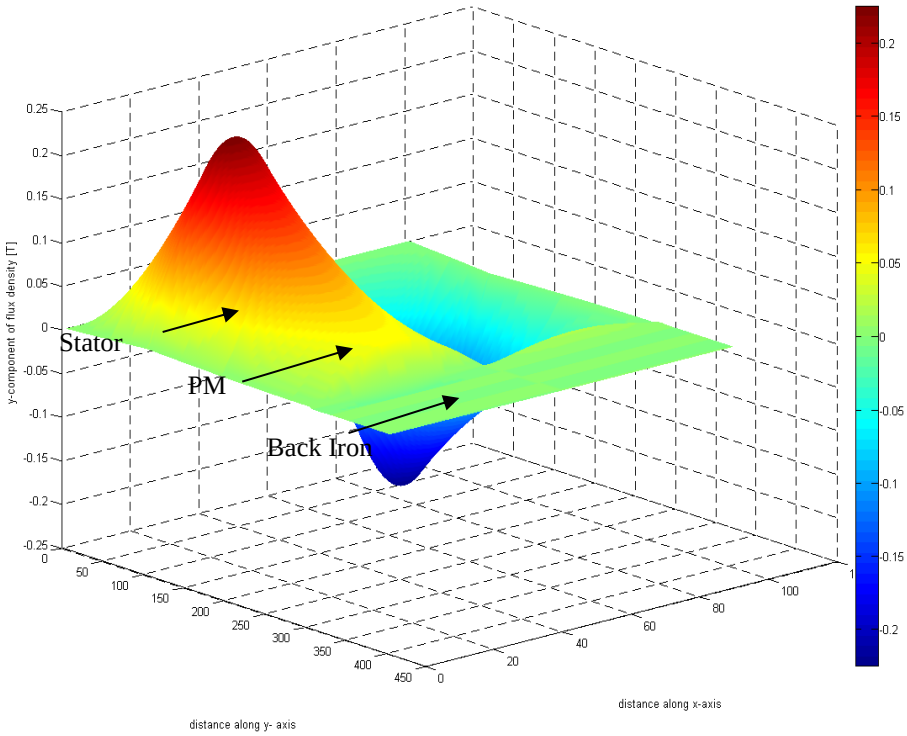

Fig.4.12: Flux density due to current sheet for fundamental harmonic

4.10.2 Induced Current Density from A_z

As shown in (4-12) (reproduced here again), the induced current density can be calculated from the calculation of time derivative of $\vec{A}$

$$\vec{J} = \sigma \vec{E}$$
$$\vec{E} = -\frac{\partial \vec{A}}{\partial t} \text{ or } \vec{J} = -\sigma \frac{\partial \vec{A}}{\partial t} \qquad (4\text{-}12)$$

We have already expressed general solution of $A_z(x, y)$ in (4-22) and (4-23). Further, because the mmf of concentrated windings is not sinusoidal, we have Fourier series decomposition of current sheet wave as excitation. This implies that each excitation will be a pure sine or cosine. The treatment of time variation is taken into account by

utilizing the periodicity of sine and cosine functions (see section 4.6.2 of this chapter) by making $A_z(x,y)$ as a sinusoidal time varying function expressed as:

$$A_z(x,y,t) = S(x,y)e^{j\omega t} \tag{4-64}$$

Here $S(x,y)$ represents the space dependent part of the solution which is solved using (4-45). Therefore, (4-12) can be written as:

$$\begin{aligned} J_z(x,y) &= -\sigma \frac{\partial \vec{A}}{\partial t} = -\sigma \frac{\partial A_z(x,y,t)}{\partial t} \\ J_z(x,y) &= -\sigma \frac{\partial}{\partial t}\left[S(x,y)e^{j\omega t} \right] \\ J_z(x,y) &= -\sigma j\omega \left[S(x,y)e^{j\omega t} \right] \end{aligned} \tag{4-65}$$

The induced current density is shown in fig. 4.13.

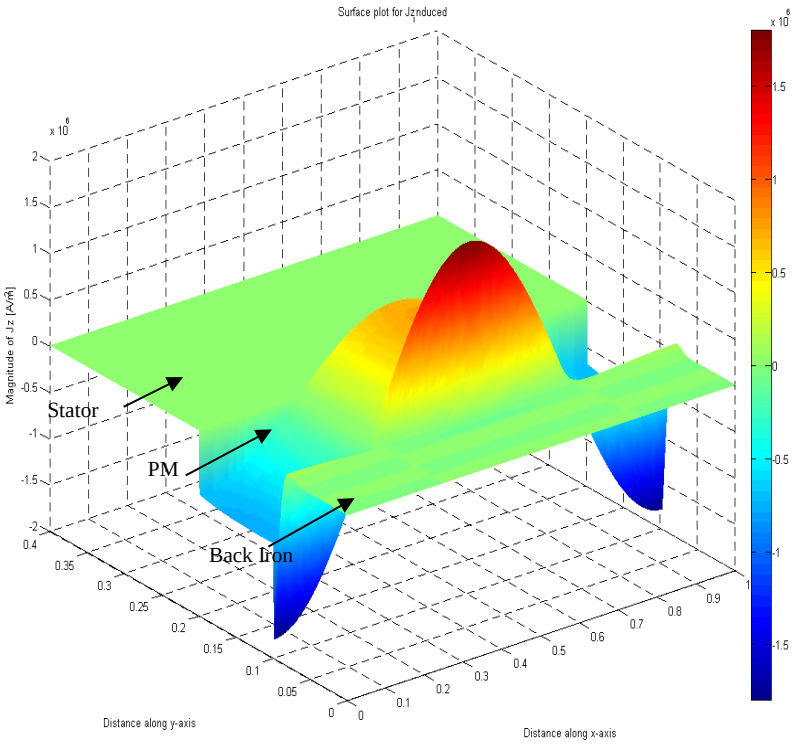

Fig.4.13: Induced current density due current sheet excitation of one harmonic

4.10.3 Eddy Current Losses from Induced Current Density

The eddy current loss is assumed to be limited by material resistance whereby loss can be easily calculated from induced current density using:

$$P_{eddy} = \iint_s \frac{J_z^2(x,y)}{\sigma} dA \qquad (4\text{-}66)$$

Here,

P_{eddy} is the eddy current losses in W; $J_z$is the induced current density in A/m²

A is area in m²; σ is conductivity in Siemens

Equation (4-66) represents eddy current loss due to one harmonic. The total loss can be calculated by adding the loss due to individual harmonic component. The loss distribution can be visualized as shown in fig. 4.14.

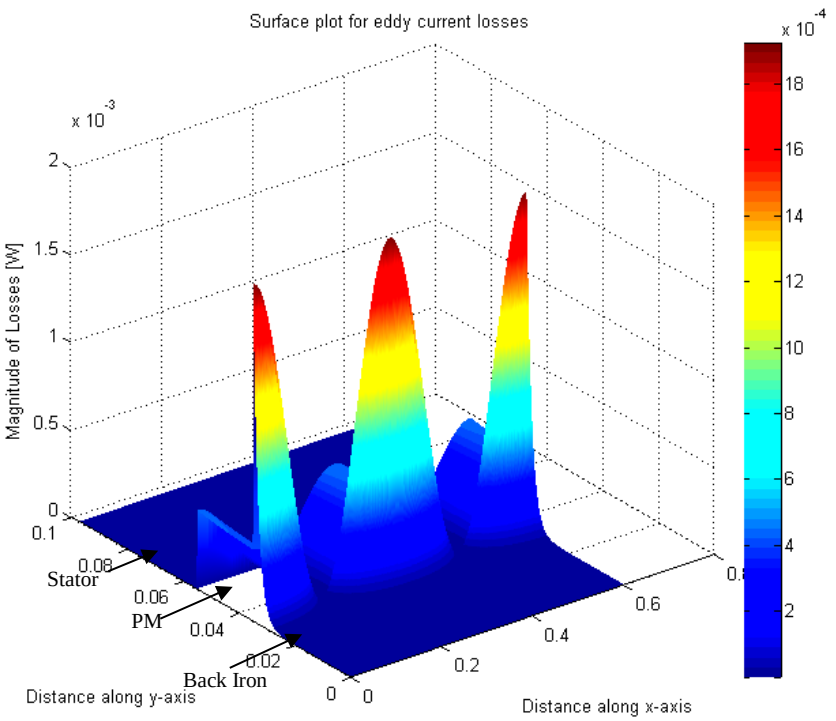

Fig.4.14: Induced eddy current losses due to current sheet excitation of one harmonic

4.11. Application of Analytical Model

The analytical model is used for determining eddy current loss trends in different slot-pole combinations of concentrated winding machines. It is clear that the assumptions used in analytical model bring some inaccuracies in the eddy current loss estimation. However, the speed of analytical modeling and independence from any special software requirement makes it very useful for short-listing and qualitatively comparing various slot-pole combinations. Modeling variables and constants are listed in table 4-1.

TABLE 4-1: MODELING CONSTANTS AND VARIABLES

Quantities kept constant	Quantities allowed to vary
a) Mechanical speed of rotor and air gap. b) Amplitude of the stator current sheet c) Materials and properties	a) Pole-pitch as per combination b) Winding factor as per slot-pole combination. c) Harmonic excitations as per Fourier decomposition

Using analytical modeling, various slot-pole combinations are modeled and dependencies on slots per pole per phase are established as shown in fig. 4.15. More results of comparisons and trends are presented in chapter 7.

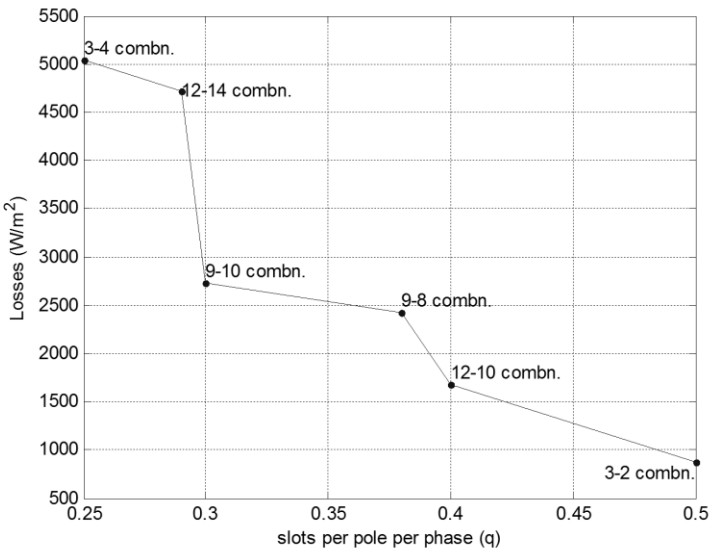

Fig.4.15: Variation of eddy current losses due to current sheet excitation for various slot-pole combinations

4.12. Summary

A generic analytical model has been developed starting from the basic Maxwell's equations. Certain assumptions have been made based on properties of large generators. A useful contribution of such a generic model is the ability to qualitatively compare various topologies having different slot-pole combinations. The analytical model is used to qualitatively compare some useful slot-pole combinations and derive trends in relation to eddy current losses.

Bibliography

[1] S.R.Holm, "Modelling and optimization of a permanent magnet machine in a flywheel," Ph.D. dissertation, pp. 62-66, Dept. Electrical Power Engineering, TU Delft, The Netherlands, 2003.

[2] P.D.Agarwal, "Eddy-Current Losses in Solid and Laminated Iron", AIEE Transactions, vol. 78, p.169 , 1959.

[3] H.Polinder, "On the losses in a high-speed permanent-magnet generator with rectifier," Ph.D. dissertation, pp. 12-16, Dept. Electrical Power Engineering, TU Delft, The Netherlands, 1998.

[4] K.J.Binns,P.J.Lawrenson and C.W. Trowbridge, "The analytical and numerical solution of electric and magnetic fields", 1995 edition, John Wiley & Sons publisher, pp. 3-6 and pp. 95-97.

[5] Pfister, P.-D.; Perriard, Y.; , "Slotless Permanent-Magnet Machines: General Analytical Magnetic Field Calculation," Magnetics, IEEE Transactions on , vol.47, no.6, pp.1739-1752, June 2011.

[6] Zhu, Z.Q.; Ng, K.; Schofield, N.; Howe, D.; , "Improved analytical modelling of rotor eddy current loss in brushless machines equipped with surface-mounted permanent magnets," Electric Power Applications, IEE Proceedings - , vol.151, no.6, pp. 641- 650, 7 Nov. 2004.

[7] Jassal, A.; Polinder, H.; Ferreira, J.A.; , "Literature survey of eddy-current loss analysis in rotating electrical machines," *Electric Power Applications, IET* , vol.6, no.9, pp.743-752, November 2012.

5. Finite Element (FE) Modeling

This chapter introduces the FE software used and the modeling procedure for large direct drive electrical machines. The chapter gives a brief introduction to the theory behind FE software and general procedure for problem setup and solution. Intermediate checks have been specified where necessary. The chapter ends with some results obtained from FE modeling

5.1. Introduction

The Finite Element (FE) method originated from the need for solving complex problems related to elasticity and structural analysis in civil and aeronautical engineering. Its development can be traced back to the work by Richard Courant [1]. Another pioneer in the field was Hrennikoff [2].Finite Element (FE) methods are being used extensively these days to simulate complex geometries and scenarios which are difficult to solve analytically. Rigorous mathematics was involved in solving electromagnetic problems when FE was not available. Earlier research in electromagnetics shows frequent use of conformal transformations, method of images etc. These days, the rigorous mathematical techniques are seldom taught in engineering disciplines. Therefore, the students from engineering back-ground find it difficult to grasp the analytical method. The analytical methods are limited in capturing the following effects:

a) Complexity of geometry
b) Material non-linearity and anisotropy
c) Interlinked transient effects like thermo-electric, motional effects etc.

The mathematical complexity of analytical models and the inaccuracy due to simplifying assumptions has made FE methods much popular. Improved graphics in FE software have made better visualization and plotting possible. Consequently, numerical analysis division of mathematics has gained tremendous momentum and a number of FE solvers are available in the market. Continuous improvements in computing speed and improved processing power have aided in overall development of FE methods.

Research is still going on for improving the quality of algorithms and making the software more user-friendly. Some of the most popular FE softwares used now-a-days are:

- ANSYS
- Vector Field's OPERA
- FLUX from CEDRAT
- FEMM – Foster Miller
- Infolytica MAGNET,
- COMSOL

All these FE software are efficient, useful and well known and it is not the purpose of this chapter to comment on features of the software. So we shift focus on the software used for this research. COMSOL Multiphysics 3.5a was used as the FE software environment. COMSOL provides an easy coupling with MATLAB. In fact COMSOL was sold as FEMLAB from MATLAB and later on developed independently as COMSOL software. Many versions of this software exist and the latest at the time of this research was COMSOL 3.5a (later versions are now available).

5.2. Finite Element Method

In essence, the Finite Element Method (FEM) is a numerical technique to solve Partial Differential Equations (PDEs) and Integral Equations (IEs). Since PDEs are easy to handle PDE's solutions are more common. In FEM, the solution of PDEs is based on either complete elimination of equations or breaking them into Ordinary Differential Equations (ODEs). These ordinary differential equations are then solved numerically by discretizing the space into smaller sub-domains and solving locally. FE formulation of a problem consists of the following basic steps:

1. *Weak Formulation* of the original boundary value problem.
2. *Discretization* of the selected domain space into cells or elements (meshing).
3. *Choice of the basic function*. This function is a piecewise linear function to get sparse matrix for the vector space.
4. *Formulation of the system* to resolve the field problem.
5. *Solution of the problem*. The solution is obtained by solving the resulting system of equations.

We will not discuss the mathematics behind these methods here as it has been widely published. Interested readers can check the following references for more details [4]-[8].

5.3. COMSOL 3.5a General Environment

The software COMSOL Multiphysics has a number of application modes and depending upon the application, a suitable mode can be chosen. Each application mode

is further sub-divided into application modules. For this research, the following application modes and modules were used:

5.3.1 Application Modes and PDE

a) COMSOL multiphysics mode and AC Power Electromagnetics module: This module is essentially a time harmonic solver. In present research this module was used to verify the solution of analytical model. The time-harmonic mode uses the following equation as the basic PDE.

$$\nabla \times (\mu_0^{-1}\mu_r^{-1}\nabla \times A_z) - \sigma v \times (\nabla \times A_z) = \sigma\left(\frac{\Delta V}{L}\right) + J_z^e \tag{5-1}$$

Here,

A_z is the z- component of vector magnetic potential
ω is the electrical frequency
σ is the electrical conductivity
V is the scalar electric potential
v is the velocity of the subdomain
J_z^e is the external current density
μ_0 is permeability of free space
μ_r is relative permeability of material

b) AC/DC mode with rotating machinery module was used: The AC/DC rotating machinery module is a transient solver which can take into account motion as well as material properties in real time. This inbuilt module has predefined conditions for modeling physical rotation and applicable boundary conditions. The transient mode uses the following equation as the basic PDE.

$$\sigma\left(\frac{\partial A_z}{\partial t}\right) + \nabla \times (\mu_0^{-1}\mu_r^{-1}\nabla \times A_z) = J_z^e \tag{5-2}$$

The symbols have the same meaning as in (5-1).

5.3.2 FE Model Setup

The purpose of using this software is to model a concentrated winding machine with permanent magnets which has design attributes similar to a generator used in a wind

turbine. In the selected topology i.e. concentrated windings, there is a problem of eddy current losses in solid conductive parts of the machine such as magnets and back iron of rotor. We have already seen in analytical modeling (chapter 4) that analytical model can't capture all the effects. On the other hand, FE software can model slotting, saturation and motion all at once. However, in order to capture eddy current losses, we need to setup the model in a useful way. The basic requirements are:

a) *Symmetry* - Since the machine in question is a large machine so modeling whole machine takes too long to solve. Thus we should use symmetry to model only a part of the machine and extrapolate the results thus obtained.
b) *Mesh size* - The phenomenon of eddy current losses has a certain skin depth and this is in the order of fraction of millimeters (mm). This means that we need a rather fine mesh in the region where we expect eddy currents to occur.
c) *Geometry accuracy* - The accuracy with which we build our geometry plays a very important part in convergence of a solution. This is critical since we are using only a part of machine to model and periodic boundary conditions. If the geometry is not accurate enough, the solver might fail to start during transient simulations.
d) *Time step and relative tolerances* - The smaller the time step, the better the results but also more the time taken for solution. Thus in order to reach an acceptable solution, the step size should not be too large to get inaccurate results and it should not be too small that it takes forever to solve the problem. There are different tolerances on different parameters and one can get a better estimate of tolerances by hit and trial.
e) *Initial values* - In order to define a good solution in transient case, a relatively accurate static model has to be solved first. The transient model gets its initial values from this solution.
f) *Boundary conditions* - The boundary conditions are of course the basis on which the solver solves the PDE. Modeling of just a section of the machine requires the use of periodic boundary conditions on east and west and symmetry/anti-symmetry can be chosen depending on geometry and physics. Similarly on the boundary between stator and rotor (which is moving), the boundary condition used is either symmetry or anti-symmetry. This condition takes the number of sections of machine into account.
g) *Physics* - This simply means the materials that we are going to use in the model. A lot of common materials are there in the library but if there are some specific materials, these can be added into the library.
h) *Motion* - Motion to simulate transient conditions is done using frames of reference. In COMSOL, there is two frames of reference viz. reference or stationary frame and moving or ALE (Arbitrary Langrangian Eulerian) frame []. Sub-domains which move during simulation are assigned movement in ALE frame and they move with respect to the fixed parts. The two reference frames are coupled using coupling

variables (called lm1, lm2 etc.). These coupling variables are linked to periodic conditions at the interface boundaries. More details will be explained later.

5.3.3 General Procedure for Problem Setup

Since COMSOL is closely coupled with MATLAB, almost all of the steps can be done in MATLAB interface as well. Drawing of geometry is for example much easily done with MATLAB as compared to the Graphic User Interface (GUI) in COMSOL. Post-processing is also very convenient with MATLAB especially for quantities which have to be derived from primary post-processing data. These are the basic advantages with COMSOL. It leads to a much better insight into the working of FE program and hence the results can be intuitively verified.
The general procedure to set-up a problem is shown in the flow chart of fig. 5.1.

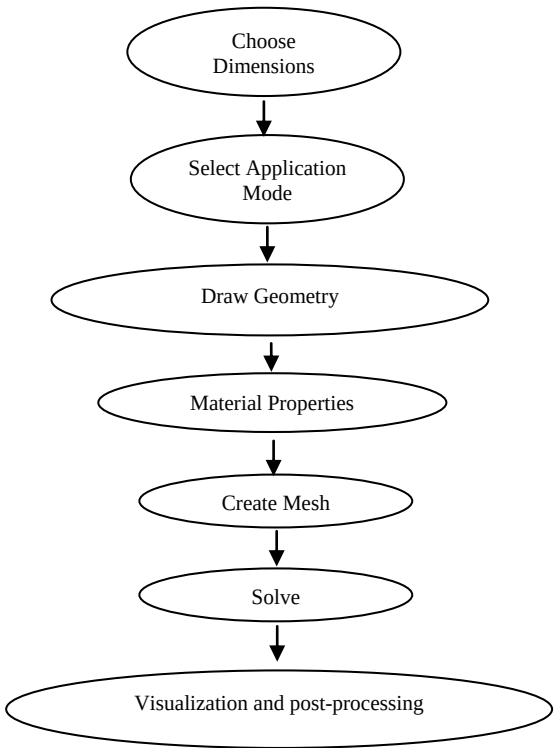

Fig.5.1: General procedure to setup a problem

.

5.4. Machine Model

There can be a number of useful slot-pole combinations for designing a machine with concentrated windings. The eddy current loss in solid conductive parts is one of

the major criteria to determine utility of a combination. Winding factor is the other important criterion [9]-[11].

Therefore we aim to compare a number of possible combinations and devise guidelines for selection. In order to keep the comparison fair, the stator dimensions, current loading, air gap velocity, thickness of magnets and rotor back-iron as well as materials has been kept same for all combinations. The dimensions that vary are length of a section containing a given number of slots and poles along with magnet span. Figure 5.2 shows the dimensions used for modeling.

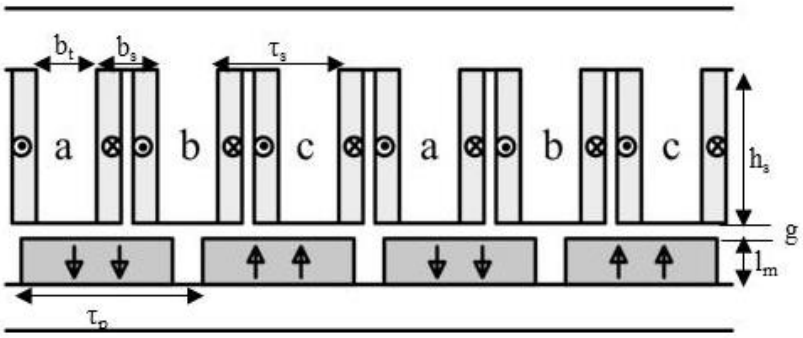

Fig.5.2: Main dimensions of a concentrated winding machine

Here the dimensions have the following meaning and values:
b_t = Tooth width
b_s= Slot width
τ_s = Slot pitch
h_s = Slot height
τ_p = Pole pitch
l_m = Magnet thickness
g = Mechanical air gap

The air gap velocity of the rotor surface has been fixed for comparison between different slot-pole combinations. Some useful combinations have been selected based on a good winding factor and these will be compared for eddy current losses in solid magnets and rotor back-iron or rotor yoke. Further, in chapter 7, a whole range of useful slot-pole combinations are analyzed and trends are formulated using FE software.

5.4.1 Geometry Drawing and Symmetry

Although it seems obvious but when drawing geometry it is better to work with relations and formulas rather than numerical values. The use of symmetry greatly

reduces the computation time. Symmetry can be defined in boundary conditions as shown in fig. 5.3. It can be periodic, anti-periodic or some potential function.

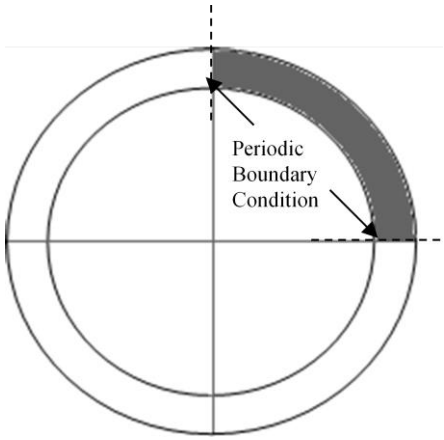

Fig.5.3: Symmetry in a machine over one quarter

Accuracy in drawing should be such that when the machine is fully completed there should be no gaps between sections anywhere.

5.4.2 Meshing

The mesh size is very important because of very small skin depth of the eddy current losses. The mesh should be fine and regular enough to simulate the skin depth where required as shown in fig. 5.4

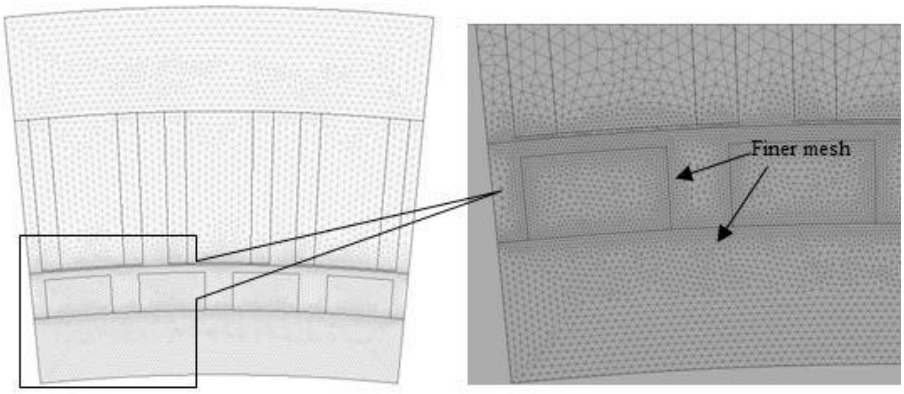

Fig.5.4: Meshing over a machine model 3 slots per 4 poles combination

There can be many possible shapes for meshing a sub-domain but triangular mesh is most common because it has the smallest possible area for any closed surface. COMSOL gives control over the size of mesh triangle in any sub-domain or along a

boundary and the rate at which the size grows within a sub-domain. There are pre-defined mesh options from extremely coarse mesh to extremely fine mesh as well.

5.4.3 Boundary Conditions

The boundary conditions are used for solution of PDE and connect various sub-domains together in solution. These boundary conditions are described using an example of 3-4 slot-pole combination (see fig. 5.5). Main conditions available to be used are:

a) Magnetic Insulation: $\vec{A} = 0$ where $\vec{A}$ is the vector magnetic potential.

b) Continuity: $n \times (\vec{H}_1 - \vec{H}_2) = 0$ where $\vec{H}_1$ and $\vec{H}_2$ represent the magnetic field on either side of boundary.

c) Periodic condition: $\vec{A}_{source} = \pm \vec{A}_{destination}$ where + means symmetry and – means anti-symmetry and $\vec{A}$ is the vector magnetic potential.

d) Periodic point condition: This is a special condition used on the points which connect the extent of the moving boundary. Coupling variables are also defined at these points.

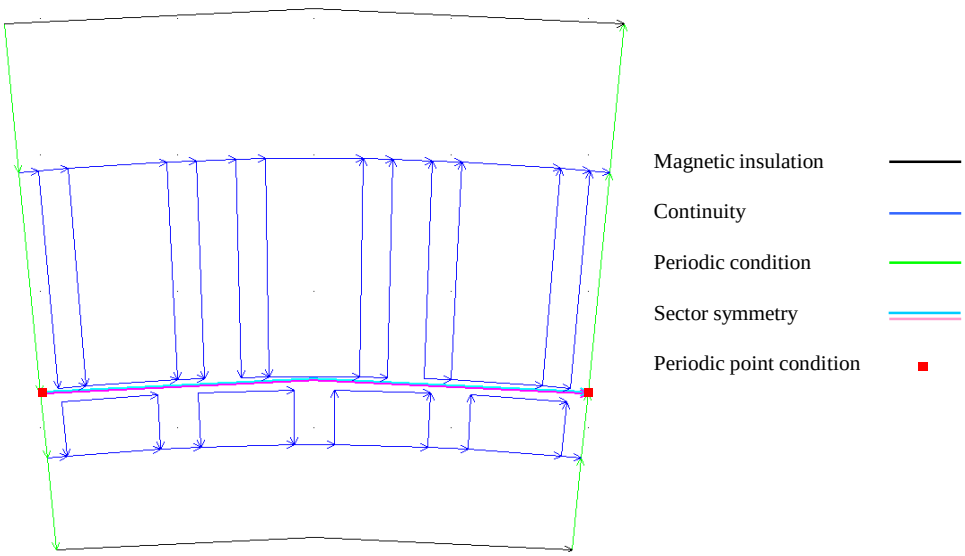

Fig.5.5: Boundary conditions shown here for a 3- 4 combination

5.4.4 Physics and Material Settings

The physics of the model can be set either by using inbuilt library or by using user-defined materials. The material and physics settings are shown in table 5-1. This can be done using Matlab or GUI but from experience, it is easier done by GUI. The material properties for each of sub-domain are shown in fig. 5.6. The material properties can be modified and a new material can be added to the existing library for future use as well.

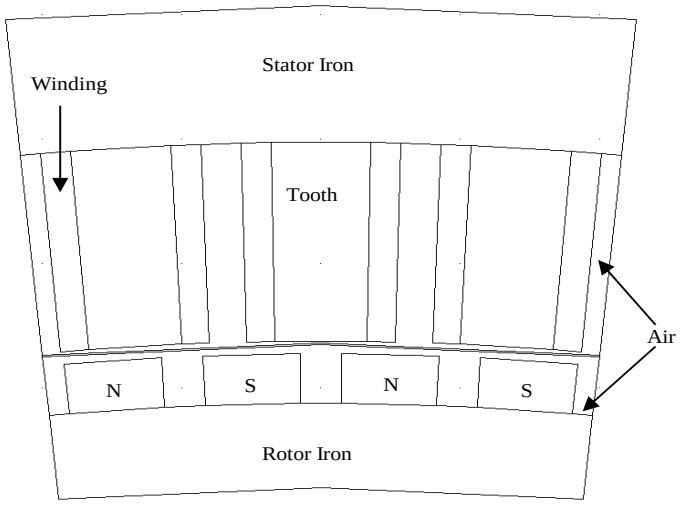

Fig.5.6: Material setting shown here for a 3- 4 combination

TABLE 5-1: PHYSICS SETTINGS

Sub-domain	Relative permeability	Electrical Conductivity (S/m)	B-H Relation	External Current Density (A/m^2)
Stator Iron	$\vec{\mu}_r = f(\vec{B})$	0	$\vec{B} = \mu_0 \vec{\mu}_r \vec{H}$	-
Tooth	$\vec{\mu}_r = f(\vec{B})$	0	$\vec{B} = \mu_0 \vec{\mu}_r \vec{H}$	-
Winding	1	0	$\vec{B} = \mu_0 \vec{\mu}_r \vec{H}$	3.5×10^6
Magnets*	1	1×10^6	$\vec{B} = \mu_0 \vec{\mu}_r \vec{H} + \vec{B}_r$ $\vec{B}_r = \pm B_r \frac{X^2}{\sqrt{X^2 + Y^2}}$	-
Rotor Iron	$\vec{\mu}_r = f(\vec{B})$	5×10^6	$\vec{B} = \mu_0 \vec{\mu}_r \vec{H}$	-
Air	1	0	$\vec{B} = \mu_0 \vec{\mu}_r \vec{H}$	-

* For magnets, X and Y are spatial coordinates to set radial flux density distribution.

5.4.5 Motion

COMSOL contains a module called AC/DC module which contains a sub-module called rotating machinery which is used for transient modeling. The effect of motion is taken into account by creating super-imposed reference frames within the rotating machinery module. These reference frames are:

a) Stationary or Reference frame – This frame shows the original position of the parts when there is no motion present. This is basically a time harmonic solver.
b) Moving or ALE reference frame – In this frame of reference, the relative motion between parts is assigned. The ALE algorithm is used to couple the solution on moving part to the solution on static part whereby computation time is lowered [12]. Since the mathematics of ALE is very specific, the details are not presented here and this is viewed just as a tool for analysis. One disadvantage is that the rotating machinery module can't model linear motion. The rotation is given by the following reference frame conversion:

$$\begin{pmatrix} X' \\ Y' \end{pmatrix} = \begin{pmatrix} \cos(2n\pi t) & -\sin(2n\pi t) \\ \sin(2n\pi t) & \cos(2n\pi t) \end{pmatrix} \begin{pmatrix} X \\ Y \end{pmatrix}$$

Here
n is rotational speed in rpm; t is time
X' and Y' are transformed coordinates at any time t
X and Y are the fixed coordinates

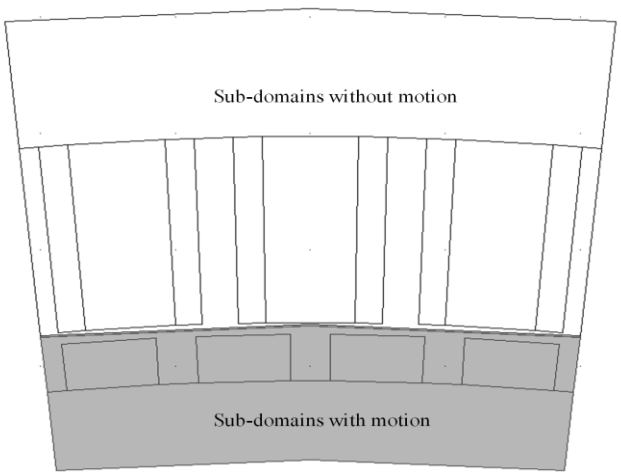

Fig.5.7: Sub-domains which are assigned motion for a 3- 4 combination

5.4.6 Visualization and Post-processing

The general post processing window gives a choice of plots which one needs to visualize on one plot for example contour plot of vector magnetic potential and surface plot of magnetic flux density can be plotted together in one figure. Further, the quantities to be plotted and the other settings of plots like color, number of lines, scaling etc. can be set from the specific visualization settings of the plot.

There are also a lot of options for defining variables and expressions using basic quantities. The post processor is coupled with Matlab and therefore the plotting options are further enhanced. Some capabilities used in this thesis are shown in table 5-2. A sample plots of useful values (w.r.t. this thesis) are shown in fig. 5.8 and fig. 5.9.

TABLE 5-2: SOME USEFUL POST-PROCESSING OPTIONS

Option	Function	Example
Cross-section Plot	Plot of quantity along a user-defined line.	Flux density plot at any y-coordinate for all x-coordinates.
Sub-domain integration	Plot of pre-defined or user-defined quantity integrated over a sub-domain and its evolution in time.	Eddy current losses, induced current density etc.
Global variables plot	Plot of user-defined variable, coupled to sub-domain or boundary.	Torque acting on the sub-domain.

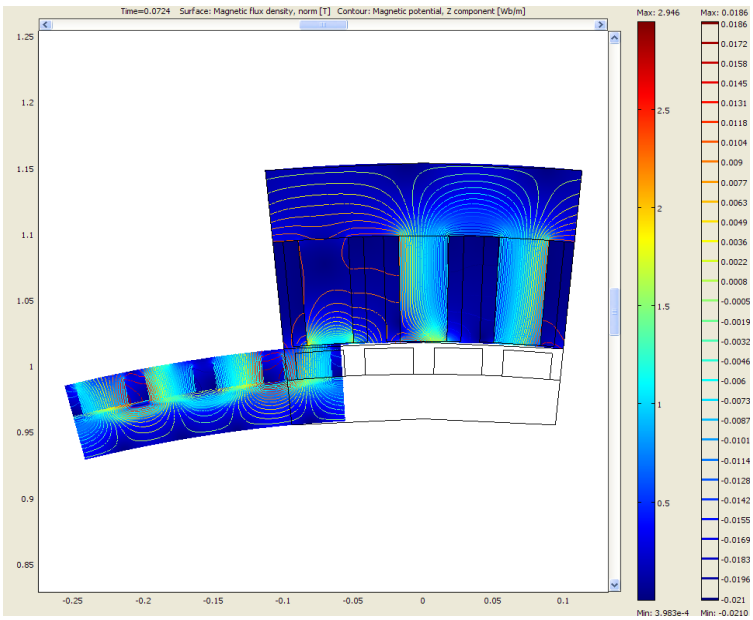

Fig.5.8: A contour plot of magnetic potential and surface plot of magnetic flux density plotted together

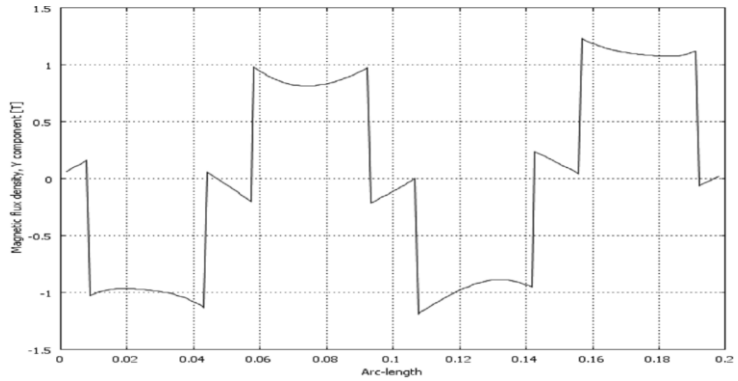

a)

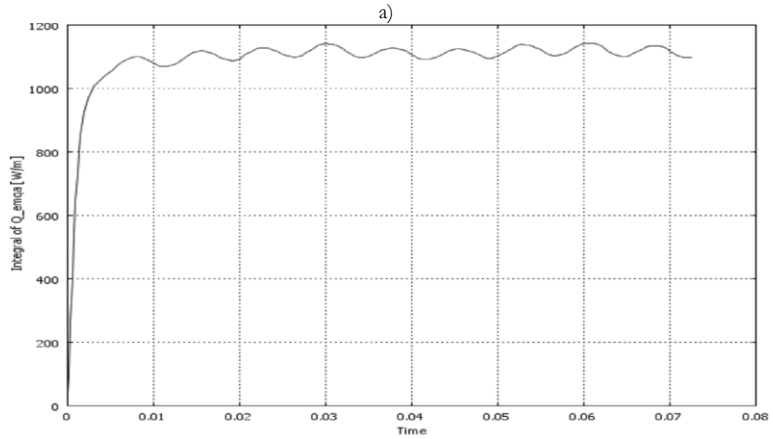

b)

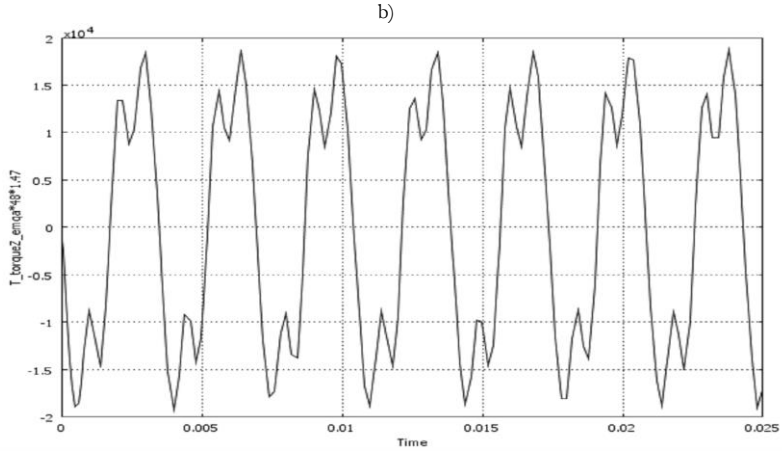

c)

Fig.5.9: a) Flux density (y-component), derived from surface plot at one time instant using cross-section plot b) Eddy current losses magnets by using sub-domain integration of resistive losses over magnets real time c) Cogging torque calculated by user defined global variable and its evolution in time.

5.5. Results of FE Modeling

5.5.1 Validation of Analytical Model

The analytical model and solution of PDE was validated with a simplified model made in COMSOL 3.5(a) FE software. This model was prepared with the same assumptions as that of analytical model to verify analytical solution itself. The geometry consists of four layers as in the analytical model. On the boundary between stator and air gap, there is a surface current density, resulting in a travelling wave of magnetic flux density in the air gap. The current sheet is responsible for flux density and losses. It is placed at the stator surface as in the analytical model. The four layers have the same material properties as in analytical model. Actual motion is present in the FE model whereas for analytical model, a modified frequency with complex harmonic excitation was used to simulate motion. The material settings for four layers are:

1. A layer with perfect iron. New material was defined in material library and material properties were chosen such that the losses in stator part can be neglected. The properties were defined as electrical conductivity $\sigma = 0$; Relative permeability $\mu_r = 4000$.
2. A layer of air with $\sigma = 0$ S; Relative permeability $\mu_r = 1$.
3. A layer of magnets with $\sigma = 1x10^6$ S; Relative permeability $\mu_r = 1$.
4. A layer of solid back iron. A new material was defined having the following properties $\sigma = 5x10^6$ S; $\mu_r = 200$.

The results are shown in table 5-3 and fig. 5.10 and 5.11. The losses for simplified models in table 5-3 do not match exactly because of numerical integration used for loss calculation in FE program.

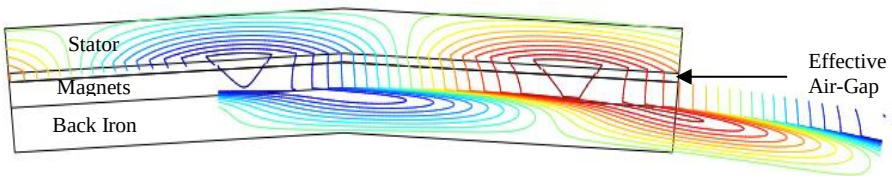

Fig.5.10: Flux lines for simplified FE model used for validation

Another reason for deviation could be the geometry curvature required to inculcate motion in the FE program. As a check, the induced current density (from which losses are calculated) for both analytical and simplified FE model was compared and found to match exactly. After initial validation of analytical model, the model was compared for eddy current loss calculation with transient FE simulations. Further, both the analytical

and FE models were compared with experiments performed on a 9 kW PM machine. These comparisons are presented in chapter 6.

TABLE 5-3: LOSS COMPARISON FOR 9-8 COMBINATION MACHINE

Harmonic	1	2	5	7	8
Losses from Analytical model (W)					
Magnets	26	74	311	0.34	1.90
Back Iron	15	28	68	0.09	0.2
Losses from simplified FE model (W)					
Magnets	24	68	301	0.14	1.40
Back Iron	18	20	74	0.06	0.6

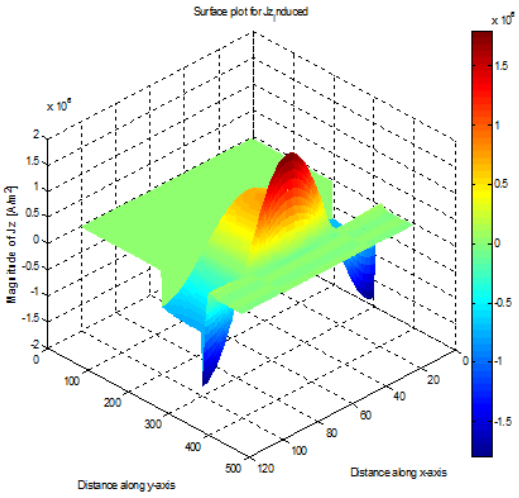

a)

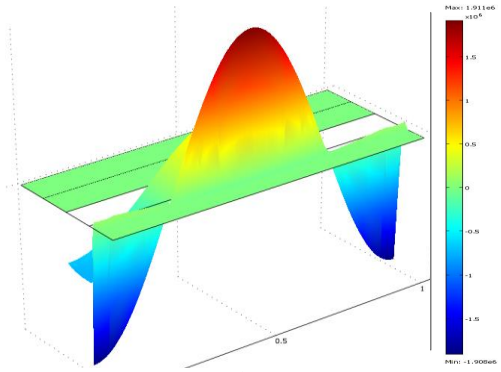

b)

Fig.5.11: Induced current density for a harmonic a) Analytical b) FE

5.5.2 Eddy Current Loss Calculation Using FE Models

The modeling method was applied on various combinations of slots and poles with many variations. There can be many useful and interesting output quantities but in context of this research, we limited to following quantities:

a) Surface plot of magnetic flux density to see if flux density is within limits.
b) Surface plot of induced current density to visualize where losses are present
c) Eddy current losses in magnets, back-iron and total using sub-domain integration

Sample output of these plots is shown in fig. 5.12-5.14. All these plots will not be shown for all the machines because plots are similar.

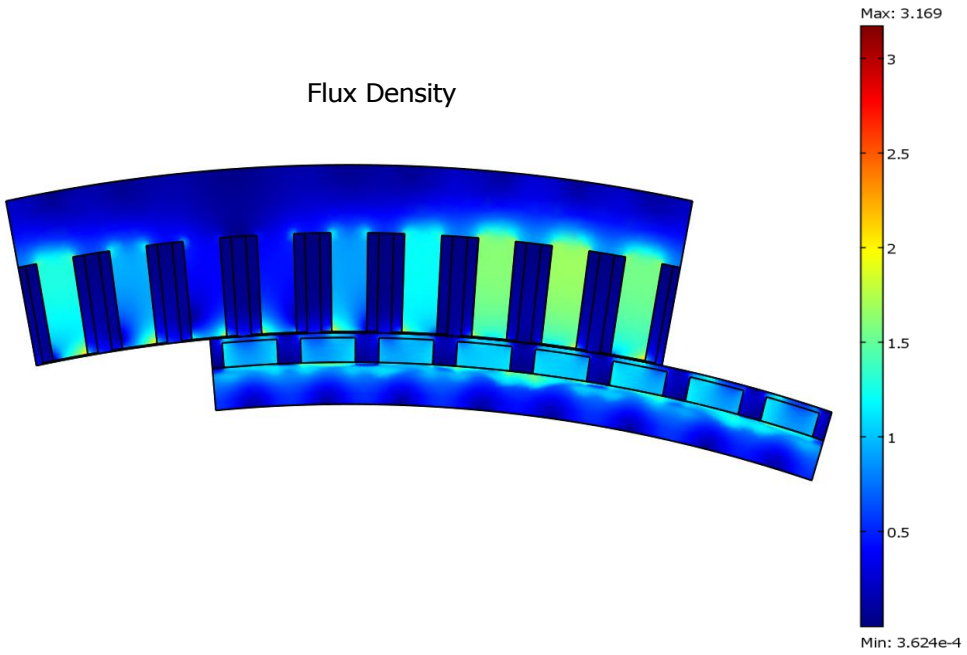

Fig.5.12: Magnetic flux density shown for a 9-8 slot-pole combination with active magnets

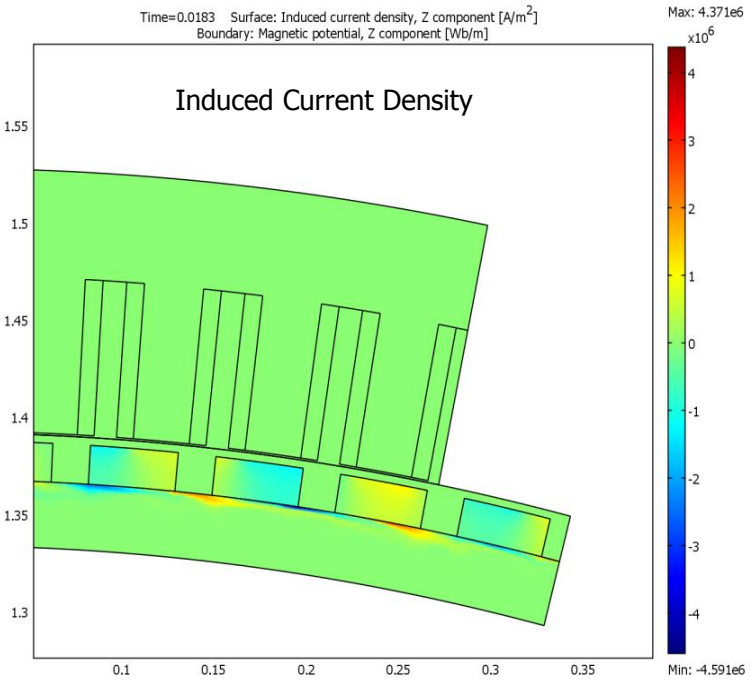

Fig.5.13: Induced current density for 9-8 combination

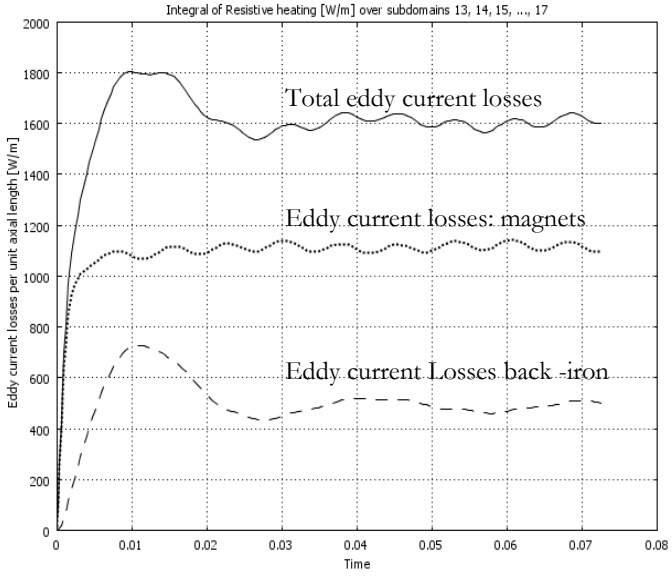

Fig.5.14: Eddy current losses in various parts of machine

5.5.2.1 Variations for models

Extensive FE modeling was done to study effects of variations in model on the eddy current losses. These variations play an important part in comparison with analytical model. The most important variations are:

a) Effect of slot opening (for ¾ slot open and ½ slot open).
b) Effect of magnetic saturation.
c) Effect of presence and absence of magnetic field of magnets.

All models are compared for these variations and then some trends have been brought out for comparison between various models.

5.5.2.2 Results for Eddy Current Losses from FE Models

Some useful combinations are analyzed for eddy current losses using the methodology explained in this chapter. The results for the loss calculations are shown in fig. 5.15 and 5.17.

The FE modeling is used for comparison and validation of the analytical model. The analytical model gives a fair match in trend of losses when compared to FE simulations. Total losses compare well in case where a higher order harmonic is responsible for losses as in 9-8, 9-10 and 12-10 combinations. The eddy current losses in the analytical model are up to 1.4 times higher than values in FE models in case of 3-4 combination. This is because losses in 3-4 combinations are produced by first harmonic which penetrates the whole conductive region. In general, the analytical model over-estimates total losses in the case where a lower order harmonic produces losses. This is because the total conductive area is higher in the analytical model and the effective air-gap calculated using carter's correction factor is estimation only.

Since magnets are represented as one region, losses in magnets are much higher than losses in back-iron as some shielding is provided by the conductive magnets.

The results for the non-linear iron case are very similar to those in linear iron case. This is due to low flux density ~ 1.2 T setup by stator currents in absence of PM magnetization whereby the skin depth increases and hence little effect of saturation comes into play.

The machines are further compared for effect of slotting by modeling semi-closed slots. The excitation conditions were same as in previous case. The rectangular slots are compared with ½ slot closed and ¾ slot closed. Use of semi-closed slots immensely reduces the losses as shown in fig. 5.16.

The computation time for the FE program in case of linear iron is in the range of 120-180 seconds and for non-linear case is 200-360 seconds. The computation time for the analytical model is 0.06 seconds. For the case when PMs are active, the computation time of FE model is about 600 seconds.

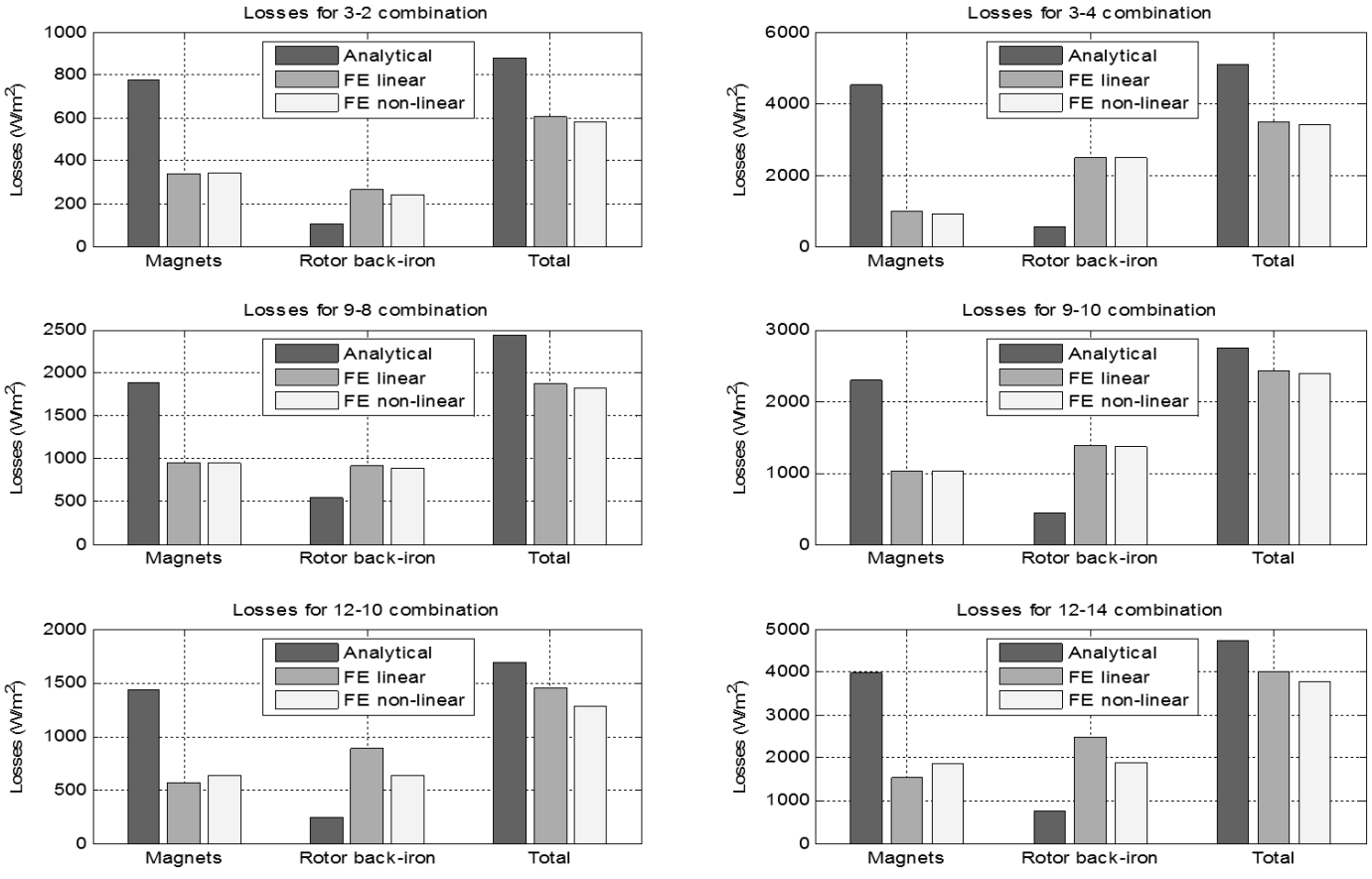

Fig.5.15: Eddy current losses in different slot-pole combinations (scale on each figure is different)

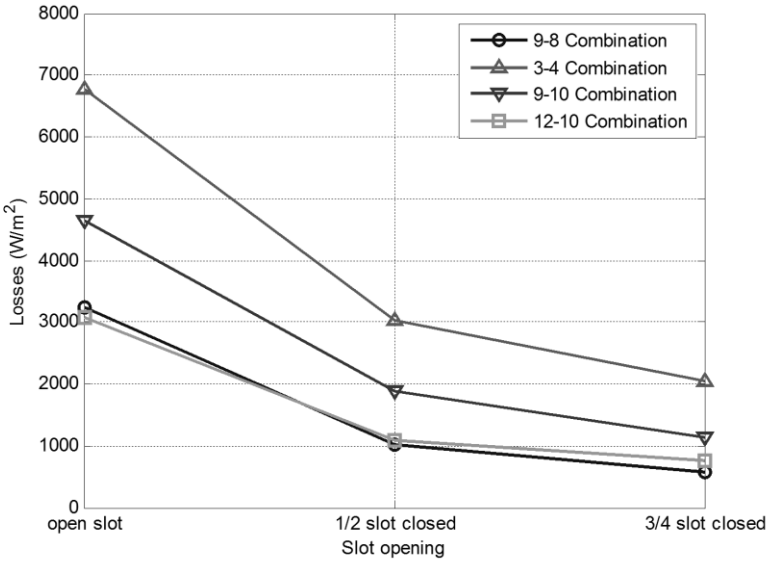

Fig.5.16: Eddy current losses with slot opening (including PM excitation as well)

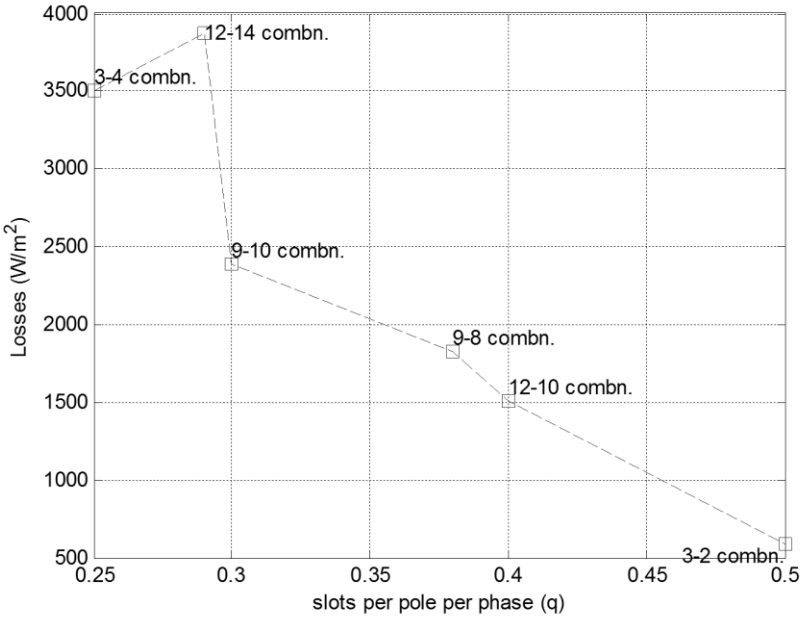

Fig.5.17: Eddy current losses with slots per pole (Only stator current excitation to compare with analytical models)

It is noteworthy to compare fig. 5.17 with fig. 4.15 at this point. It is shown by plotting both graphs in same figure. The comparison brings out a limitation in analytical modeling where a lower order harmonic is responsible for the eddy current losses. It can be seen that in 3-4 slot-pole combination, the analytical model over-estimates the losses while FE model predicts lower losses. In this particular combination, 2nd harmonic produces torque whereas 1st harmonic is mainly responsible for losses. The low frequency of 1st harmonic allows it to penetrate deeper in the conducting surfaces. Since the analytical model assumes magnets as a continuous layer (and not separate magnets), the area used for integrating induced current density is larger. This leads to higher loss estimation. In other cases also, the analytical model predicts higher losses however the deviation is smaller. It can be seen that the results (atleast trends) are comparable.

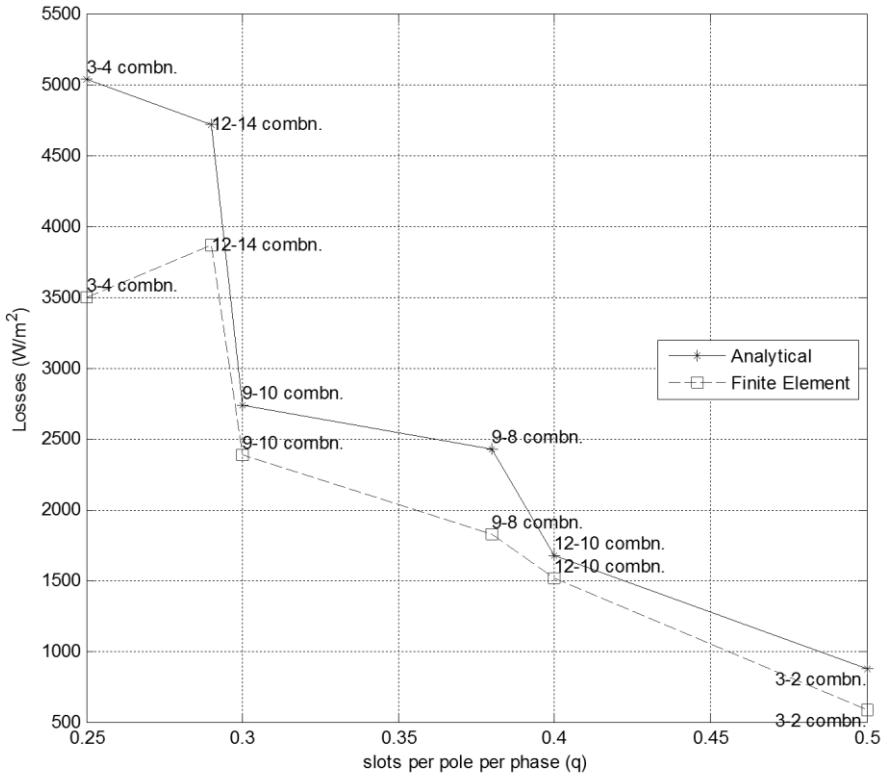

Fig.5.18: Eddy current loss calculation with slots per pole per phase: A comparison between analytical and FE methods for the case of only stator current excitation

5.6. Summary

Finite Element modeling methodology has been explained and some results thus obtained have been presented. The FE method is more accurate than the analytical method. However, similar trends from analytical and FE models could be derived with some exceptions. The analytical model overestimates losses in case where a lower order harmonic is responsible for losses (explained in description of fig. 5.18). The effect of slotting in presence of the PM field and motion produces appreciable losses which can't be ignored. On the other hand these losses are expected to be similar for different slot-pole combinations as long as the stator dimensions are similar.

Bibliography

[1] Pelosi, G.; , "The finite-element method, Part I: R. L. Courant [Historical Corner]," *Antennas and Propagation Magazine, IEEE* , vol.49, no.2, pp.180-182, April 2007.

[2] Hrennikoff, H., "Solutions of Problems in Elasticity by the Framework Method", Journal of Applied Mechanics, A 169-175, 1941.

[3] Courant, R., "Variational Methods for the Solution of Problems of Equilibrium and Vibration", Bulletin of American Mathematics Society, Vol. 49, 1-23, 1943.

[4] Oliveira, E., "Theoretical Foundation of the Finite Element Method", International Journal of Solids and Structures", Vol. 4, pp. 926-952. 1969.

[5] A.B.J Reece, T.W. Preston, "Finite Element Methods in Electrical Power Engineering", Oxford University Press, 2000.

[6] Nicola Bianchi, "Electrical Machine Analysis Using Finite Elements", CRC Press, 2005.

[7] A.Bondeson, T.Rylander, P. Ingelstrom, Computational Electromagnetic, Springer, 2005.

[8] F. Vermolen, D.Lahaye, "Introduction to Finite Elements", Lecture Notes, TU Delft, 2008.

[9] J. Cros, P. Viarouge, "Synthesis of high performance pm motors with concentrated windings", IEEE Transactions on Energy Conversion, vol. 17, pp. 248–253 (2002).

[10] F. Magnussen, C. Sadarangani, **"**Winding factors and Joule losses of permanent magnet machines with concentrated windings," in Proc. of the 2003 IEEE International Electric Machines and Drives Conference**,** 2003, pp. 333 – 339, vol.1.

[11] Bianchi, N.; Bolognani, S.; Fornasiero, E.; , "An Overview of Rotor Losses Determination in Three-Phase Fractional-Slot PM Machines," Industry Applications, IEEE Transactions on , vol.46, no.6, pp.2338-2345, Nov.-Dec. 2010.

[12] J. Donea et.al. **,** "Encyclopedia of computational mechanics", chapter 14, vol. 1, John-Wiley publishers 2011.

6. Experimental Analysis

This chapter aims at validating the FE and analytical modeling. The concept and methodology are explained first. Thereafter, the framework for carrying out various types of experiments is presented. The equipment and their specifications are briefly explained. This is followed by detailed explanation of procedure of the experiments. The deviations in results between various methods are documented and the reasons for deviation have been brought out.

6.1. Introduction

Experimental analysis is the most trusted tool when it comes to practicality of eddy current loss analysis. Analytical modeling involves a lot of assumptions whereby the results are inaccurate. FE modeling can take into account many non-linearities but generally 2d analysis is done and there are material anisotropies, edge effects, physical non-uniformities in dimensions etc. which might lead to deviation between experimental and FE results. Further, even the experiments are not perfect owing to measuring inaccuracies. However, the experiments bring us closest to the real physical scenario. The aim of the experiments performed is to validate various eddy current loss models.

6.2. Experimental Setup

The experimental setup aims at validating both analytical and FE models developed in the course of this research. Although FE modeling can take into account more 2d effects than the analytical models (slotting, material non-linearity etc.) but it is difficult to include material anisotropies, edge effects, physical non-uniformities etc. These 3d effects are difficult to incorporate even in 3d FE analysis because the material properties differ from specimen to specimen. Therefore experiments are needed to validate the models and bring out deviations. For the present research, the experiments are conducted in two phases:

I. Static tests – Tests without actual motion
II. Rotary tests – Tests where real machine motion is utilized.

The theory and rationale behind tests is explained further in the following sections.

6.3. Static Tests

Static tests imply that there is no moving part involved in the experimental setup. The test is conducted for three different metallic rings which are made from aluminum, copper and mild-steel. The purpose of these tests is to validate the formulation of the analytical model as the test setup represents simplest rotor structure (only a ring) and no physical motion. The schematic for these tests is shown in fig. 6.1.

6.3.1 Static Tests – Procedure

The following steps explain the procedure for conducting static tests.

1. A fixed voltage and frequency is applied to the stator (alone) of machine to create a rotating field.
2. The power taken to set-up the flux in air is measured. This power can be expressed as: $P_{in1} = P_{Fes} + P_{Cus}$; where P_{Fes} is stator iron loss and P_{Cus} is copper loss in the stator.
3. Now the stator is covered by a metallic ring and power input is measured again keeping current same as before. This power can be expressed as:
   $P_{in2} = P_{Fes} + P_{Cus} + P_r$; where P_r is the power lost in the ring.
4. The power input will be different in the two cases (without and with ring). This difference in power indicates eddy current losses in the ring. Therefore power loss in the ring $P_r = P_{in2} - P_{in1}$

It is assumed that the stator iron losses are same for both operations which is not exactly true. This is because the magnetic field setup by the stator current changes when there is ring compared to the case without ring. Copper and Aluminum ring have very low relative permeability. Therefore inductance remains fairly constant when compared with the case without the ring. Thus we can say that this assumption of constant stator losses is valid. In case of mild steel ring, the permeability is very high. Therefore the change in inductance compared with the case without any ring is large. In this case the assumption is expected to bring more deviation in results. However since it is difficult to estimate stator iron losses especially for low flux densities, the assumption is made anyways.

The assumption is verified by measuring the inductance and resistance of the setup with and without the rings and explained in section 6.3.3 on the results of the static tests (see fig. 6.8 and 6.9)

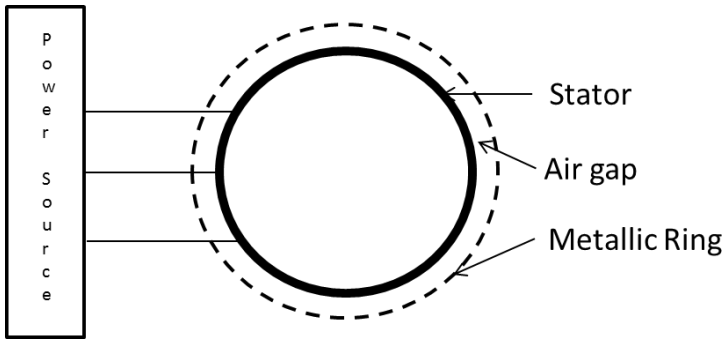

Fig.6.1: Static tests - schematic of the arrangement

6.3.2 Static Tests – Apparatus

The apparatus for the static tests consists of the following equipment:

a) Power supply – 6 kW, Variable frequency (17-1000) Hz, with inbuilt voltage, current and power measurement (see fig. 6.2).
b) Stator with 3-phase winding and open slots (fig. 6.3)
c) Stator with 3-phase winding and semi-closed slots (fig. 6.3)
d) Rings of copper, aluminum and ST37 steel (fig. 6.4)
e) Voltage, current and power measurement

The machine parameters are shown in table 6-1 and 6-2. The total setup is depicted in fig. 6.5.

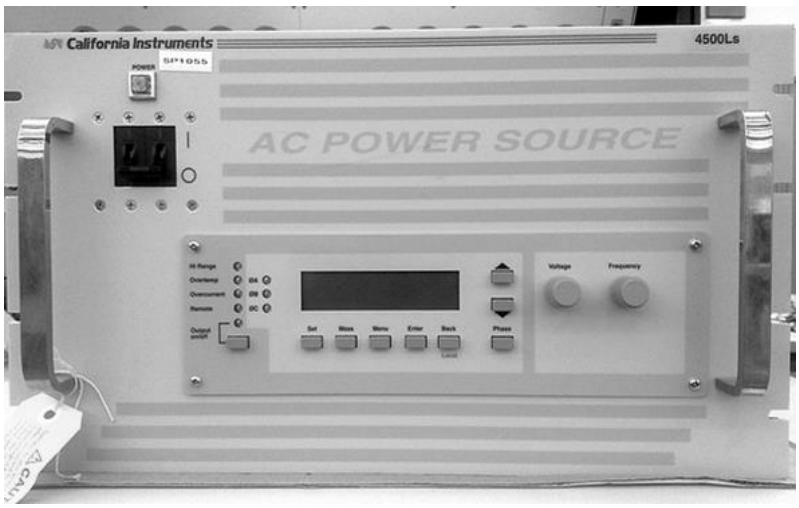

Fig.6.2: Power Supply (with inbuilt voltage, current and power measurement)

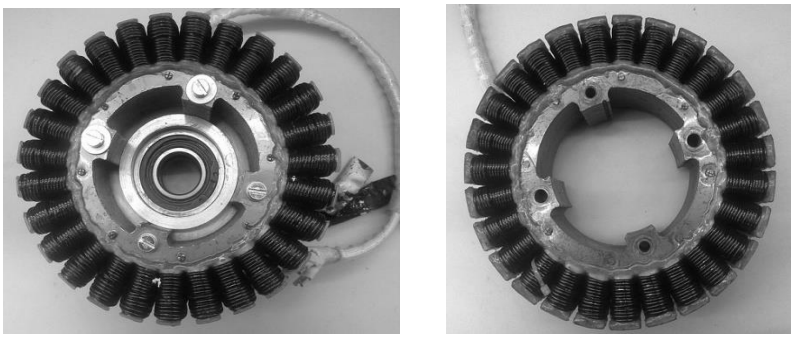

a) b)

Fig.6.3: Stators a) open slots b) semi-closed slots

TABLE 6-1: MACHINE PARAMETERS: DIMENSIONS

Parameter	Description	Open slot	Semi-closed slot
N_t	number of tooth	27	27
N_p	number of pole	18	18
N_c	number of turns for each coil	15	15
r_s	air gap radius	91 mm	91 mm
r_{si}	inner radius stator	46 mm	46 mm
h_s	slot height	30 mm	26 mm
h_{so}	slot opening height		4 mm
b_t	tooth width	8 mm	8 mm
b_{tt}	tooth width with edges		18 mm
h_{sy}	height of stator yoke	10 mm	10 mm
τ_s	sloth pitch	21.17 mm	21.17 mm
l_g	air gap length	2 mm	2 mm
r_m	permanent magnet surface radius	93 mm	93 mm
l_m	magnet length	5 mm	5 mm
b_p	magnet width	24 mm	24 mm
l_s	stack length	56 mm	56 mm
Rated Current		10 A	10 A
Rated Speed		3600 rpm	3600 rpm
Rated Power		9 kW	9 kW

TABLE 6-2: MACHINE PARAMETERS: MATERIAL PROPERTIES

Parameter	Description	Value
ρ_{fe}	back iron resistivity	$2x10^{-7}$ Ω.m
ρ_m	magnet resistivity	$1.3 x10^{-6}$ Ω.m
B_{rm}	magnet remanent flux density	1.2 T
μ_{rfe}	relative permeability back iron	200
μ_{rm}	relative permeability magnet	1.05

a) b) c)

Fig.6.4: a) copper ring b) aluminum ring c) ST37 steel ring

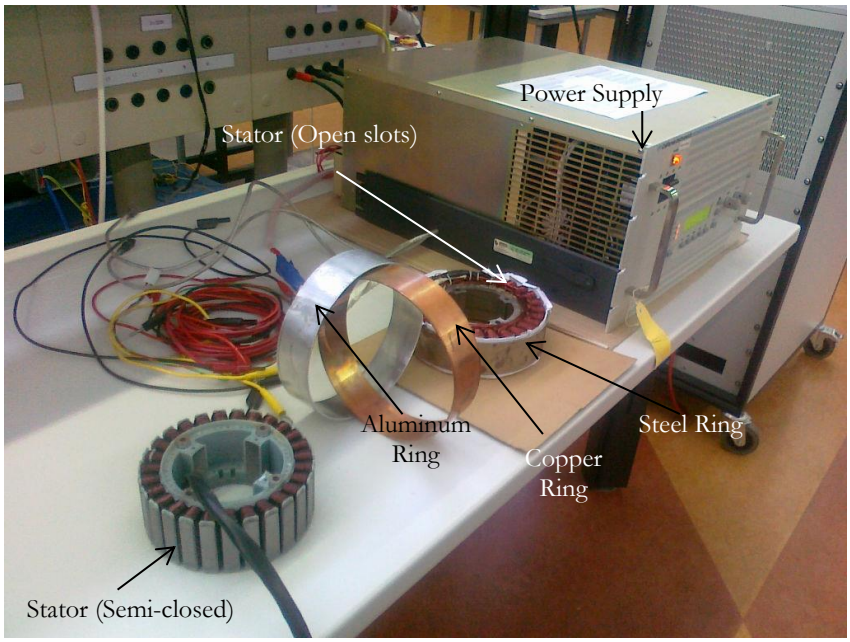

Fig.6.5: Experimental setup

6.3.3 Results Static Tests

The results for the static tests are shown in this section in fig. 6.6 for open slot machine and in fig. 6.7 for semi-closed slot machine. The eddy current loss calculation for the three rings of different materials and stators with open slots as well as semi-closed slots are presented.

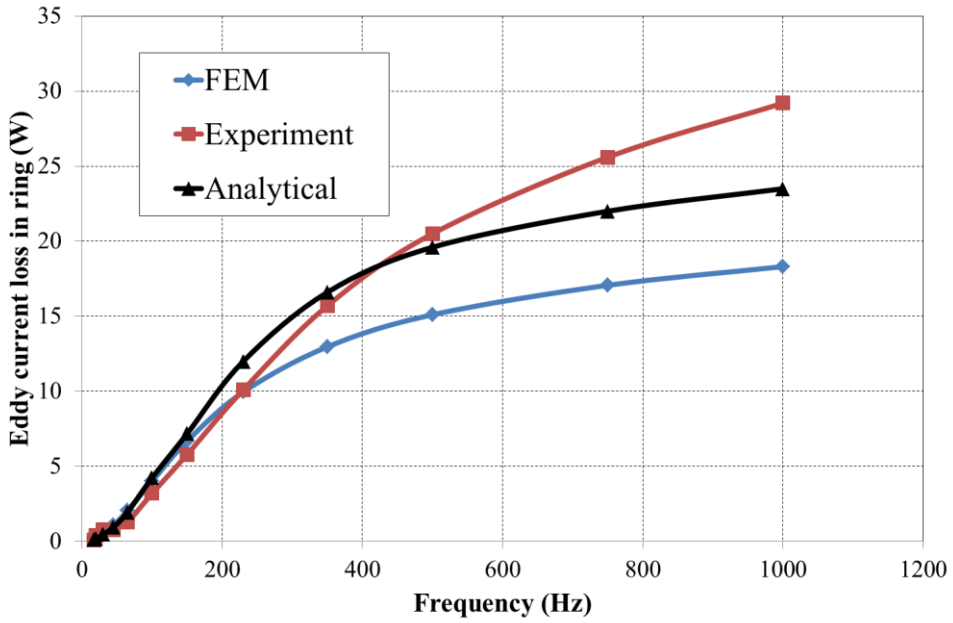
FEM
Experiment
Analytical
Eddy current loss in ring (W)
Frequency (Hz)
0
5
10
15
20
25
30
35
0
200
400
600
800
1000
1200

a)

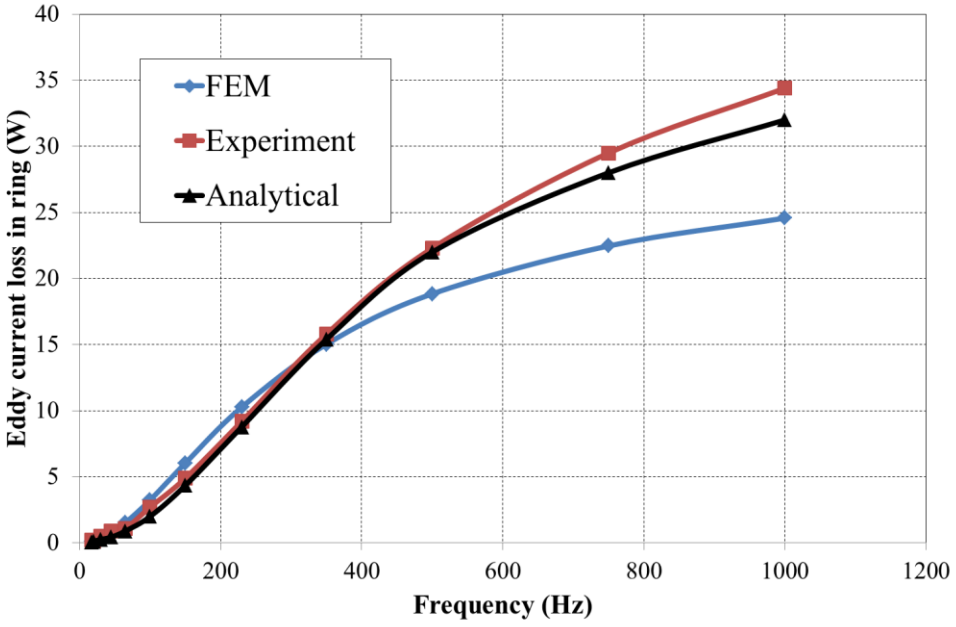
FEM
Experiment
Analytical
Eddy current loss in ring (W)
Frequency (Hz)
0
5
10
15
20
25
30
35
40
0
200
400
600
800
1000
1200

b)

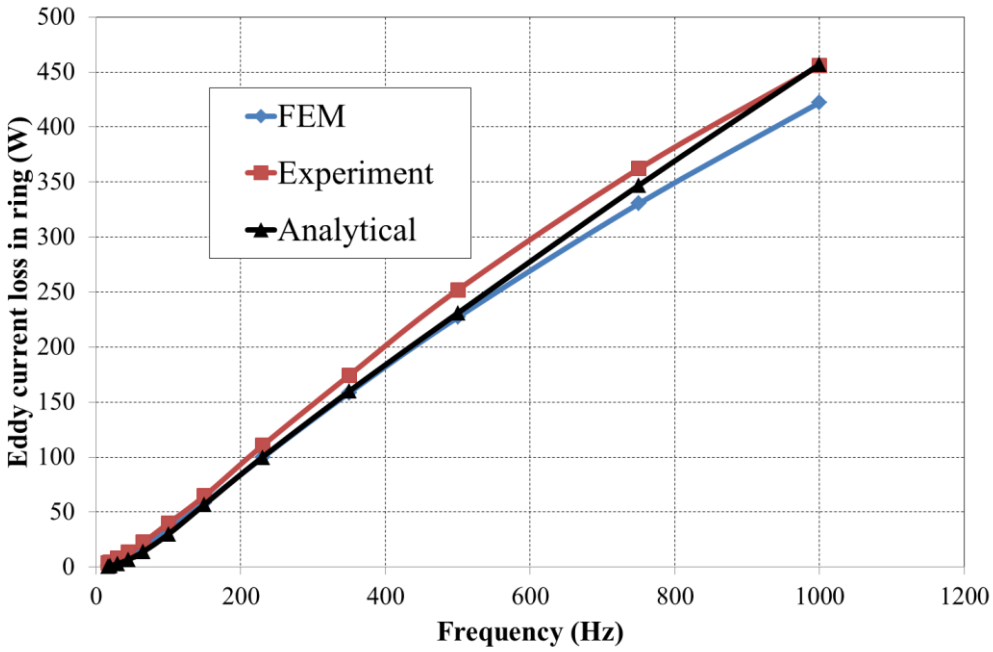

c)

Fig.6.6: Comparison of Losses for a) Copper ring b) Aluminum ring c) ST37 steel ring for open slot machine

In case of aluminum and copper, the experiments show higher losses. This is because of end effects where the eddy currents get crowded at the edges of the ring. Since the axial length of the machine is very small compared to pole pitch, the end effects are rather pronounced. The FE and analytical models are for large machines where axial length is much larger than the pole pitch therefore 2d only. The experimental losses include end effects. It can be seen that both analytical and FE models overestimate losses at lower frequencies while they underestimate losses at higher frequencies.

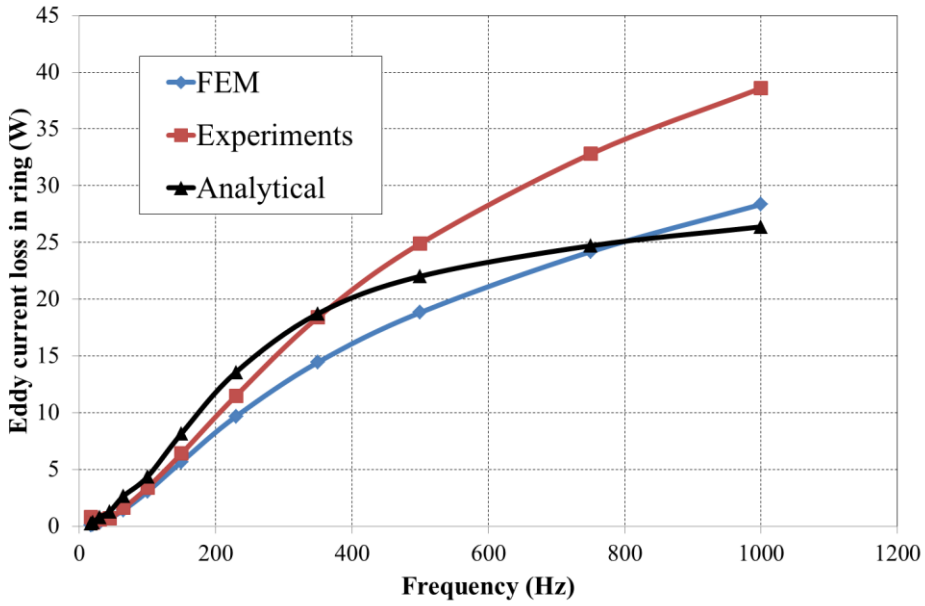
FEM
Experiments
Analytical
Eddy current loss in ring (W)
Frequency (Hz)
0
5
10
15
20
25
30
35
40
45
0
200
400
600
800
1000
1200

a)

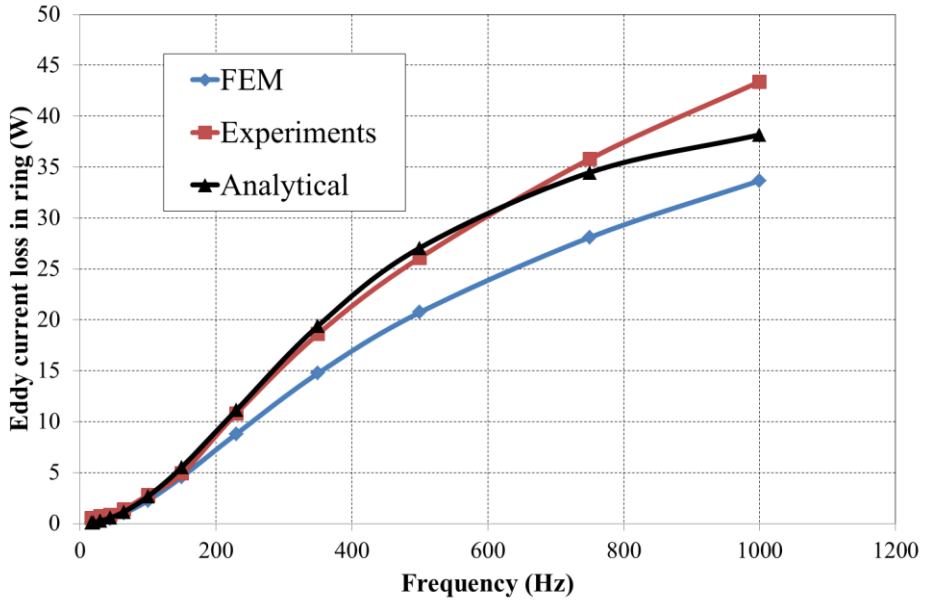
FEM
Experiments
Analytical
Eddy current loss in ring (W)
Frequency (Hz)
0
5
10
15
20
25
30
35
40
45
50
0
200
400
600
800
1000
1200

b)

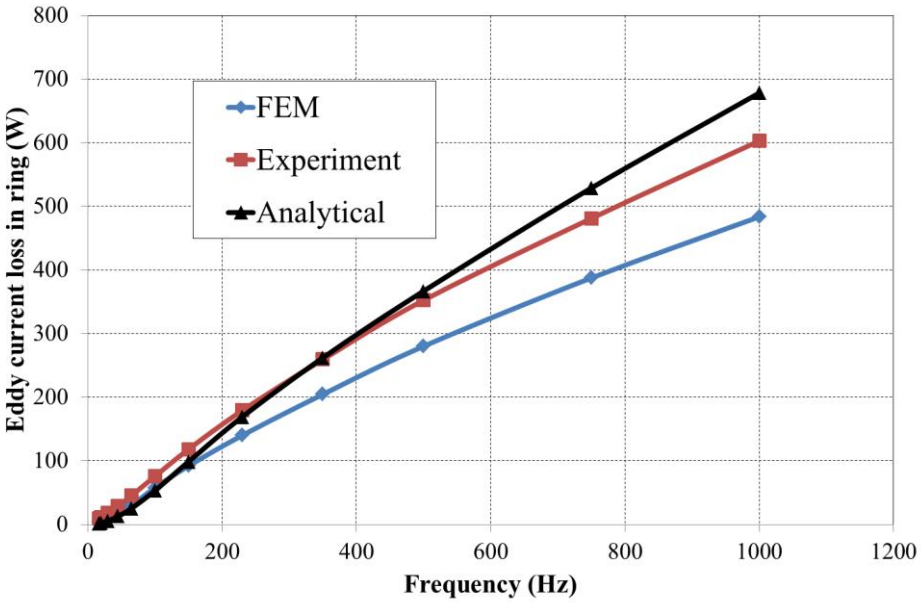

c)

Fig.6.7: Comparison of Losses for a) Copper ring b) Aluminum ring c) ST37 steel ring for semi-closed slot machine

In order to understand the deviation, the impedance of stator with ring mounted is measured for difference frequencies and results are shown in fig. 6.8 and 6.9.

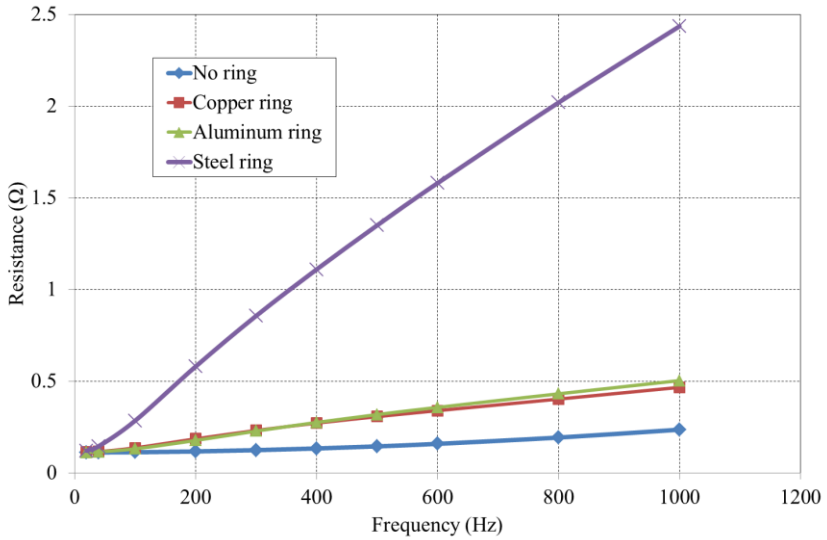

a)

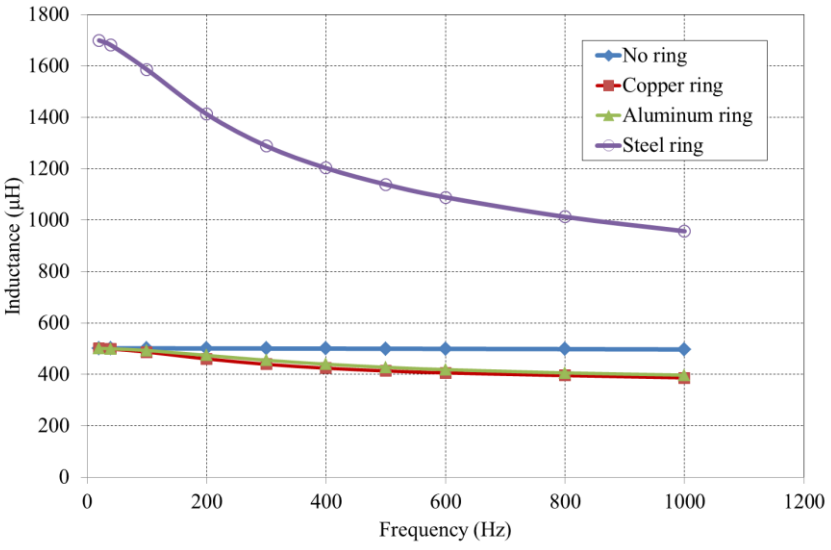

b)

Fig.6.8: Effect of frequency on a) resistance b) inductance of the open slot machine

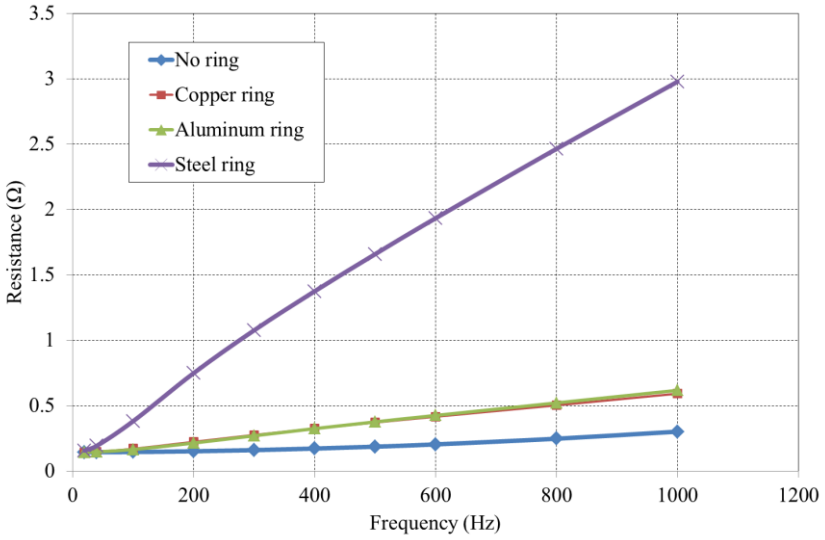

a)

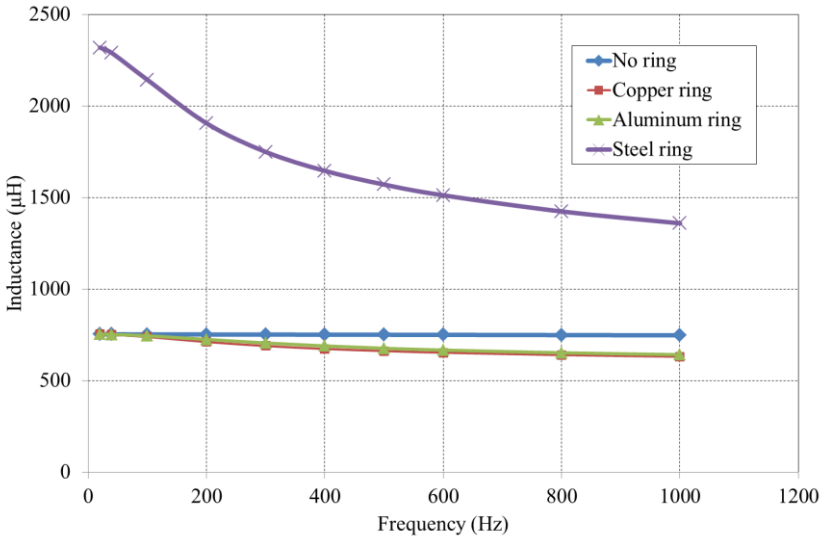

b)

Fig.6.9: Effect of frequency on a) resistance b) inductance of the semi-closed slot machine

At low frequencies, the reaction field is negligible and therefore the circuit's inductance is high and resistance is low as observed from the machine terminals.

However the resistance in actual machine is higher than in FE or analytical models because of end effects. This phenomenon is verified by using a thermal camera. Immediately after the tests, the setup is put inside a cardboard box and pictures are taken with the thermal camera through a slit sized to the camera sensor. This is done to eliminate any error in thermal image due to reflection of light. The pictures shown in fig. 6.10 clearly show end effects i.e. the edges of the rings have higher loss concentration than the central part of the ring.

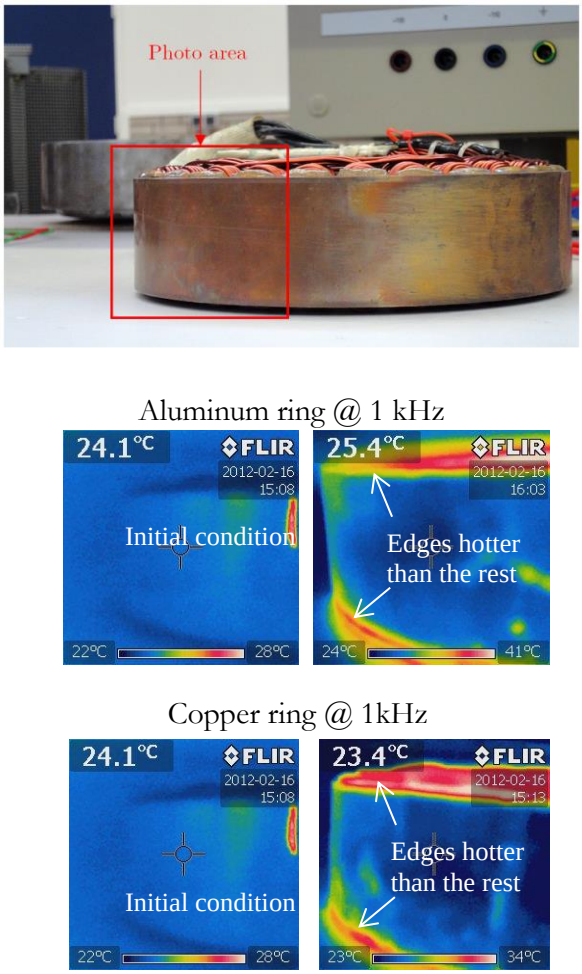

Fig.6.10: Thermal pictures of the rings immediately after tests. Note higher temperature on the edges of the ring

The over-estimation of eddy current losses for low frequencies and under-estimation at high frequencies can be further explained by taking increased resistance due to end effects into account.

Since losses are limited by resistance, power measured at stator terminals is given by:

$$P = \frac{U^2}{R}$$

P is power measured; U is voltage and R is resistance.

Thus increased resistance due to end effects leads to lower losses in experiments for low frequencies.

At higher frequencies, the reaction field is strong and thus inductance reduces and resistance increases as seen at machine terminals. The current flow seen from machine terminals is governed by inductance and power is given by:

$$P = I^2 R$$

Thus, an increase of resistance leads to higher losses. It can be seen from fig. 6.6 and 6.7 that the models still predict correct order of magnitude of losses.

The losses in case of the non-linear ST-37 steel are higher in analytical model compared to experimental and FE (which also takes non-linearity into account). This is because of local saturation at high frequencies which has not been taken into account in analytical model.

6.4. Rotary Tests – Main Principle

Rotary tests imply that there is a rotating part involved in the experimental setup. The principle of power balance is used to calculate losses in the rotor back-iron and magnets. This method involves measurement of input power supplied to the prime mover and the output power of the concentrated winding machine.

The machine considered here, is a generator and feeds a known load. If the machine is operating at synchronous speed, the losses due to torque-producing component are not present therefore we can assume that all the losses are occurring due to harmonics. These losses comprise of copper and iron losses. We can separately calculate copper losses for the machine and the remaining losses are the iron losses.

The power balance equation can be written as

$$P_{in} = P_{pm\_m} + P_{mech} + P_{gen} + P_{load} \tag{6-1}$$

Here,

P_{in} = Electrical power input

P_{pm_m} = Power lost in prime-mover

P_{mech} = Mechanical power at shaft

P_{load} = Power taken by load

$P_{gen} = P_{Cus} + P_{Fes} + P_{Fer}$ = Power loss in generator

P_{Cus} is copper loss in stator; P_{Fes} is iron loss in stator; P_{Fer} is iron loss in rotor

The total losses can be separated to obtain the copper and Iron losses. The manufacturer's data for stator can be used to estimate the iron losses in the stator laminations. The rest of losses can be separated assuming that eddy current losses are the major contribution towards iron losses in solid rotor. In order to separate iron losses in rotor due to stator currents and PM magnetization, the same test is performed when magnets are replaced by un-magnetized magnets. This ensures that the losses are only due to stator excitation.

6.4.1 Rotary Tests – Apparatus

The apparatus for rotary tests shown in fig. 6.11 and 6.12 consists of the following main components:

1) DC Power supply (600 V, 60 A, 36 kW) for armature
2) DC Power supply (340 V, 1.92 A) for field excitation
3) DC machine as prime mover (30 kW)
4) Stator with 3-phase winding and open slots
5) Stator with 3-phase winding and semi-closed slots
6) Rotor with magnets
7) Rotor with un-magnetized magnets
8) Voltage, current and power measurement
9) Spring balance for torque measurement and fixing mechanism
10) Resistive load for loading the machine
11) Speed measurement (Encoder fixed to DC machine)

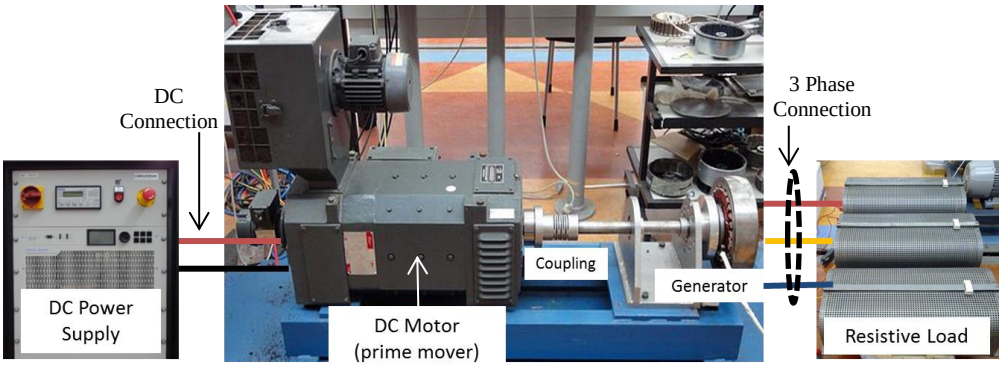

Fig.6.11: Rotary tests - schematic of the arrangement

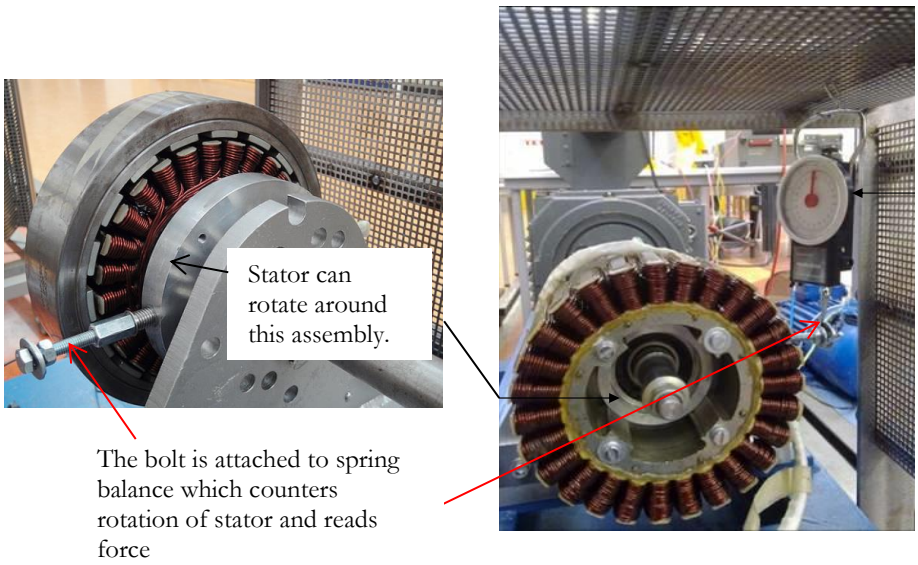

Fig.6.12: Stator and mechanism of torque measurement for the 9 kW PM machine

6.4.2 Variations in Rotary Tests

The rotary tests are conducted on the machine and compared with FE simulations to bring out the differences. The method of power balance and direct torque measurement are used to measure losses in the machine. The separation of iron losses into stator and rotor losses is carried out by calculating the stator iron losses from manufacturer's datasheet. A correction factor of 1.55 (to account for punching and processing of

laminations) is used to estimate losses in the stator. Same rotary tests are conducted on both open slot and semi-closed slot machine. Further, the rotary tests are conducted for the cases tabulated in table 6-3.

TABLE 6-3: EXCITATION CASES

Case	Excitation	Validation
I	PM but no stator currents	Losses: PM only (slotting)
II	Stator currents + PM	Losses: Combined
III	Stator currents only	Losses: Stator Currents

The detailed account of procedure for measurement is given in the subsequent sections

6.4.2.1 Measurement of the prime mover and mechanical losses

It is necessary to measure the prime mover and mechanical losses before we proceed with loss measurements with different cases mentioned in table 6-3. The prime mover and mechanical losses are two separate entities and therefore calculated from the experimental results. These losses are calculated for three different cases viz. unloaded shaft, shaft with stator only and shaft with rotor only. The case with both stator and rotor can't be considered because that would lead to some electromagnetic power exchange and extra losses.

The input power is the power absorbed from the DC power supply (connected with the armature) by the DC motor which acts the prime mover.

$$P_{in\_dc} = U_{dc} I_{dc} \tag{6-2}$$

Here P_{in_dc} is the input DC power; U_{dc} is the DC armature voltage;

I_{dc} is the armature current.

Out of this input power, some power is lost in the DC motor armature. This power is simply calculated by

$$P_{cu\_dc} = I_{dc}^2 R_{dc}$$
$$R_{dc} = \frac{U_{dc}}{I_{dc}} \tag{6-3}$$

Here P_{cu_dc} is the copper loss of the prime mover; R_{dc} is the armature resistance. The armature resistance is also verified by measuring after running the machine for some time

The power balance can now be established as:

$$P_{in\_dc} = P_{cu\_dc} + P_{m\_pm} \tag{6-4}$$

P_{m_pm} is the mechanical power lost due to friction and other rotational losses in prime mover and assembly.

Further, the mechanical power loss P_{m_pm} is calculated from three different measurements:

1. First the shaft is not loaded and rotated at different speeds (100-1500 rpm in steps of 100 rpm). The voltage, current and power of the DC motor is recorded at all different speeds. The mechanical power lost in this operation is calculated using (6-3). This power is called P_{m_pm0} i.e. the mechanical loss without the influence of the mass of rotor and stator.
2. Secondly, only the rotor is mounted onto the shaft and the voltage, current and power of the DC motor is recorded at the same speeds in as in 1.The mechanical power lost is calculated using (6-4). This power is called P_{m_pm1} i.e. is the mechanical loss with only the influence of the mass of rotor.
3. Step 2 is repeated using the stator instead of the rotor. The mechanical power loss is called P_{m_pm2} i.e. the mechanical loss with only the influence of the mass of stator.

Finally the mechanical loss at a certain speed is calculated by using

$$P_{m\_pm} = P_{m\_pm1} + P_{m\_pm2} - P_{m\_pm0} \tag{6-5}$$

These measurements provide us with the amount of prime mover and mechanical losses at various speeds. This result is independent of the load so it can be used in both no-load and on-load tests.

Results: The measurement results for both open-slot and closed-slot machines at different speeds are shown in fig. 6.13.

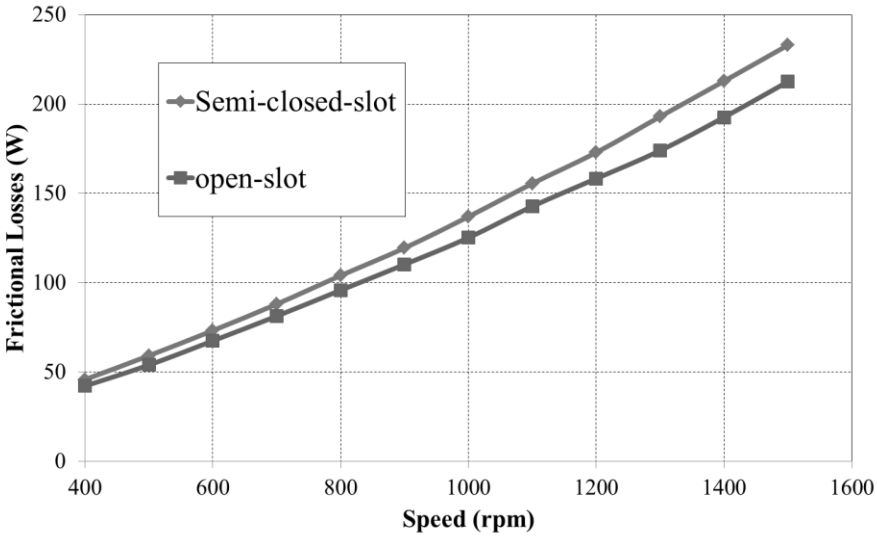

Fig.6.13: Frictional losses for open-slot and semi-closed slot machine

The mechanical loss measured with the semi-closed-slot machine is a little bit higher than with the open-slot machine. This could be due to the slightly higher mass of the semi-closed-slot stator. Each curve shows an almost linear relationship. This implies that most of the mechanical loss comes from bearing losses, because bearing losses vary linearly with speed while air friction losses have a quadratic or even cubic variation with speed.

6.4.3 Rotary Tests Case I: PM excitation but no stator current

There are mainly two sources of magnetic field excitation. The first source is stator currents and the second source is the presence of permanent magnets (PMs). Even in the absence of stator currents, there can be eddy current losses in the machine stator and rotor due to effect of slotting (see fig. 6.14). The losses exist because of change of flux density in stator iron and rotor iron as the magnets pass under stator teeth and slot (air).

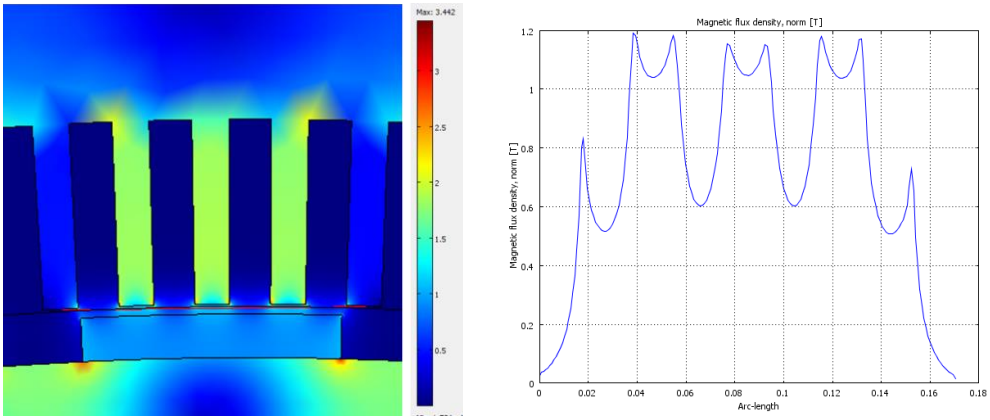

Fig.6.14: Effect of slotting on flux density: Pulsation under teeth and air part of stator alternately

In order to capture these losses, the machine is run on different speeds with no current in the stator (as in a no load test) and losses are estimated.

6.4.3.1 Procedure for the no-load test (Case I)

In this test both the stator and rotor are mounted on the setup. The terminals of PMSG remain open circuited and therefore no current flows in the stator winding. The rotor is driven by the prime mover and the stator is kept stationary by the spring balance arrangement which also measures force. The power balance for this condition can be expressed by modifying (6-1):

$$P_{Fer} = P_{in} - P_{m\_pm} - P_{Fes} \tag{6-6}$$

Here, the meaning of symbols is same as in eq. (6-1)

Equation (6-6) can also be written as:

$$P_{Fer} = P_{mech} - P_{Fes} \tag{6-7}$$

Here P_{mech} is the mechanical power at the shaft measured by using the spring balance.

The spring balance measures mass in kg. The mass in kg is converted into force by multiplying it by g (acceleration due to gravity). This force is then multiplied by the perpendicular distance between the center of the stator and the point of contact of the spring balance hook. The mechanical power can be calculated by multiplying torque with mechanical rotational speed.

$$T_{mech} = mgr$$
$$P_{mech} = T_{mech}\omega_m \tag{6-8}$$

Here T_{mech} is the mechanical torque; m is the mass shown by spring balance;
g is acceleration due to gravity; ω_m is the mechanical rotational speed
r is the perpendicular distance from center of stator to spring balance hook

In this case the electromagnetic power is converted into iron losses (both stator iron and rotor iron) and magnet losses in the machine. It is evident that in the power flow model we have to know the stator iron loss, otherwise only the total iron loss in the machine can be found out. The power is measured at different speeds. The speed range is chosen from 100rpm to 1500rpm with a step size of 100rpm.

6.4.3.2 Separation of Stator and Rotor Iron Losses

The iron losses measured in the tests are the sum of stator and rotor iron losses. Here in this chapter, a method utilizing finite element simulations is used to give an estimation of stator iron losses. The fact that the iron losses in ferromagnetic materials depend on the flux density and its frequency is utilized. Eddy current loss per unit volume can be written as:

$$P_e = K_e f^2 B_m^2 \tag{6-9}$$

K_e is the eddy current loss coefficient; f is the frequency; B_m is the peak magnetic flux density which is a sinusoidal function.

The eddy current loss coefficient is usually hard to determine as it is not a constant. This makes the application of (6-9) rather difficult. Manufacturers of ferromagnetic materials therefore provide the users with curves or look-up tables. The curves or tables show the iron losses as a function of the peak value and the frequency of flux density as shown in fig. 6.15. The material used for the stators in this thesis is M-19-29-Ga fully processed non-oriented silicon steel. Its dependence on peak flux density at various flux densities is provided by the manufacturer.

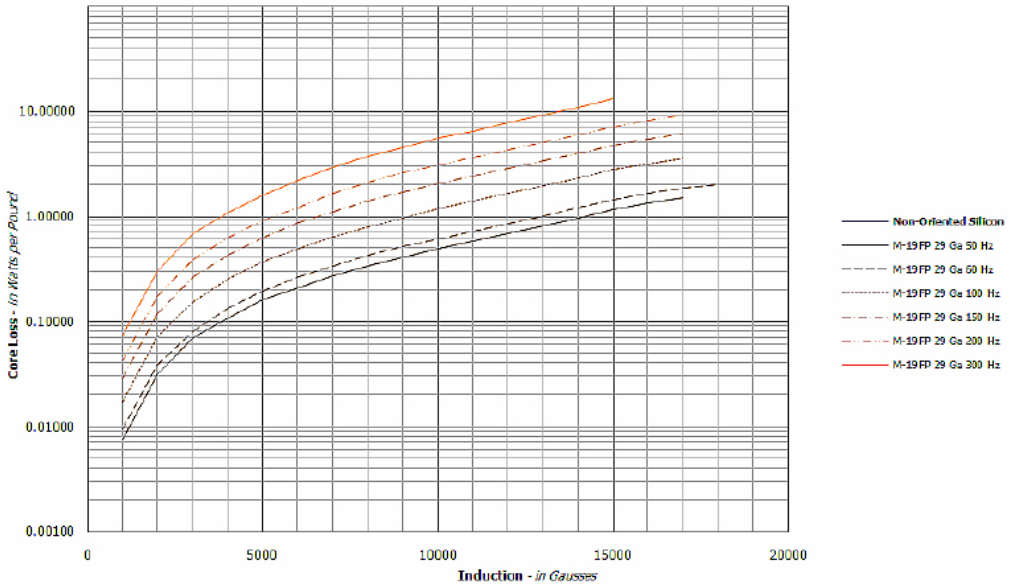

Fig.6.15: Eddy current loss as a function of frequency and flux density

The unit for the flux density is Gauss and for the iron loss is Watt/ Pound. The conversion of these units to SI units follows:

1 Gauss= 0.0001 Tesla ; 1 Watt/Pound=2.20462 Watt/kg

Now the peak values of flux density in the stator iron is estimated. Finite element simulations are used again to solve for the flux density. Using the same geometry and the same parameters of the actual machine, the finite element simulation can provide a relatively precise prediction of flux density in various parts of the stator i.e.in the stator teeth, the tooth caps and the stator yoke (see fig. 6.16). The frequency is the frequency of operation obtained according to the number of poles and the rotational speed of machines. The frequency is calculated as:

$$f = \frac{\omega_m p}{120} \tag{6-10}$$

f is the electrical frequency; ω_m is the mechanical speed in rpm and p is the number of poles

With the peak values of flux density written in Table 6-4, the iron loss per unit mass can be found in each region

TABLE 6-4: PEAK FLUX DENSITY IN VARIOUS PARTS OF STATOR

Stator Part	Tooth	Yoke	Tooth cap
Open slot machine	1.5 T	0.9 T	NA
Semi-closed slot machine	1.65 T	0.95 T	1.40 T

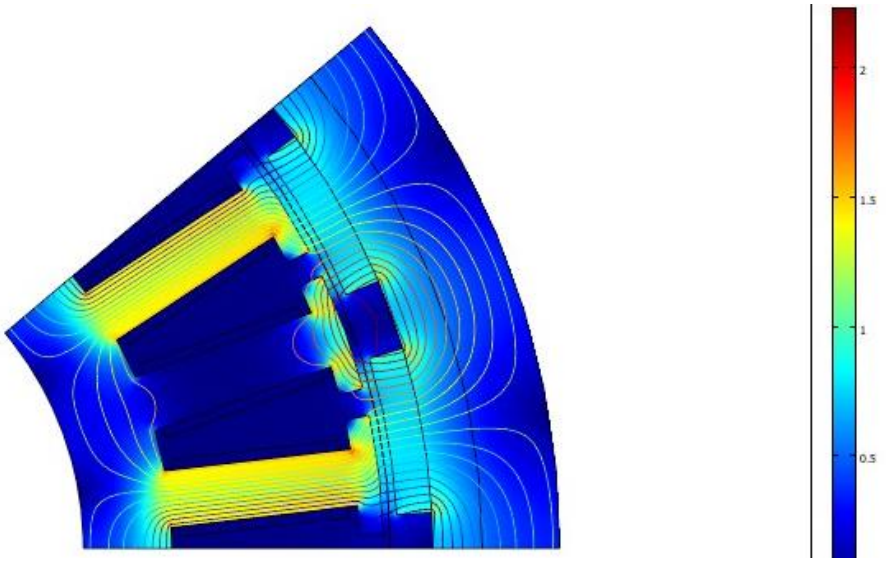

Fig.6.16: Flux density in various parts of stator for estimating stator losses

The mass used is the amount of stator iron material found after subtracting the mass of copper used in winding from total stator mass. Further, since flux density in different parts is different, the mass is calculated using following steps:

1. The total mass of the stator is measured.
2. The total stator iron mass is obtained after the mass of copper windings is deducted.
3. The mass of teeth, tooth caps or yoke is calculated from the geometrical volume after multiplying the volume with the mass density of the stator iron which is uniform.
4. The part of stator yoke in which the flux density hardly varies is deducted. The effective yoke mass contributing to iron losses is approximately 0.6 time of the total mass of yoke. The mass of each region is summarized in Table 6-5.

TABLE 6-5: MASS OF VARIOUS PARTS OF STATOR

Stator Part	Tooth	Effective Yoke	Tooth cap
Open slot machine	2.55 kg	0.99 kg	NA
Semi-closed slot machine	2.02 kg	0.89 kg	0.56 kg

5. Thereafter the iron loss is calculated in each region with its own mass and iron loss per unit mass. The total stator iron loss is subsequently obtained by adding the losses in all regions of the stator iron.

It should be noticed that this stator iron loss is not absolutely accurate but is an estimate. The accuracy is dependent on several factors. One decisive factor is the deterioration of the iron material during its production process. Some processes such as punching and heat treatment can lead to higher iron losses in the iron. A correction factor is thus introduced to take the increase of iron losses due to production process into account. According to experience, the correction factor for iron losses of the open-slot stator is 1.45 and for the semi-closed-slot stator is 1.55. This difference exists because the latter stator has tooth caps which complicate its production and bring about relatively more iron losses than the former.
At this stage, we have the total iron losses measured from the power balance method. In order to get the rotor iron losses, we can simply subtract the estimated stator losses from the total iron losses.

6.4.3.3 Results – Case I

The results for the no load tests i.e. case I are shown in the following figures.

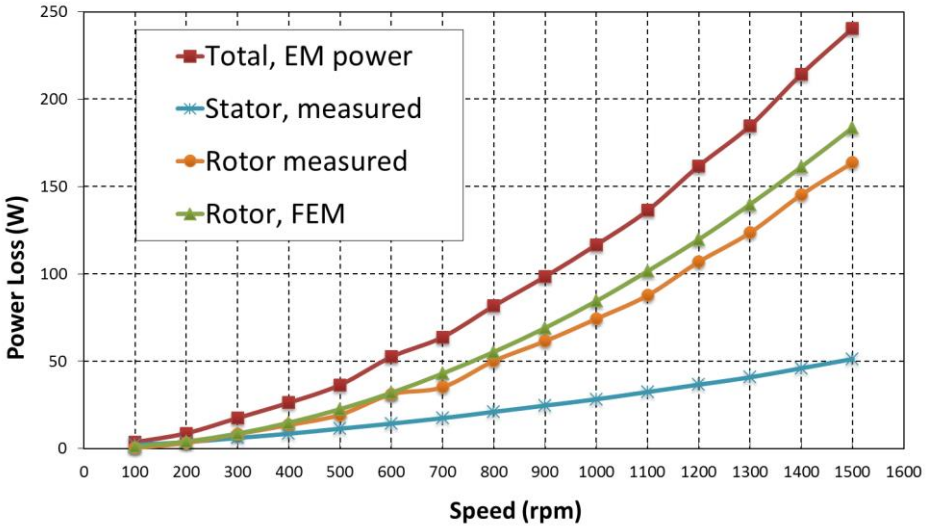

Fig.6.17: No load losses (due to slotting) for open slot machine

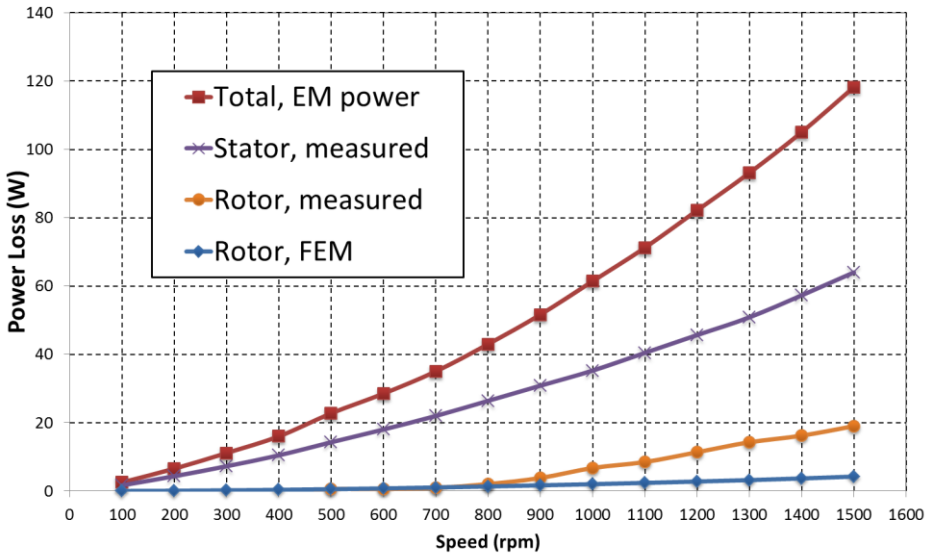

Fig.6.18: No load losses (due to slotting) for semi-closed slot machine

The two machines behave quite opposite to each other in terms of the eddy current

losses in the rotor. In case of the open slot machine, most of iron losses occur in the rotor whereas in case of semi-closed slot machine, losses are higher in the stator. This is because of very little amplitude of flux density pulsations in case of semi-closed machine.

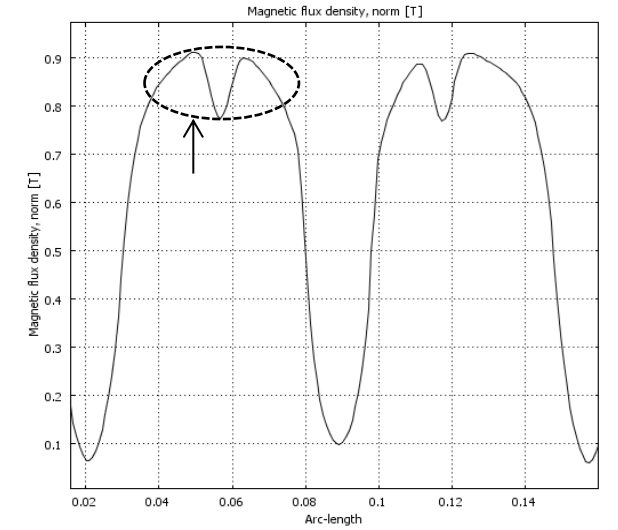

a)

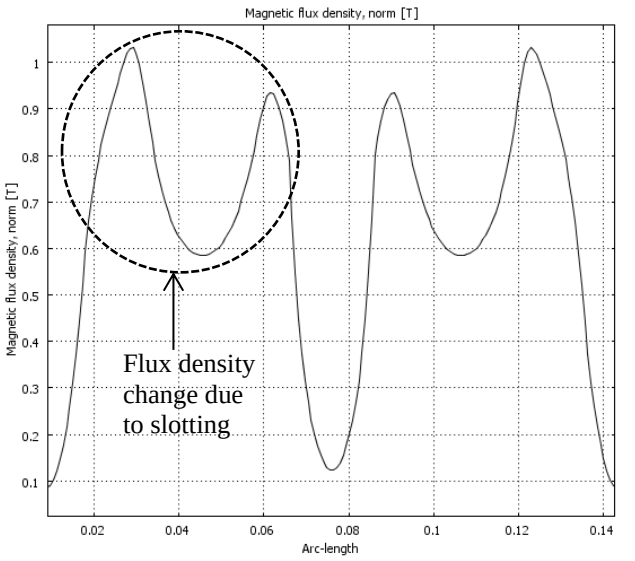

b)

Fig.6.19: Flux density change in the air-gap of a) semi-closed slot machine has very low change of flux density b) open slot machine has much larger change in flux density

6.4.4 Rotary Tests Case II: PM excitation with stator current

In order to find the influence of armature currents together with magnets on iron losses, we connect the machine used as a generator (PMSG) to a purely resistive load. Therefore there is a current flow in the stator windings due to generated voltage and connection of load. The resistors are adjusted for various values and the PMSG is rotated at different speeds. The idea is to keep the current constant while the speed changes.

6.4.4.1 Procedure for the on-load test (Case II)

For each load condition (current at a particular value) and speed, the total iron loss is measured by using the power balance method. The power flow can be written as:

$$P_{Fe} = P_{mech} - P_{Cus} - P_{Load} \tag{6-11}$$

Here, P_{Cus} is the copper loss in the stator; P_{Load} is the power consumed by load.
The copper loss in the PMSG is calculated as

$$P_{Cus} = (I_a^2 + I_b^2 + I_c^2)R_s \tag{6-12}$$

Here R_s is the resistance of each phase of the stator winding. R_s at different frequencies is found by looking up the results in fig 6.8 and 6.9. These resistance values are adjusted for the temperature rise using the standard temperature coefficient of resistance of copper at 0.00393 ohm/^{0}C.
I_a, I_b and I_c are the currents in each phase

The output power is calculated as the sum of power lost in all three-phase loads:

$$P_{Load} = U_a I_a + U_b I_b + U_c I_c \tag{6-13}$$

U_a, U_b and U_c are the voltages across the load resistors

We do not use the load resistance to calculate the power dissipated here because:

1. The load resistance can be measured only when the PMSG is offline while voltages can be measured on line.

2. The load resistance is quite sensitive to temperature. Precise measurement is difficult especially when the resistor is offline, because the temperature of the resistor decreases fast.

The RMS values of current for the both PMSGs are selected as 4A, 7A, 10A and 13A. The chosen speeds for both PMSGs are 600rpm, 800rpm, 1100rpm, 1200rpm, 1300rpm, 1400rpm and 1500rpm. Too low speeds (e.g. 100 rpm, 300rpm) could lead to unacceptable errors in measurement so they are not used.
The rotor iron losses are calculated by estimating the stator losses and subtracting them from the total iron losses measured experimentally. The details of this procedure are already explained in section 6.4.3.2 (separation of stator and rotor iron losses).

A note on temperature of magnets: The magnets used in the rotor of the PMSGs are rare-earth type. The remanent magnetic flux density is dependent on temperature. Therefore, it is important to adjust the value of remanent flux density (B_r) for modeling purposes. It becomes all the more important in the on-load test because different values of current lead to different values of losses and hence different temperature of magnets as shown in table 6-6.

TABLE 6-6: TEMPERATURE OF MAGNETS IN DIFFERENT EXPERIMENTS

Current	Temperature of Magnets in Open Slot Machine (^{0}C)	Temperature of Magnets in Semi-closed Slot Machine (^{0}C)
No Load	70	70
4 A	70	70
7 A	75	75
10 A	80	75
13 A	90	75

6.4.4.2 Results – Case II: Stator currents and PM excitation

This case represents the actual scenario which brings out deviations from FE models. Since analytical model is limited by complex geometry and FE model is 2d, this case presents the most "close to reality" scenario. The losses due to end effects and other material non-linearities are also present in these measurements. The results of these experiments are shown in fig. 6.20 for open slot machine and in fig. 6.21 for semi-closed slot machine.

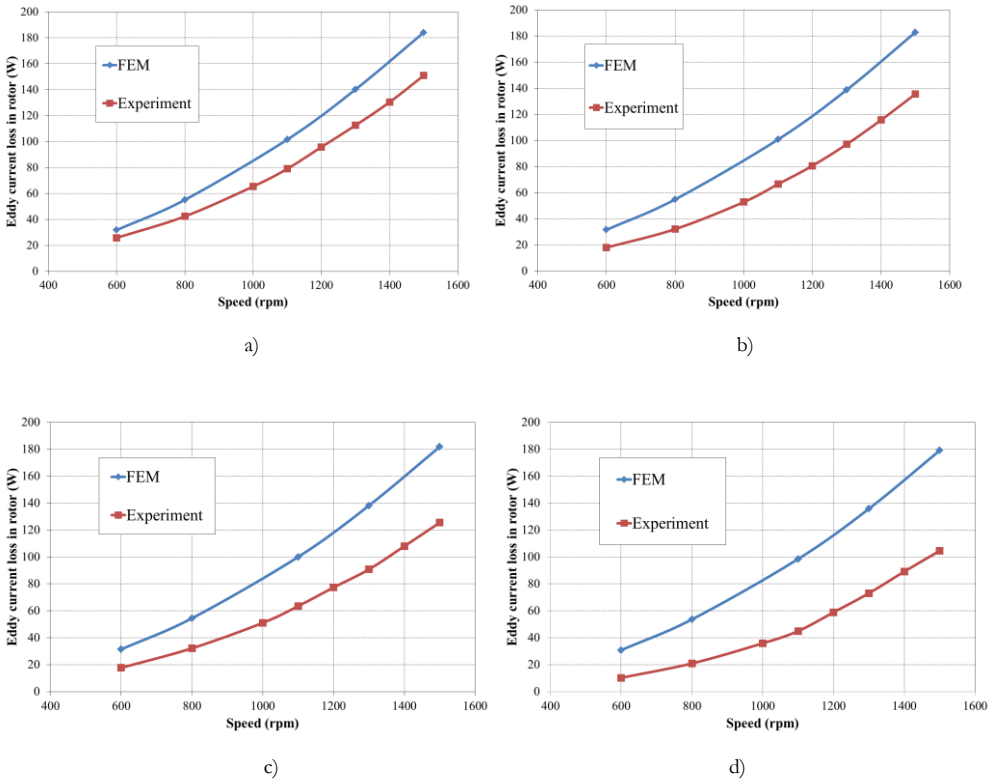

Fig.6.20: Losses due to both stator currents and PMs in open slot machine for a current of a) 4A b) 7A c) 10A d) 13A

The FE method predicts higher losses than the experimental measurements. As we load the stator more, the difference between the experimental and FE values of the losses increases. It may be noted that the FE model predicts almost same amount of losses for all different current loading whereas the experimental values decrease as the current loading increases. In general, the eddy current losses increase with speed. This is expected because the eddy current losses increase as square of frequency.

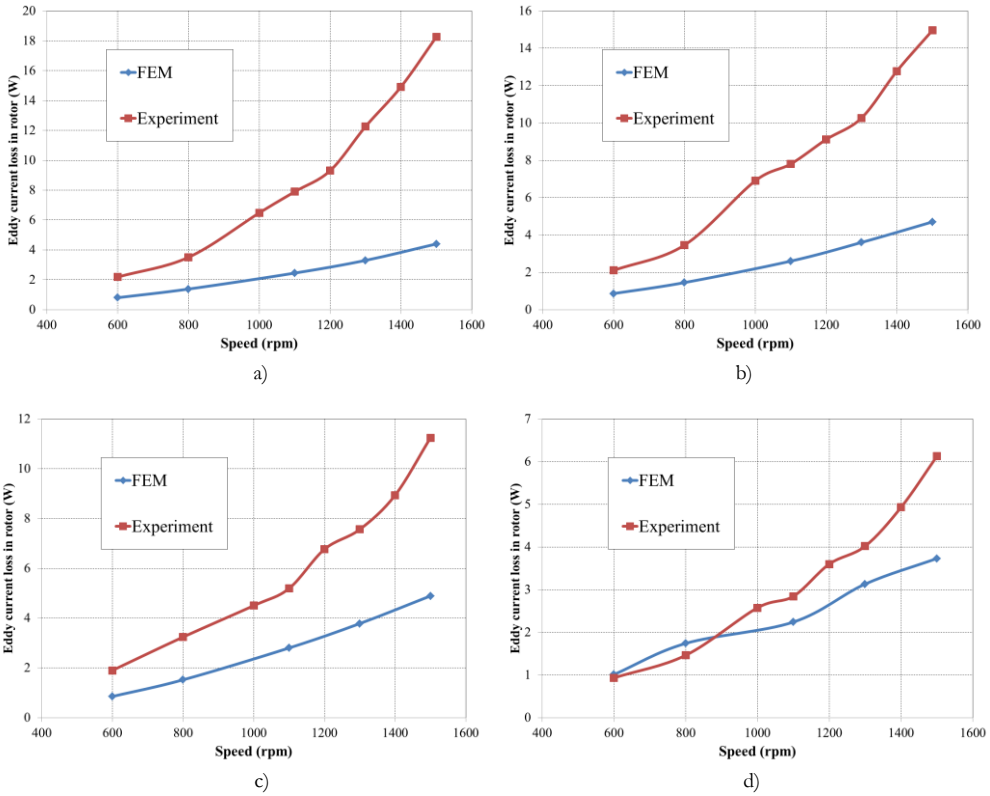

Fig.6.21: Losses due to both stator currents and PMs for semi-closed slot machine for a current of a)4 A b) 7 A c) 10 A d) 13 A

In case of the semi-closed slot machine, the FE method predicts lower losses than the experimental measurements. As we load the stator more, the difference between the experimental and FE values of the losses decreases. It may be noted that the FE model predicts almost the same amount of losses for all different current loadings except when the current increases to 13 A. As seen in the case of open-slot machine, the experimental loss values decrease as the current loading increases. This difference in loss prediction can be explained by:

a) The stator iron loss: The FE model is a 2d model whereby, the laminations and current induced in laminations can't be modeled. Therefore, the stator losses are not included in the model. This results in almost constant loss prediction by FE model although current is varied. On the other hand, the iron losses in the stator are estimated and subtracted from the total iron loss in experimental results. The results from the experiments show that as we increase the stator current, losses in the stator increase whereas the iron losses in the rotor decrease. This is a direct consequence of using

power balance. Since the quantity of interest is resulting from difference of two large quantities, the measurements are very sensitive. The actual power values and resulting stator iron loss calculation is shown in fig. 6.22 for the case of 4 A loaded condition of semi-closed slot machine. This case is chosen because the rotor iron losses are very low as compared to the other power measurements.

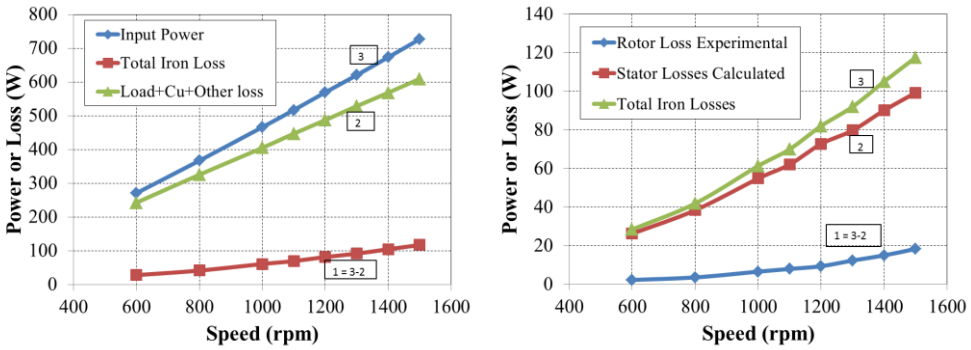

a) b)

Fig.6.22: Loss Calculation Procedure: a) Total Iron Losses from Experiments b) Rotor Iron Losses deduced after estimating stator iron losses

In fig. 6.22 (a), the total iron losses (curve 1) are deduced by subtracting power dissipated in load + copper losses (curve 2) from input power at shaft curve 3. This is shown as curve 1 = curve 3 – curve 2 in the figure.

Similarly, fig. 6.22 (b) shows the rotor losses (curve 1) deduced by subtracting stator losses calculated (curve 2) from total iron losses (curve 3). Notice the scale change from fig. 6.22 (a) to fig. 6.22 (b).

b) The inaccuracy in torque measurement: The inaccurate measurement of torque to calculate input mechanical power to the generator can be a reason for deviation. This is all the more important in the case of semi-closed slot machine because the space harmonic content of mmf is low and therefore the induced eddy current losses are low(~10 W) compared to losses in case of open slot machine (~100 W).

c) End effects: The FE model being 2d, is not capable of handling all the end effects which can be prominent for the machines used for experiments (axial length comparable to pole pitch). The end effect means that the induced current circulates in loops in the solid conductive parts as shown in fig. 6.23. The induced current circulates along x- axis as well as along z-axis. The 2d model doesn't consider the current (and hence the loss) along the path of x-direction. This factor might be ignored if we are comparing larger PM machines having axial length >> pole pitch so that the current loop has a much

larger length than width.

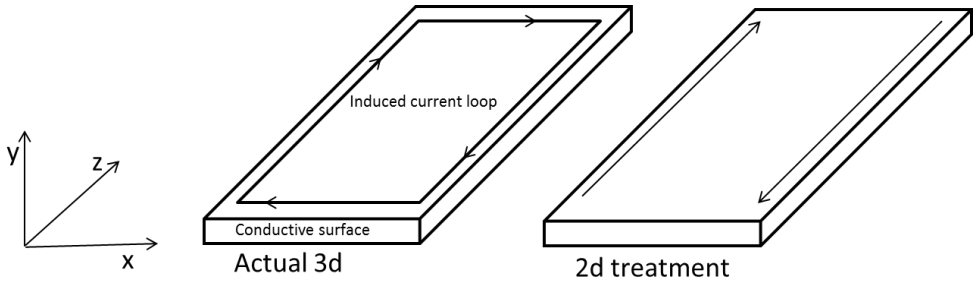

Fig.6.23: Eddy current loop in 3d and 2d treatment of induced current.

d) Effect of Phase angle: It has been assumed in the FE model that the phase angle between current and EMF is zero. In reality, there can be a phase difference due to different loading conditions. A fictitious phase angle was given to see the effect of such a variation. Since normally this angle is small for purely resistive load, even if it is a factor responsible for deviation, the magnitude is not considerable.

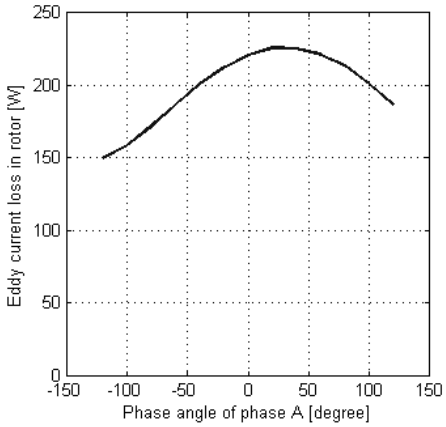

Fig.6.24: Effect of phase angle of current on eddy current loss calculation

6.4.5 Rotary Tests Case III: No PM excitation, only stator current

This case is a special case which is supposed to validate the analytical model because these are the conditions actually used in the analytical modeling. The PMs are replaced by un-magnetized magnets of the same material. This leads to the condition that eddy

current losses are present but the effect of PM field is not present. The analytical model is based on this scenario. The underlying idea is that the effect of slotting is primarily the same for different slot-pole combinations as long as stator geometry is same. This means that the eddy current losses due to PM field and slotting are more or less constant across the range of slot-pole combinations. It is the stator current excitation that defines the trend.

6.4.5.1 Procedure for Case III: Only stator currents no PM field

In this test both the stator and rotor (with un-magnetized PMs) are mounted on the setup. The terminals of the machine are connected to a variable frequency power supply such that a constant current of 9 A is made to flow through the stator at a particular frequency.

The rotor is driven by the prime mover and the purpose is to rotate the rotor at corresponding synchronous speed so that load torque is zero. The machine acts as a motor and all the mmf in the airgap is due to stator currents. The rotor tries to rotate under the effect of the torque producing harmonic but the prime mover rotates the rotor at synchronous speed and counters the load torque.

Therefore the electromagnetic energy exchange can be seen as limited to the machine part where iron losses are induced by the stator field (space harmonics). These iron losses are responsible for the counter-torque at synchronous speed. The power flow can be simply written as:

$$P_{Fe} = P_{ac} - P_{Cus} \tag{6-14}$$

Here, P_{Cus} is the copper loss in the stator; P_{ac} is the power supplied to stator, measured directly from the power supply. The copper loss in the PM machine is calculated as:

$$P_{Cus} = (I_a^2 + I_b^2 + I_c^2)R_s \tag{6-15}$$

Here R_s is the resistance of each phase of the stator winding. I_a, I_b and I_c are the currents in each phase. The main steps for experiment are:

The stator is supplied by variable frequency supply and the rotor is rotated at synchronous speed shown in table 6-7. The total iron losses are estimated from the power balance. Then, the rotor iron losses are calculated by estimating the stator losses and subtracting them from the total iron losses measured experimentally. The details of this procedure are already explained in section 6.4.3.2 (separation of stator and rotor iron losses).

TABLE 6-7: FREQUENCY AND CORRESPONDING ROTATIONAL SPEED

Frequency (Hz)	Rotation speed (rpm)
45	300
90	600
135	900
180	1200
225	1500

6.4.6 Results – Case III: Stator current excitation only

As discussed in sections 3.1 and 3.2, the concentrated windings induce losses in the solid conductive parts of the machine. In order to capture these losses, the machines' PMs are replaced with un-magnetized magnets so that eddy current losses due to stator currents can still exist while losses due to PM field are absent.

In principle, this could lead to validation of loss calculation in the analytical model. However because of only stator currents present and a relatively large air gap, lot of flux doesn't cross the air gap. Thus the losses in rotor are expected to be rather low. Consequently in order to proceed with meaningful results very sensitive torque measurements are required. The results are presented in figs. 6.25-6.27. No definite validation can be confirmed.

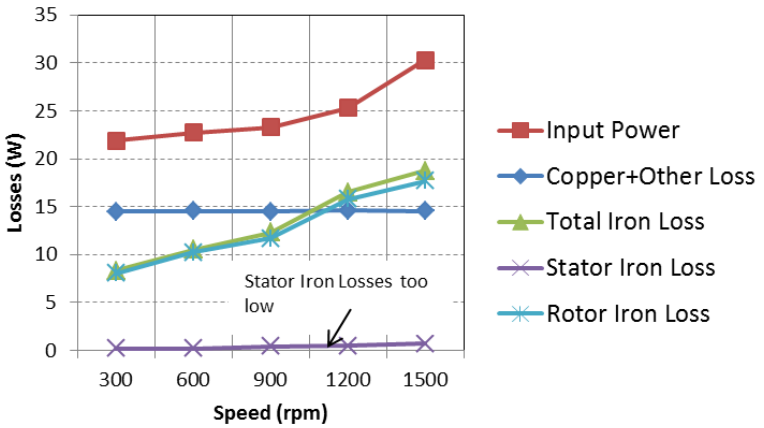

Fig.6.25: Losses calculation (shown for the case of open slot machine)
Here, Rotor Losses = Input power – Copper losses – Stator iron losses;

Fig. 6.25 shows the calculation process used to find out the rotor losses. The input power is measured at different speeds and copper losses are subtracted. The remaining losses are mainly iron losses in stator and rotor. From the total iron losses, the stator iron losses are subtracted to find out rotor iron losses. It can be seen that the copper

losses are dominant and stator losses are under-estimated. Therefore, the rotor losses calculated are over-estimated. However, if we look at fig. 6.26 and fig. 6.27, the experimental losses are still higher. This discrepancy is the result of very low torque available to measure and hence measurement inaccuracy. Hence both measurements and calculations are uncertain and nothing concrete can be concluded from these set of experiments.

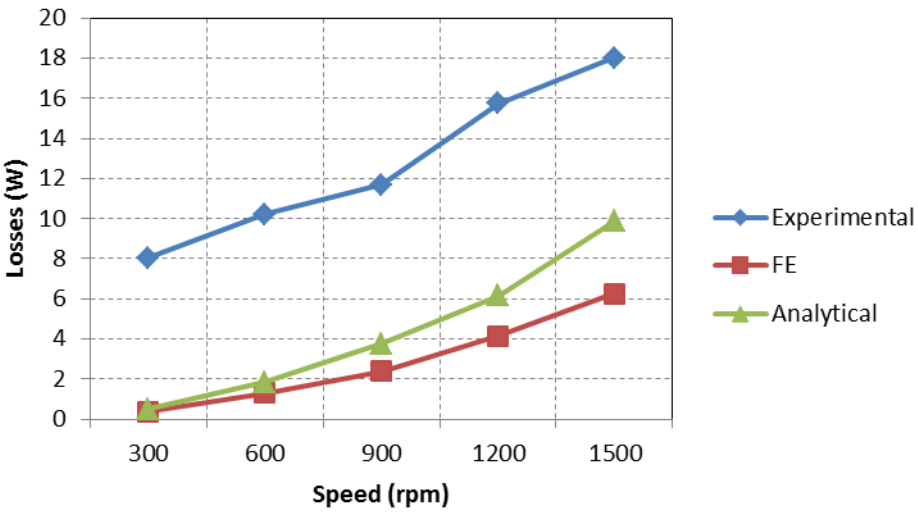

Fig.6.26: Losses due to stator current excitation only and no active PM field for open slot machine

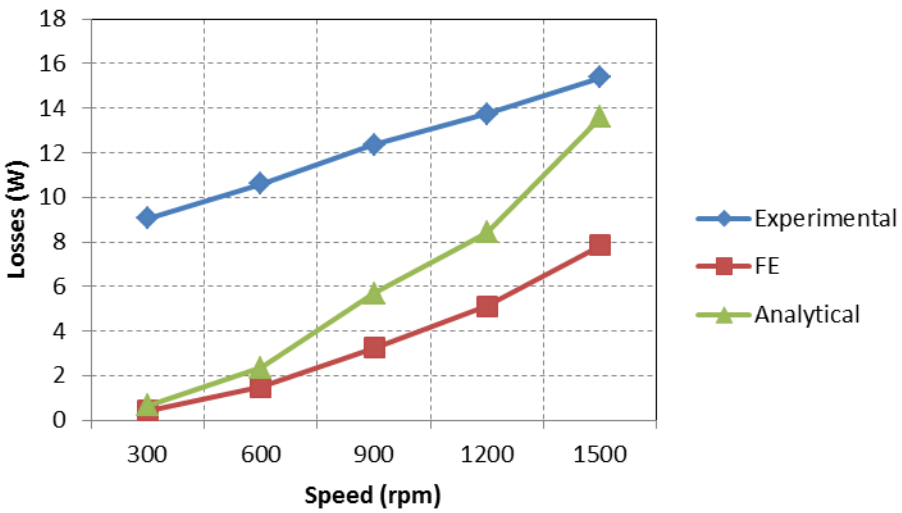

Fig.6.27: Losses due to stator excitation only and no active PM field for semi-closed slot machine

The reasons for deviation between FE, analytical and experimental results can be:

a) Inaccuracy in the torque measurement.
b) Under-estimation of stator iron losses because of 2d analysis used whereas in reality, end effects are considerable.

6.5. Summary

A framework for carrying out experiments in order to validate eddy current modeling techniques has been presented. These experiments are conducted in various stages leading to comparison of various aspects of models in each stage. The method of measurements and the results thereof are documented. Two sets of experiments are conducted i.e. stationary for validating analytical models and rotary for validating both FE and analytical models. The static set of experiments fairly validates the analytical model formulation. In the rotary tests, the eddy current losses in the rotor due to different excitations of the machine are separately analyzed and compared with models for validation. The excitations used for loss calculation are stator slotting effect, winding space harmonics and both excitations combined.

.

Bibliography

[1] S.R.Holm, "Modelling and optimization of a permanent magnet machine in a flywheel," Ph.D. dissertation, pp. 62-66, Dept. Electrical Power Engineering, TU Delft, The Netherlands, 2003.

[2] H.Polinder, "On the losses in a high-speed permanent-magnet generator with rectifier," Ph.D. dissertation, pp. 12-16, Dept. Electrical Power Engineering, TU Delft, The Netherlands, 1998.

[3] K.J.Binns,P.J.Lawrenson and C.W. Trowbridge, "The analytical and numerical solution of electric and magnetic fields", 1995 edition, John Wiley & Sons publisher, pp. 3-6 and pp. 95-97.

[4] J. Cros, P. Viarouge, "Synthesis of high performance pm motors with concentrated windings", IEEE Transactions on Energy Conversion, vol. 17, pp. 248–253 (2002).

[5] F. Magnussen, C. Sadarangani, **"**Winding factors and Joule losses of permanent magnet machines with concentrated windings," in Proc. of the 2003 IEEE International Electric Machines and Drives Conference**,** 2003, pp. 333 – 339, vol.1.

[6] H. Polinder, M.J. Hoeijmakers, M. Scuotto, "Eddy-current losses in the solid back-iron of permanent-magnet machines with concentrated fractional pitch windings," in Proc. of the 2006 IEE International Conference on Power Electronics, Machines and Drives, Dublin, 4-6 April 2006, pp. 479-483.

[7] A.K.Sawhney , A course in Electrical Machine Design, 5th edition, Dhanpat Rai and Co. Publishers, pp.122-127.

[8] Haylock, J.A.; Mecrow, B.C.; Jack, A.G.; Atkinson, D.J.; , "Operation of fault tolerant machines with winding failures," Energy Conversion, IEEE Transactions on , vol.14, no.4, pp.1490-1495, Dec 1999.

7. Trends and Design Guidelines

This chapter aims at bringing out trends in eddy current loss depending upon the slot-pole combination used. Since the eddy current loss analysis is not the only major factor influencing the design, other indicators of machine performance such as cogging torque, balanced winding layout etc are briefly explained. The purpose is to present a more complete picture of design selection. This information might be trivial for electrical machine design experts but for a general reader and students this additional information is useful and hence included. The FE models are used to determine effect of selecting a slot-pole combination on eddy current losses in rotor of machine. The overall goal is to draw some trends and guidelines on selecting slot-pole combinations for concentrated winding topology for wind turbines.

7.1. Introduction

The performance of electrical machines is governed by many factors. Different types of machines have different sensitivities to machine parameters. As discussed throughout this thesis, eddy current losses are of prime importance when we discuss PM machines with concentrated windings. There are many other design characteristics which define machine performance in general. Some of the important aspects which need due attention at an initial stage of design are:

a) Winding factor
b) Balanced windings
c) Cogging Torque
d) Rotor force balance

These are not all the parameters which have to be considered for an optimal machine design but are some important parameters for an initial design. There is a lot of literature available on utility of these design parameters. Therefore, these are just introduced here to give an overview. Once these parameters are chosen, a unique slot-pole combination

geometry can be obtained. The weight, cost, reliability and other performance parameters can then be derived for a particular design.

The primary comparison is still the eddy current loss analysis in this particular chapter. The trend analysis is based on a stator chosen to represent approximately a 1.25 MW wind turbine generator. The specifications for this configuration are mentioned in table 7.1. The number of rotor poles was varied keeping the ratio of pole-pitch to magnet span constant. Further, the air-gap velocity for the rotor surface was kept constant for all the slot-pole combinations listed in table 7-2.

TABLE 7-1: SPECIFICATION OF ANALYZED MACHINE

Stator Parameters	
Outer radius	1527.9 mm (NB: specified: circumference 9.6 m)
Yoke thickness	55 mm
Slot height	80 mm
Slot width	50 % of slot pitch
Coil current	2750 A (peak)
Current angle	0 °
Stator μ_r	4000
Airgap	5 mm
Stack length	1 m
Power range	1.1-1.3 MW
Surface speed	4 m/s (~27.5 RPM)
Rotor Parameters	
Magnet thickness	20 mm
Magnet span	70 % of pole pitch
Yoke thickness	35 mm
Magnet resistivity	1 μΩm
Yoke resistivity	200 nΩm
Yoke μ_r	200
Magnet remanent flux density B_r	1.2 T
Magnet μ_r	1

7.1.1 Slot-pole Combinations Used

TABLE 7-2: DIFFERENT SLOT-POLE COMBINATIONS ANALYZED

S No.	Combination		Winding Factor	Number of poles for 144 slots	Slots/pole/phase q
	slot	pole			
1	3	2	0.866	96	0.50
2	3	4	0.866	192	0.25
3	9	8	0.945	128	0.38
4	9	10	0.945	160	0.30
5	12	10	0.933	120	0.40
6	12	14	0.933	168	0.29
7	18	14	0.902	112	0.43
8	18	22	0.902	176	0.27
9	24	22	0.949	132	0.36
10	24	26	0.949	156	0.31
11	36	26	0.867	104	0.46
12	36	34	0.953	136	0.35
13	36	38	0.953	152	0.32
14	36	46	0.867	184	0.26
15	48	34	0.859	102	0.47
16	48	38	0.907	114	0.42
17	48	46	0.954	138	0.35
18	48	50	0.954	150	0.32
19	48	58	0.907	174	0.28
20	48	62	0.859	186	0.26
21	72	50	0.848	100	0.48
22	72	58	0.912	116	0.41
23	72	62	0.933	124	0.39
24	72	70	0.955	140	0.34
25	72	74	0.955	148	0.32
26	72	82	0.933	164	0.29
27	72	86	0.912	172	0.28
28	72	94	0.848	188	0.26
29	144	98	0.837	98	0.49
30	144	106	0.874	106	0.45
31	144	110	0.89	110	0.44
32	144	118	0.917	118	0.41
33	144	122	0.928	122	0.39
34	144	130	0.944	130	0.37
35	144	134	0.95	134	0.36
36	144	142	0.955	142	0.34
37	144	146	0.955	146	0.33
38	144	154	0.95	154	0.31
39	144	158	0.944	158	0.30
40	144	166	0.928	166	0.29
41	144	170	0.917	170	0.28
42	144	178	0.89	178	0.27
43	144	182	0.874	182	0.26
44	144	190	0.837	190	0.25

7.2. Results: Eddy Current Loss Trends

The results for the eddy current loss analysis are presented in this section. There are two different excitations responsible for the eddy current losses in solid conductive parts of the analyzed machine. The first excitation is due to the current in the stator winding. The second excitation source is the pulsation of magnetic field due to effect of slotting. The effect of these different excitations is elaborated on the conductive parts of the machine. Three simulations are executed for each slot-pole combination:

1. One with the rated remanent flux density of the PMs and no stator currents, thus providing the losses due to slotting.
2. One without PM magnetization, but with nominal stator currents, thus providing the losses due to space harmonics due to the stator current.
3. One with both magnets and currents applied, to confirm that the superposition of 1 and 2 applies.

In figures 7.1 and 7.2 the back-iron and magnet eddy current losses are presented.

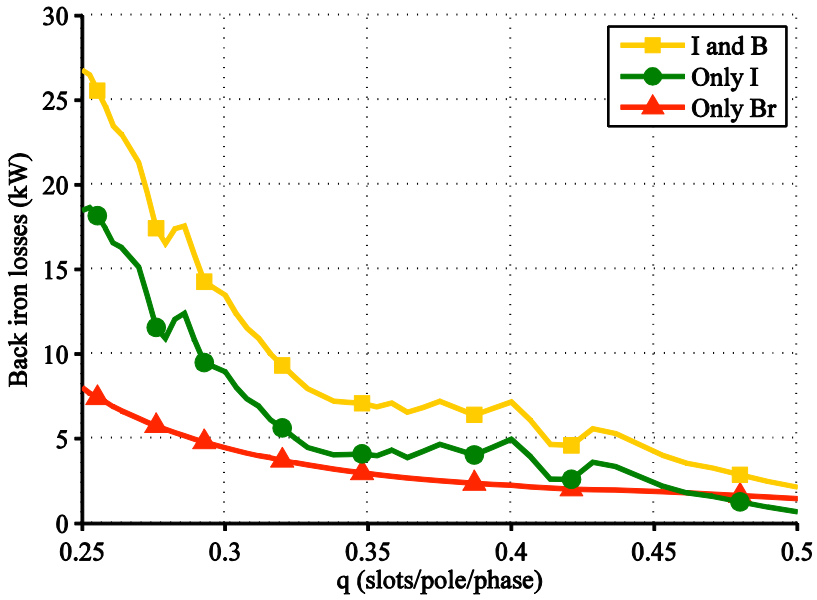

Fig.7.1: Losses in the solid rotor back-iron due to stator currents only (I), PMs only (Br) and combined field (I and B)

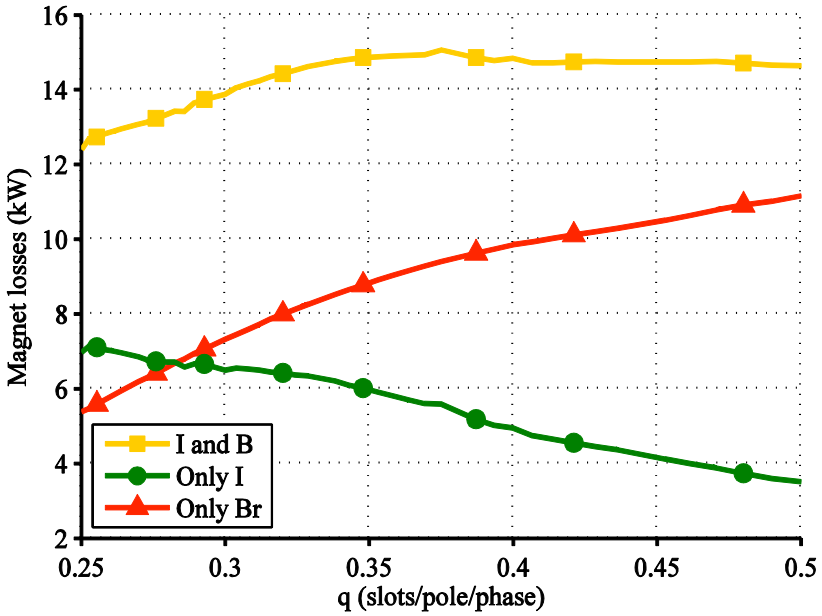

Fig.7.2: Losses in the magnets due to stator currents only (I), PMs only (Br) and combined field (I and B)

A brief inspection reveals that superposition principle can be applied for the two different excitations. In the case without currents but with PM active, some shielding of the magnet eddy current losses due to back iron eddy-currents can be observed for low values of slots per pole per phase i.e. q.

In the losses due to space harmonics no shielding effects are visible and the losses increase with decreasing q (i.e. increasing electrical frequency). As a result, the relative variation in magnet losses is 22 % over the full range of q, while the minimum and maximum iron losses differ by more than 10 times.

It can be seen from fig. 7.3 that the trend for loss analysis is mainly governed by the rotor back-iron losses and total magnet losses are more or less comparable for different slot-pole combinations. This means that if we want to find trends within slot-pole combinations, then analytical model which gives a qualitative comparison of losses due to stator currents alone is sufficient.

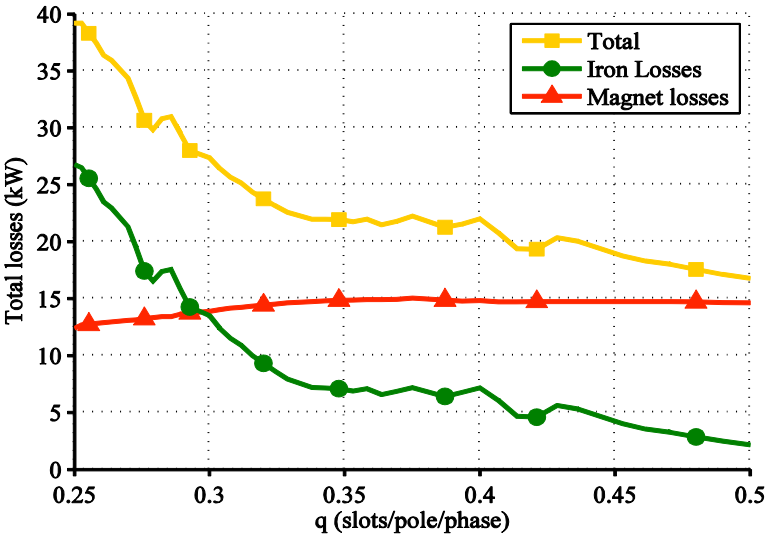

Fig.7.3: Total losses in the machine due to combined field

For q > 0.35 the losses remain relatively constant and the decision for a certain slot-pole combination should be based on other criteria. One possibility is to consider the mechanical power, shown in fig. 7.4 which shows a peak around q = 0.35.

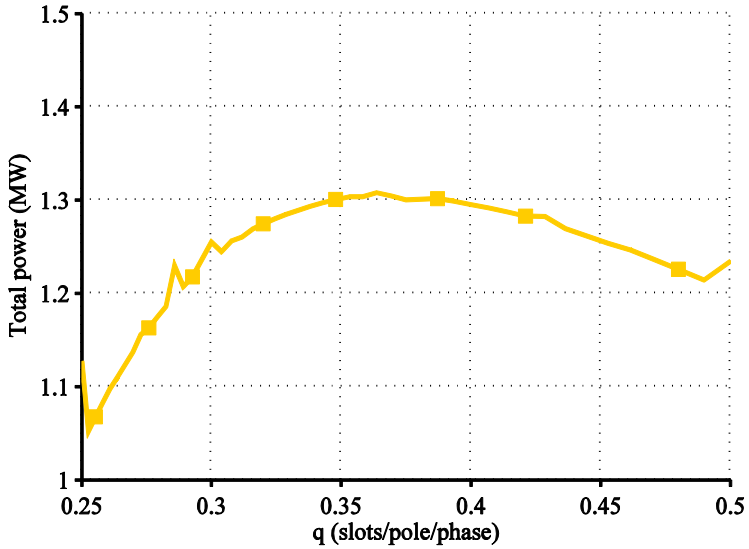

Fig.7.4: Mechanical power as a function of q for chosen topologies

The rotor losses relative to the mechanical power are presented in fig. 7.5 again showing that any slot-pole combination with q > 0.35 performs similar from a rotor loss perspective.

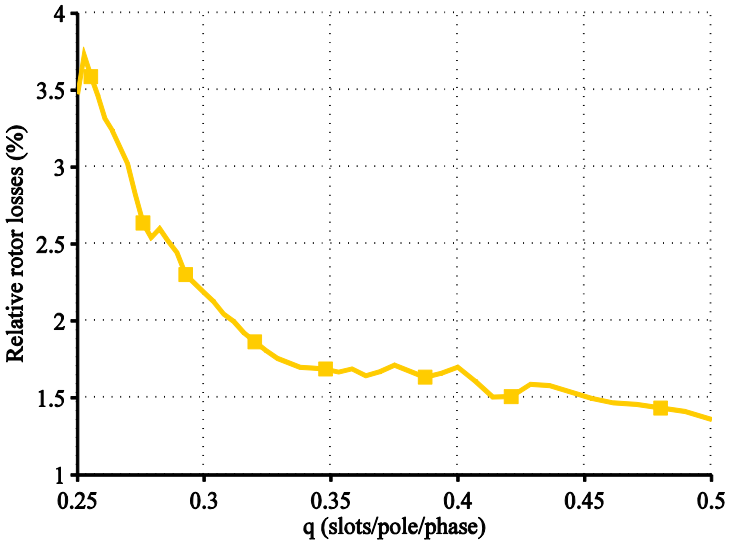

Fig.7.5: Total rotor losses as a fraction of mechanical power

7.3. Other Design Considerations

As mentioned in the introduction section, in a complete design of machine, eddy current losses are not the only design criteria. There are many other design considerations which result in an optimal design. The important ones are mentioned in this section as a general guideline. These have been introduced to lay emphasis on totality of eddy current loss analysis in context of a complete machine design.

7.3.1 Winding Factor

There are many definitions of winding factor, available in literature [7]. In very simple words, to form a concept, winding factor can be defined as:

"T*he ratio of the phasor sum of emf generated by individual coils of a distributed winding to maximum emf that can be generated with a full pitch, concentrated winding*".

Winding factor is in a way an indicative of how "efficiently" emf can be generated by a given sequence of connected coils. If all coils were full pitch and concentrated, it would mean a winding factor of 1. The winding factor is made up of three components

a) Distribution factor: To take into account the fact that the coils are distributed along the stator periphery and not at one place.

b) Pitch factor: This reduction factor takes into account the effect of short-pitching of coils i.e. if the coil may doesn't span full pole pitch or 180 degrees electrical.

c) Skewing factor: To take stator and/or rotor skewing into account. In this thesis this factor is ignored for all relevant calculations.

The winding factor is then given as multiplication of the distribution factor, pitch factor and skewing factor. The significance of winding factor lies in the fact that average electromagnetic torque of a machine is directly proportional to the winding factor. A lower winding factor results in a lower torque or in other words, to get the same torque, we need a bigger machine. As shown in fig. 7.6, the winding factor for fractional slot windings tends to decrease substantially for $q<0.25$ and for $q>0.5$ [2] and [3]. Due to this reason, in the trend analysis, the q values were chosen to vary from 0.25-0.5.

It may be noted that for q = 1, the winding factor is only 0.5. This is because of the assumption made in [3] that the phase spread is assumed to be 60 electrical degrees (which is common). For a 3 phase system and q =1, there are 3 slots under one pole. Since one pole spans 180 electrical degrees, one coil will spread 60 electrical degrees. Therefore as shown in equations (5)-(9) in [3], the distribution factor =1 however the pitch factor = 0.5 resulting in a winding factor of 0.5.

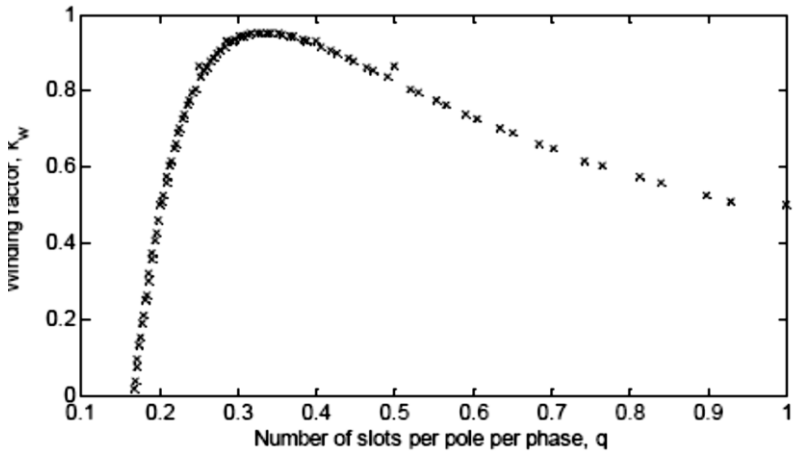

Fig.7.6: Variation of winding factor with slots per pole per phase 'q' [3]

7.3.2 Balanced Set of Windings

In most cases of electrical machine design, we use 3-phase windings. The 3-phase windings of a machine must be balanced in order to avoid noise, torque-ripple and unbalanced forces on machine structural parts.

"A balanced winding has coils arranged in such a way to produce a symmetrical system of equally time-phase displaced emfs of identical magnitude, frequency and waveform."

It is quite easy to know if a slot-pole combination will yield a balanced winding or not because it depends only on the number of slots and poles.
In order to obtain a balanced winding:

"The slots per phase for each periodic part of machine should be an integer number and not a fraction."

Periodic part of the machine simply means the set of slots and poles which repeats itself as we go around machine periphery. The number of periodicities of a slot-pole combination is given by Greatest Common Divider (GCD) of number of slots and number of pole-pairs. Mathematically, the condition for balanced winding may be expressed as:

$$\frac{1}{3}\frac{S}{\mathrm{GCD}\,(S,\,\mathrm{p})} = Integer$$

Here, S is the number of slots, p is the number of pole pairs, 3 is number of phases.

7.3.3 Cogging Torque

The cogging torque is produced by the interaction of PMs with the stator teeth. The PMs always try to align themselves in such a position that magnetic reluctance is minimized.

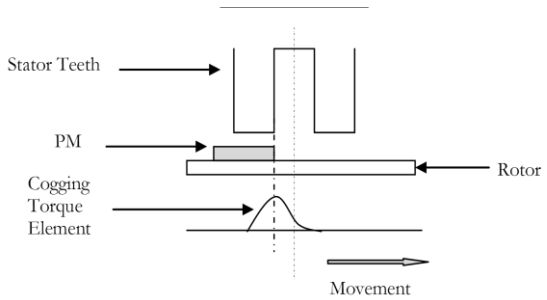

Fig.7.7: Cogging elements contributing to the cogging torque

The magnets on the rotor interact with stator teeth, trying to position themselves in the lowest magnetic reluctance path or in other words they have a preferred position. This phenomenon is called cogging. Figure 7.7 shows that when a magnet edge is near a tooth and approaching, it experiences a pull towards the tooth. This leads to a sudden torque in direction of movement. Similarly when a magnet edge leaves a tooth, it experiences a pull creating a torque against the movement.

Each of this interaction leading to a sudden torque is called a cogging torque element. Net Cogging torque can be expressed as the sum of all such interactions around the rotor periphery. If all of these individual contributions add up, it can lead to a very high cogging torque.

Cogging torque presents problems during start-up of the machine. It may also introduce a torque ripple in total electromagnetic torque. In case a long shaft is used in a machine, and cogging torque is high, it can lead to shaft fatigue. The cogging torque can be easily calculated and negotiated as explained in [4]-[6]. It is shown in these references that magnet span relative to pole-pitch, slot-pole combination and positioning of magnets are the most important factors in negotiating cogging torque.

7.3.4 Rotor Force Balance

The rotor force here refers to the radial outward pull caused on the rotor surface due to magnetic force of attraction between PMs and the stator iron. If due to any reason, the PMs are placed on the rotor in such a way that the distribution of magnets on rotor surface is unsymmetrical, it can lead to local deformation of the rotor and unbalanced magnetic pull. This leads to undue stress on the shaft and bearings.

Such unbalanced pull can also result from manufacturing tolerances, especially parts which define air-gap and low shaft stiffness. More information regarding calculation of this unbalance force is available in [7]

7.4. Summary

The chapter presents trends in eddy current loss evaluation for surface mounted PM machines. The transient 2d FE model developed in chapter 5 is used for that purpose. Some other basic guidelines regarding design of machines are then presented. These other basic guidelines are known in literature but are presented here to put eddy current loss analysis in the overall perspective of machine design. All the guidelines together can be used while designing surface mounted PM machines with fractional slot windings.

Bibliography

[1] J. Cros, P. Viarouge, "Synthesis of high performance pm motors with concentrated windings", IEEE Transactions on Energy Conversion, vol. 17, pp. 248–253 (2002).

[2] F. Magnussen, C. Sadarangani, **"**Winding factors and Joule losses of permanent magnet machines with concentrated windings," in Proc. of the 2003 IEEE International Electric Machines and Drives Conference**,** 2003, pp. 333 – 339, vol.1.

[3] Skaar, S.E., Krovel, O., Nilssen, R.: "Distribution, coil span and winding factors for PM machines with concentrated windings", ICEM-2006, Chania (Greece), Sept.2006, paper 346.

[4] Z. Q. Zhu and D. Howe, "Analytical prediction of the cogging torque in radial-field permanent magnet brushless motors." IEEE Trans. Magn., vol. 28, no. 2, pp. 1371–1374, Mar. 1992.

[5] T. Li and G. Slemon, "Reduction of Cogging Torque in Permanent Magnet Motors", IEEE Transactions on Magnetics, Vol. 24, No.6, Nov. 1988.

[6] N. Bianchi and S. Bolognani, "Design Techniques for Reducing the Cogging Torque in Surface-Mounted PM Motors", IEEE Transactions on Industry Applications, Vol. 38, No.5, Sep. 2002.

[7] A.K. Sawhney "A Course in Electrical Machine Design", Dhanpat Rai and Sons, edition 1997.

8. Conclusions & Recommendations

This chapter summarizes the findings and contributions of the thesis.

8.1. Conclusions

Electrical machine design is a complex and iterative process. There are many different points of view which define the framework of a machine design. A particular design might be best for an application while redundant for another application.

Given this background, we can say that we don't generally go for the technically best possible design but for the most optimum design to suit a requirement. In order to simplify this process, a design engineer might have to shuffle through a variety of designs before selecting the one which is eligible for further optimization. This is where the modeling process is used and having analytical and FE models help during this stage.

This thesis is focused on one aspect of evaluating a design i.e. eddy current loss evaluation in double layer fractional slot windings. However, this thesis highlights other aspects of machine design such as history and trends, manufacturing technology, validation of models and some aspects of machine performance as well. In the following text, we will go through the main interest points presented in each chapter and also highlight contributions of this research work.

Chapter 2: In this chapter, the manufacturing methods for large PM machines used in the industry today are explained. Manufacturing experience for an actual 2 MW PM generator is shared. This knowledge of manufacturing processes is valuable as it provides the reader with details which are not very obvious. This chapter brings out limitations and challenges of current technology which are helpful in forming the thesis objective.

- The large number of coils and manual labor involved in winding manufacture make assembly of generator rather tedious. More time spent on machine manufacture also means higher cost and lower through-put.
- In addition to the material costs, the present winding technology adds a large cost to an already expensive machine. Therefore, it makes sense to explore other methods to wind the generator.

Chapter 3: Eddy current loss analysis in rotating electrical machines is an old and intriguing field. This chapter presents an interesting literature survey on historical development of eddy current loss analysis in rotating electrical machines. This is an important contribution of this thesis as such a survey has not been done before. The survey is completed with many trends in development of analysis methods for the eddy current loss analysis resulting in a journal paper (Chapter 3, [115]).

Chapter 4: In this chapter, an analytical model is developed starting from the basic Maxwell's equations. The strength of this analytical model is its generic nature and simplicity. Although the analytical modeling theory for the eddy current loss analysis already exists but in the field of large direct drive wind turbines the application is rather new. Therefore this work in that sense is a contribution. Due to large size, many safe assumptions can be made which simplifies the model and makes it very generic. Some important conclusions from this chapter are:

- The solution time for the analytical model is in the order of 1-10 seconds depending on the accuracy desired. The model can be adapted very quickly for various slot-pole combinations and an easy comparative study or trend analysis can be performed.
- The solution of this model doesn't require any special expensive software which is a distinct practical advantage. The model can be programmed even in Microsoft Excel. Here however, Matlab was used.
- The eddy current loss trends for various useful slot-pole combinations are derived in this chapter which is a contribution.
- The model also has some limitations (as in over-prediction of losses) especially when a low order harmonic produces eddy current losses.

Chapter 5: In this chapter Finite Element modeling is explained. Some useful slot-pole combinations are compared for eddy current losses and the results thus obtained are presented. The conclusions drawn from the chapter are:

- The FE method is more accurate than the analytical method as it includes the effects of slotting and magnetic saturation.
- In general, analytical model predicts similar trends for eddy current losses when compared with FE model. However in slot-pole combinations where a low order harmonic is responsible for losses, analytical model predicts higher losses.
- The effect of slotting in presence of the PM field and motion produces appreciable losses. These losses can't be ignored but are rather easy to include in a FE calculation.
- A mixed approach of use of analytical and FE models can produce useful results in short time.

Chapter 6: Experiments to validate analytical and FE models developed in chapter 4 and 5 are presented in this chapter. Since experiments are the most close to actual situation in the real machine, they can be used for validation. The extent of deviation from experimental values is documented and reasons are deduced. This is a contribution of this chapter. The eddy current losses are studied for three different excitation cases i.e. PM field only, bringing out effect of slotting; Stator field and PM field bringing out the combined effect of slotting and winding harmonics; Only stator field and no PM field bringing out the effect of only winding harmonics. The following conclusions may be drawn:

- In case of the open slot machine, the eddy current losses due to PM field only (slotting) as well as combined field (PM and stator current) are appreciable and therefore are easier to measure. Both analytical and FE models can be used to predict the approximate amount of losses.
- In case of semi-closed slot machine, the eddy current losses are very low. The present setup can't measure the losses accurately enough therefore the analytical and FE models can't be fully validated for this case.
- In case of excitation with stator current only and no PM field, the experimental results remain inconclusive due to very low amount of losses and measurement inaccuracies.
- 3d effects contribute to substantial mismatch between models and experimental measurements.
- Very sensitive torque measurements are needed to validate the loss models for cases where losses are very low (~10 W)

Chapter7: The purpose of this chapter is to apply the FE modeling method to a number of useful slot-pole combinations and bring out trends in eddy current losses w.r.t. slot-pole combination. The main contribution of this chapter comes from the validation of assumptions used for analytical modeling. It can be concluded that:

- Superposition principle can be used to find total eddy current losses due to slotting effect and winding mmf space harmonics.
- The slotting effect is more or less constant for a given stator geometry, type of magnet and air-gap velocity.
- The power loss due to the winding mmf space harmonics sets the trend for variation of eddy current losses amongst various slot-pole combinations.
- The trend analysis shows that the value of slots per pole per phase (q), around 0.35-0.40 presents a very good operating region in terms of low eddy current losses and high winding factor.

– The slot-pole combinations 12-10 and 9-8 have acceptable eddy-current losses and very high winding factor. The combination 3-2 has very low eddy current losses but also a lower winding factor.

8.2. Thesis Deliverables Revisited

In the section 1.6, the thesis objective, some deliverables from the thesis are listed. Here we take a look at the final status of these deliverables.

a. A simple and generic analytical model for predicting eddy current losses.

This deliverable was completely achieved and a generic analytical model has been developed in chapter 4.

b. Validation of the analytical model using FEM; Validation of analytical and FE models formulation using experiments to bring out effect of simplifications used for models.

The analytical model formulation was validated in chapter 5 with FEM and with experiments in form of static tests in chapter 6. The analytical loss calculation for the experimental machines matched fairly with FEM. However there was significant deviation from the experimental results. Especially in the case where eddy current losses were low, analytical and FE models could not be fully verified experimentally. The main reasons for deviation are 3d effects and inaccurate torque measurements. Therefore this deliverable was partially achieved.

c. Deduction of trends in eddy current losses for various slot-pole combinations

Eddy current loss trends were drawn for a large span of useful slot-pole combinations both analytically and with FEM. Apart from some over-estimation on lower order harmonics, similar trends were obtained by both analytical and FE methods.

d. Design guidelines for PMDD generators with respect to eddy current losses.

Based on the trend analysis for eddy current losses done in chapter 4, 5 and 7, useful slot pole combinations with acceptable losses and winding factors have been identified and recommended. Some other design guidelines are explained briefly to present a perspective of loss analysis in overall design.

8.3. Recommendations for Further Research

This research deals with a very complex phenomenon of eddy current loss modeling. The diffused nature of the induced currents, material anisotropies, measurement inaccuracies and the fact that losses occur inside the material (hence difficult to measure) are some of the main aspects which make this topic very complex. This research is an attempt to provide the machine designer with some modeling methodology to select some useful topologies (at an early design stage) for more rigorous design optimization. However, there are many topics for further research which have been recognized during this work which are mentioned below:

- Since many discrepancies/mismatches amongst models in prediction of losses have been attributed to 3d effects, a natural first recommendation is to investigate eddy current losses in 3 dimensions.
- The experiments can be performed on a more elaborate setup with very accurate torque measurement to gain more confidence in experimental values. This can lead to a better model validation.
- It is also recommended to conduct experiments on a larger number of slot-pole combinations to validate the trend analysis as well.

9. Appendices

9.1. Example of Solution of Partial Differential Equation

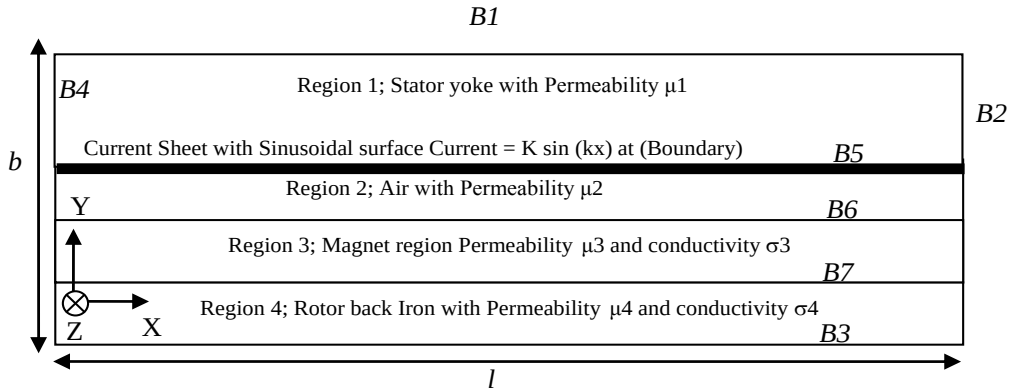

Fig.9.1: Sinusoidal current sheet exitation

Region 1 is iron having permeability $\mu 1$
Region 2 is air, having permeability $\mu 2$
Region 3 is magnets, having permeability $\mu 3$ and conductivity $\sigma 3$
Region 4 is iron, having permeability $\mu 4$ and conductivity $\sigma 4$

The boundary *B1* is located at y = b; *B3* is at y = 0; *B5* is at y = 3b/5; *B6* is at y = 2b/5 and *B7* is at y = b/5

Subscripts 1, 2, 3 and 4 define the region where the quantity is present.

Now using boundary condition on boundary $B1 \Rightarrow A_{z1(x,y=b)} = 0$

$$A_{z1} = \sin kx(g_1 e^{ky} + h_1 e^{-ky}) = 0$$
$$\Rightarrow g_1 e^{kb} + h_1 e^{-kb} = 0 \qquad (9\text{-}1)$$

Using boundary condition on boundary $B3 \Rightarrow A_{z4(x,y=0)} = 0$

When y=0

$$g_4 e^{ky} + h_4 e^{-ky} = 0$$

$$\Rightarrow g_4 + h_4 = 0 \tag{9-2}$$

On boundary B5, when y = 3b/5, we know that

$$A_{z1(x,3b/5)} = A_{z2(x,3b/5)}$$

$$g_1 e^{\left(\frac{3kb}{5}\right)} + h_1 e^{-\left(\frac{3kb}{5}\right)} = g_2 e^{\left(\frac{3kb}{5}\right)} + h_2 e^{-\left(\frac{3kb}{5}\right)} \tag{9-3}$$

On boundary B5 where y = 3b/5, we get

$$\frac{1}{\mu_1}\left(\frac{\partial A_{z1}}{\partial y}\right) - \frac{1}{\mu_2}\left(\frac{\partial A_{z2}}{\partial y}\right) = K \sin kx$$

$$\Rightarrow \frac{1}{\mu_1}\left(g_1 \sinh\left(\frac{3kb}{5}\right) + h_1 \cosh\left(\frac{3kb}{5}\right)\right) - \frac{1}{\mu 2}\left(g_2 \sinh\left(\frac{3kb}{5}\right) + h_2 \cosh\left(\frac{3kb}{5}\right)\right) = \frac{K}{k} \tag{9-4}$$

On boundary B6, when y=2b/5, we know that

$$A_{z2(x,2b/5)} = A_{z3(x,2b/5)}$$

$$\sin(kx)\left(g_2 \cosh\left(\frac{2kb}{5}\right) + h_2 \sinh\left(\frac{2kb}{5}\right)\right) = \sin(\alpha x).\left(g_3 \cosh\left(\frac{2\gamma_3 b}{5}\right) + h_3 \sinh\left(\frac{2\gamma_3 b}{5}\right)\right)$$

Here, $\gamma = \sqrt{k^2 + j\beta^2}$; $k = \alpha$ ($\because$ Excitation is same)

Thus,

$$\left(g_2 \cosh\left(\frac{2kb}{5}\right) + h_2 \sinh\left(\frac{2kb}{5}\right)\right) = \left(g_3 \cosh\left(\frac{2\gamma_3 b}{5}\right) + h_3 \sinh\left(\frac{2\gamma_3 b}{5}\right)\right)$$

(9-5)

Also on boundary B6,

$$\frac{1}{\mu_2}\left(\frac{\partial A_{z2}}{\partial y}\right)-\frac{1}{\mu_3}\left(\frac{\partial A_{z3}}{\partial y}\right)=0$$

$$\Rightarrow \frac{k}{\mu_2}\left(g_2\sinh\left(\frac{2kb}{5}\right)+h_2\cosh\left(\frac{2kb}{5}\right)\right)-\frac{\gamma}{\mu_3}\left(g_3\cosh\left(\frac{2\gamma_3 b}{5}\right)-h_3\cosh\left(\frac{2\gamma_3 b}{5}\right)\right)=0 \quad (9\text{-}6)$$

On boundary B7, when y=b/5, we know that

$$A_{z3(x,b/5)}=A_{z4(x,b/5)}$$

$$\sin(kx)\left(g_3\cosh\left(\frac{kb}{5}\right)+h_3\sinh\left(\frac{kb}{5}\right)\right)=\sin(\alpha x).\left(h_4\sinh\left(\frac{\gamma_4 b}{5}\right)\right)$$

Here, $\gamma=\sqrt{k^2+j\beta^2}$; $k=\alpha$ ($\because$ Excitation is same)

Thus,

$$\left(g_3\cosh\left(\frac{\gamma_3 b}{5}\right)+h_3\sinh\left(\frac{\gamma_3 b}{5}\right)\right)=h_4\sinh\left(\frac{\gamma_4 b}{5}\right) \quad (9\text{-}7)$$

Also on boundary B7,

$$\frac{1}{\mu_3}\left(\frac{\partial A_{z3}}{\partial y}\right)-\frac{1}{\mu_4}\left(\frac{\partial A_{z4}}{\partial y}\right)=0$$

$$\Rightarrow \frac{\gamma_3}{\mu_3}\left(g_3\sinh\left(\frac{\gamma_3 b}{5}\right)+h_3\cosh\left(\frac{\gamma_3 b}{5}\right)\right)-\frac{\gamma_4}{\mu_4}\left(h_4\cosh\left(\frac{\gamma_4 b}{5}\right)\right)=0 \quad (9\text{-}8)$$

Equations (9-1) to (9-8) can be written in matrix form as shown below:

$$\begin{pmatrix} \cosh kb & \sinh kb & 0 & 0 & 0 & 0 & 0 \\ \cosh\left(\frac{3kb}{5}\right) & \sinh\left(\frac{3kb}{5}\right) & -\cosh\left(\frac{3kb}{5}\right) & -\sinh\left(\frac{3kb}{5}\right) & 0 & 0 & 0 \\ \frac{\sinh\left(\frac{3kb}{5}\right)}{\mu_1} & \frac{\cosh\left(\frac{3kb}{5}\right)}{\mu_1} & \frac{-\sinh\left(\frac{3kb}{5}\right)}{\mu_2} & \frac{-\cosh\left(\frac{3kb}{5}\right)}{\mu_2} & 0 & 0 & 0 \\ 0 & 0 & \cosh\left(\frac{2kb}{5}\right) & \sinh\left(\frac{2kb}{5}\right) & -\cosh\left(\frac{2\gamma_3 b}{5}\right) & -\sinh\left(\frac{2\gamma_3 b}{5}\right) & 0 \\ 0 & 0 & \frac{k\sinh\left(\frac{2kb}{5}\right)}{\mu_2} & \frac{k\cosh\left(\frac{2kb}{5}\right)}{\mu_2} & \frac{-\gamma_3\sinh\left(\frac{2\gamma_3 b}{5}\right)}{\mu_3} & \frac{-\gamma_3\cosh\left(\frac{2\gamma_3 b}{5}\right)}{\mu_3} & 0 \\ 0 & 0 & 0 & 0 & \cosh\left(\frac{\gamma_3 b}{5}\right) & \sinh\left(\frac{\gamma_3 b}{5}\right) & -\sinh\left(\frac{\gamma_4 b}{5}\right) \\ 0 & 0 & 0 & 0 & \frac{\gamma_3\sinh\left(\frac{\gamma_3 b}{5}\right)}{\mu_3} & \frac{\gamma_3\cosh\left(\frac{\gamma_3 b}{5}\right)}{\mu_3} & \frac{\gamma_4\cosh\left(\frac{\gamma_4 b}{5}\right)}{\mu_4} \end{pmatrix} \begin{pmatrix} g_1 \\ h_1 \\ g_2 \\ h_2 \\ g_3 \\ h_3 \\ h_4 \end{pmatrix} = \begin{pmatrix} 0 \\ 0 \\ \frac{K}{k} \\ 0 \\ 0 \\ 0 \\ 0 \end{pmatrix} \tag{9-9}$$

We have the following physical constants for the geometry

$K = 2 \times 10^6$ A/m

$\mu 0 = 4\pi.10^{-7}$

$\mu 1 = 4000\ \mu 0$

$\mu 2 = \mu 0$

$\mu 3 = 1.09\ \mu 0$

$\mu 4 = 200\ \mu 0$

$\sigma 3 = 5 \times 10^6$

$\sigma 4 = 3 \times 10^6$

After solution, we can find out the constants to define A_z everywhere in the domain.

$$\begin{pmatrix} g_1 \\ h_1 \\ g_2 \\ h_2 \\ g_3 \\ h_3 \\ h_4 \end{pmatrix} = \begin{pmatrix} -0.7365 + j0.6381 \\ 0.8907 - j0.7717 \\ -0.1042 + j0.2675 \\ -0.1480 - j0.1629 \\ -0.1676 + j0.2150 \\ 0.0883 - j0.0181 \\ -0.0035 - j0.0013 \end{pmatrix} \tag{9-10}$$

Thus, the complete solution can be written as:

$$\begin{aligned} A_{z1} &= \sin kx\ ((-0.7365 + j0.6381)\cosh ky + (0.8907 - j0.7717)\sinh ky) \\ A_{z2} &= \sin kx\ ((-0.1042 + j0.2675)\cosh ky + (-0.1480 - j0.1629)\sinh ky) \\ A_{z3} &= \sin kx((-0.1676 + j0.2150)\cosh \gamma_3 y + (0.0883 - j0.0181)\sinh \gamma_3 y) \\ A_{z4} &= \sin kx((-0.0035 - j0.0013)\sinh \gamma_4 y) \end{aligned} \tag{9-11}$$

To verify the results, a case where we know k was taken up. The value of k can be found out easily by comparing the periodicity of sine with length of the domain l
If there is one period of sine within length l then:

$$k = \frac{2\pi}{l}$$

If there are n periods of sine within length then

$$k = \frac{2n\pi}{l} \tag{9-12}$$

n=3 was taken for analysis and comparison with FEM. The FEM model results and the analytical results are compared below.
The electrical frequency for this simulation was 10 Hz as the depth of penetration was clearly visible at this frequency.

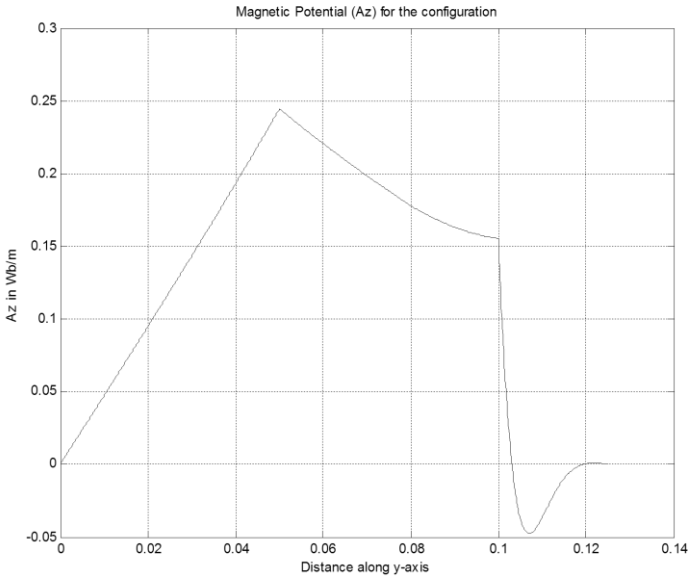

Fig.9.2: Plot for A_z for x = 0.84 m and f = 10 Hz

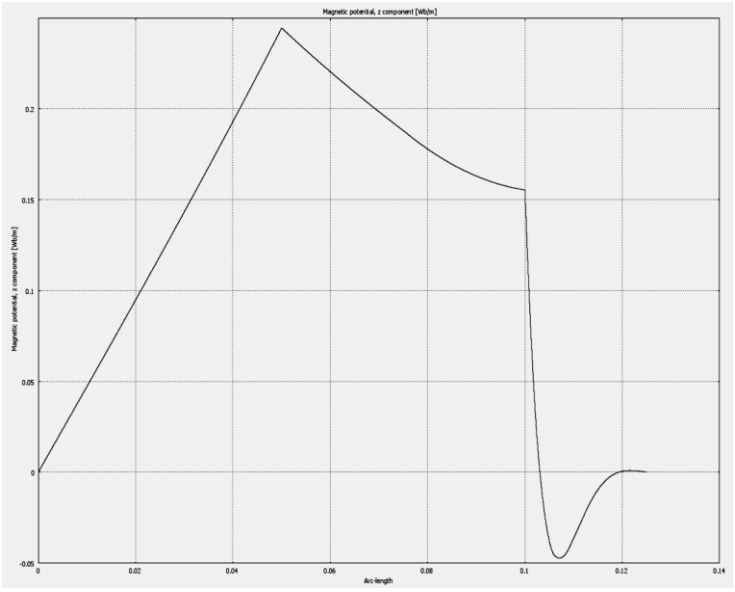

Fig.9.3: Plot for A_z for x = 0.84 m and f = 10 Hz from FE software

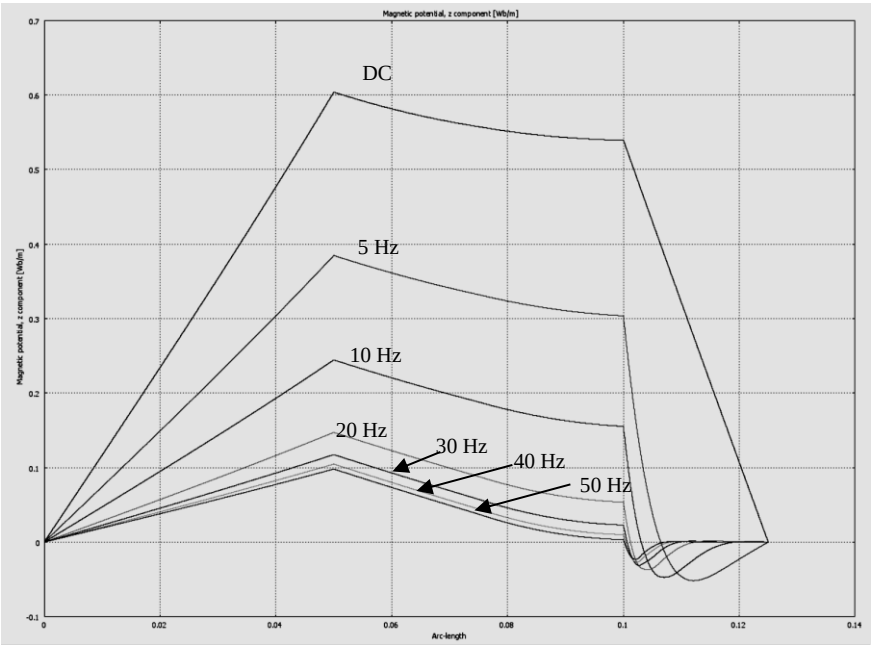

Fig.9.4: Plot for A_z for x = 0.84 m and different frequencies

9.2. Some Settings of the Used FE Software

9.2.1 Solver Settings

Once the problem is set-up as explained in chapter 5, the solver is configured for solution. There are two solvers used during set up of transient problems pertaining to machines. These solvers are static (time harmonic) solver and transient solver. The important settings for each of these solvers are mentioned below:

a) Static Solver: The most important settings are the relative tolerance and the number of iterations allowed for solution. Generally, smaller the relative tolerance, higher the number of iterations required to reach the desired accuracy.
b) Transient Solver: The transient solver requires more settings because the results from the static solver are used as initial conditions for the transient solver. The first step is to define how to obtain initial conditions.

The important settings for configuring the transient solver are:

1) The time step size, the relative tolerance and the absolute tolerances: This is very critical in determining the solution accuracy. There is a global relative tolerance and

there is an absolute tolerance for the solution. Different variables to be solved must be assigned individual absolute tolerance. The tolerance for the variable (depending upon the values that variable can assume) is assigned as product of relative tolerance and absolute tolerance. For example the values that A_z can take are very small as compared to the values taken by coupling variable lm_1 therefore different absolute tolerances are assigned to these variables.

2) The time steps stored in the output and restrictions on time steps taken by the solver.
3) The number of iterations required for each time step.
4) The update of Jacobian matrix: This means refresh rate of the Jacobian used to solve the PDE during iterative solution process. The higher refreshing rate means more accurate solution. This parameter can be set to update at each of the iterations, at each time step or minimal update. The time taken is inversely proportional to the accuracy.

The settings for the solvers are shown here. These settings are not the only possible settings but just serve as an example. For different machines and different mesh sizes, these settings can be different.

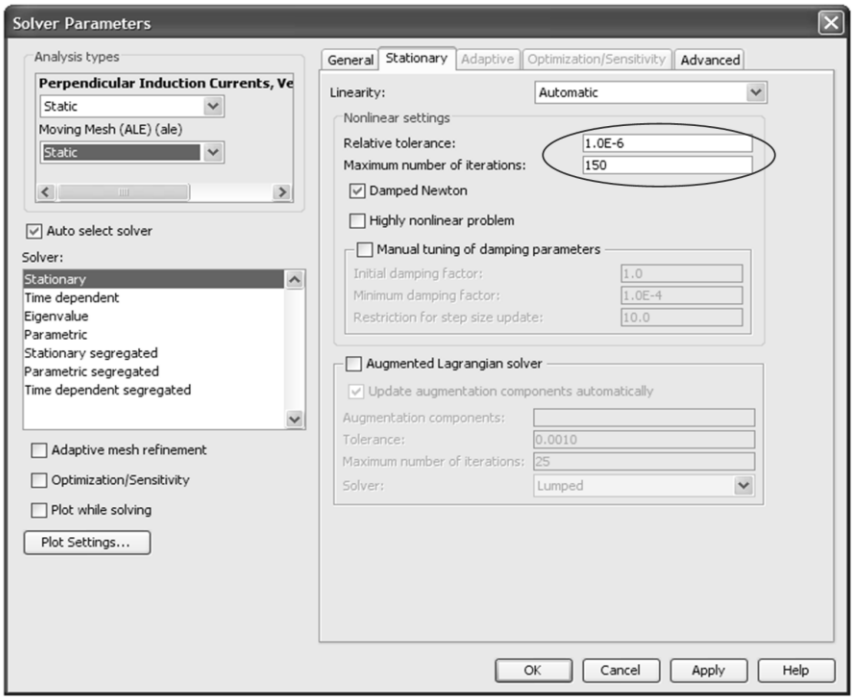

Fig.9.5: Settings for stationary solver

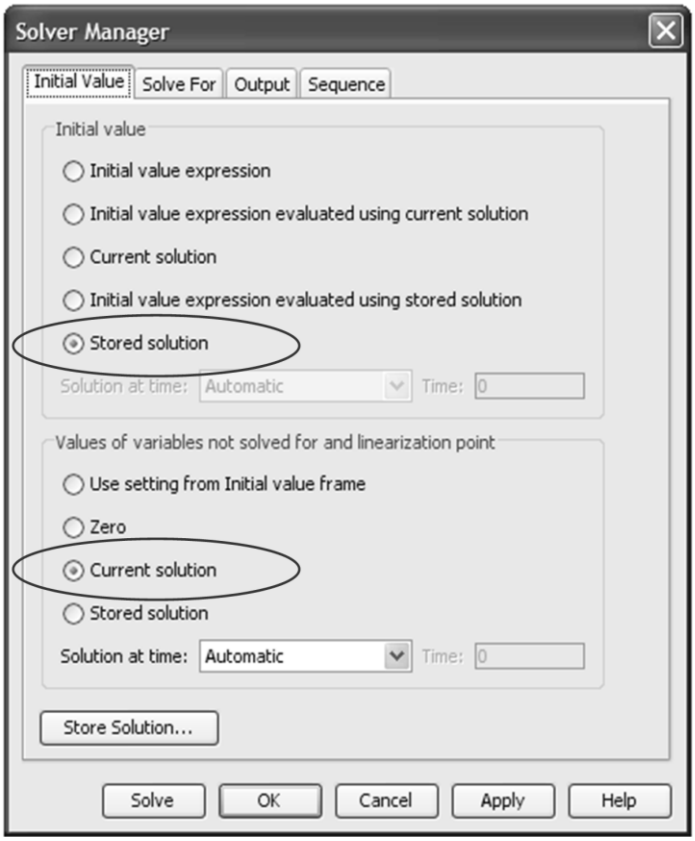

Fig.9.6: Settings for the initial conditions for the transient solver

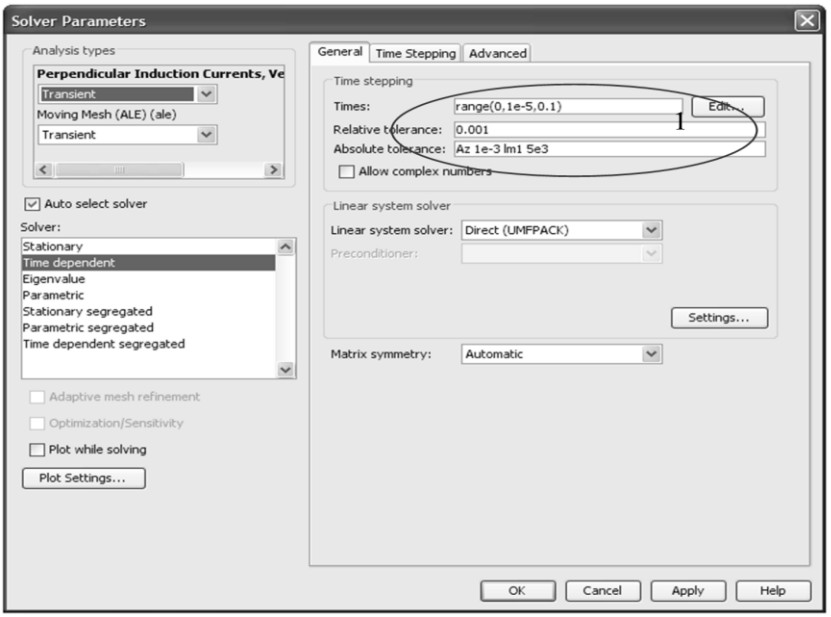

Fig.9.7: Settings for the initial conditions for the transient solver

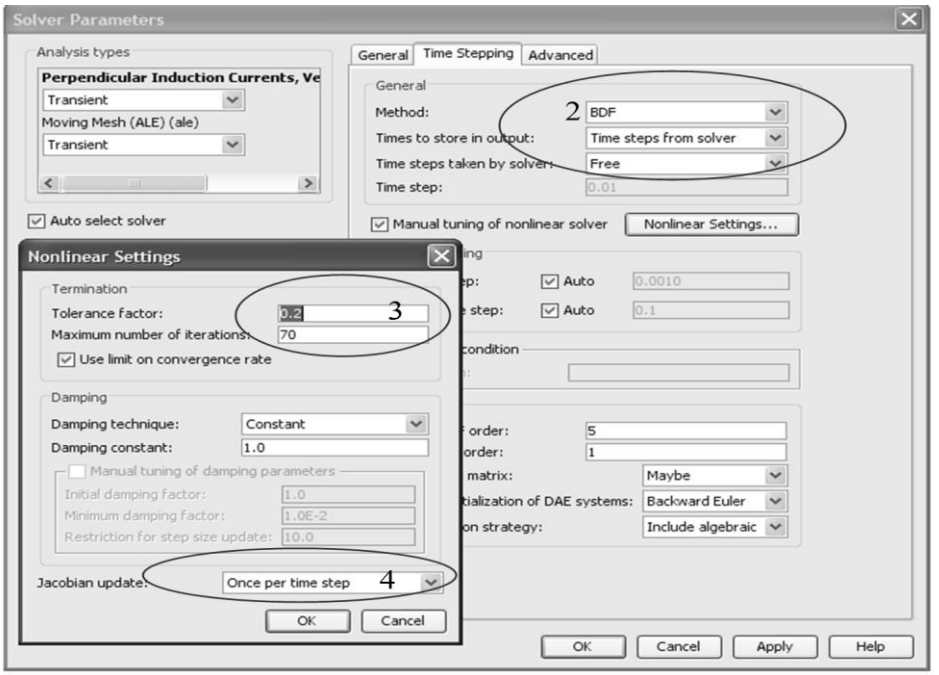

Fig.9.8: Settings for time stepping, non-linear solver and Jacobian matrix update

While the solver is running, it displays the reciprocal of step size and relative error during convergence of iteration. These quantities give useful information for determining if the solution is converging or not. If the solver is changing step size very frequently, it means that the solver is not able to solve the problem. This instability of solution is seen as peaks in the reciprocal of step size and very low slope of the relative error for the iteration. If such a situation occurs, it is better to look for geometrical inaccuracies, insufficient meshing of sub-domains and periodic boundary conditions as check. Visualization in FEM is an added advantage during analysis. This helps in understanding the physics better. The effects that can't be captured by analytical methods are very well captured and can be seen without any further imagination. Visualization also serves as a check on the solution. If there is something wrong, it is visible. A sample of good and bad solutions is shown in the figure below:

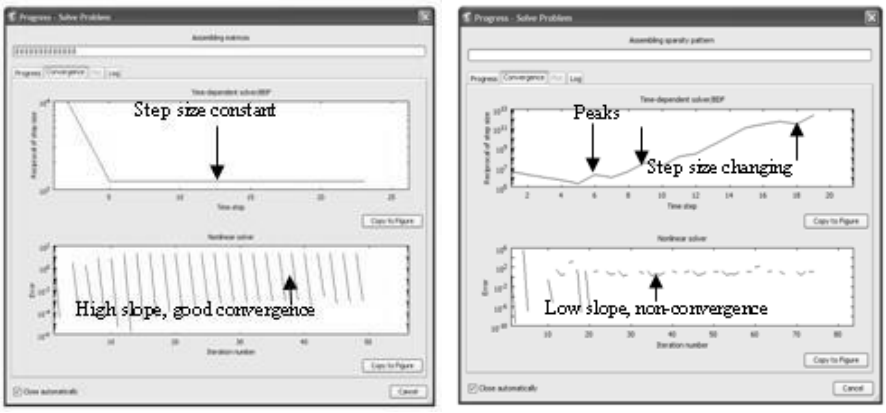

a) b)

Fig.9.9: a) Good solution b) Unstable solution

Summary

Eddy current loss modeling for design of PM generators for wind turbines

PhD Thesis

By Anoop Jassal

Background

The main motivation for this thesis comes from manufacturing experience of a 2 MW direct drive Permanent Magnet (PM) generator for wind turbine. The reference generator uses a distributed winding for stator and an inner rotor with surface mounted permanent magnets. It was found that a substantial amount of cost for such a generator comes from manufacturing process of distributed windings. The use of concentrated windings can reduce the winding cost and hence overall cost of generator. Another motivation for this research comes from the trend of wind turbines being installed in large offshore wind turbine parks. These wind turbine parks require lighter, cheaper and more efficient generators which are more reliable and modular in construction to lower overall installation costs.

However, the use of concentrated windings introduces additional losses in the solid conductive parts of the rotor due to eddy currents induced by harmonics of winding mmf. The eddy current losses need to be analyzed so that the concentrated windings can be safely installed in the generator.

Main Goal

This thesis focuses on the modeling, analysis and validation of the eddy current loss models suitable for PM generators for wind turbines. The modeling approach is a mixed use of analytical and Finite Element (FE) methods. A simplified generic analytical model for predicting eddy current losses at an early design stage is formulated. However, due to simplifying assumptions, analytical method leads to a qualitative analysis rather than quantitative. The detailed analysis for the most promising topologies selected by analytical method is carried out with Finite Element (FE) method. Both analytical and FE methods

need some validation/verification whereby experiments are performed for comparison. Design guidelines are developed thereafter.

Literature Survey

A detailed literature survey outlining the development of various methodologies concerning eddy current loss calculation in rotating electrical machines was conducted. The idea of this survey is to answer two basic questions viz.

- What type of work has already been done in the field of eddy current loss calculation?

- Which fields of rotating electrical machines have been thoroughly covered and in which fields can we contribute?

This survey summarizes useful contributions from eminent scientists and brings out various trends in the methods used for calculation of eddy current losses.

Modeling of Eddy Current Losses

Two modeling methodologies are used to evaluate eddy current losses.

A) Analytical modeling

B) Finite Element (FE) modeling

Analytical model is based on simplifying assumptions which are frequently used in literature. Maxwell's equations are solved for magnetic vector potential on a simplified geometry using proper boundary conditions. The induced current density is calculated from the magnetic vector potential and then the eddy current losses are calculated from the induced current density. The input for the model is derived from the Fourier decomposition of the linear current density in the stator (which is assumed slot-less). The utility of the analytical model is a quick qualitative comparison for eddy current losses amongst various possible slot-pole combinations. No expensive software is needed to solve the analytical model which is an advantage.

FE modeling is done in 2 dimensions with COMSOL software version 3.5a. The FE model includes all geometrical effects and material non-linearities except 3d effects. This might be valid for machines with long axial length and small pole pitch (which is generally the case with large direct drive generators). Many useful slot-pole combinations over the whole range of slots/pole/phase were analyzed and trends regarding eddy current losses were deduced. Assumptions used in

analytical models were verified with FE analysis. It was deduced that analytical model over-estimates the eddy current losses for the case when a lower order harmonic is responsible for eddy current losses. The assumption that losses due to slotting are more or less similar for same geometry of stator slots was validated. This means that the eddy current loss trend amongst various slot-pole combinations is governed by stator current induced eddy current losses.

Experimental Analysis

The experimental analysis aims at validating both analytical and FE models. The experiments were conducted on two 9 kW PM machines, one with open slots and another with semi-closed slots. The principle of power balance is used to deduce combined rotor losses (rotor back-iron and magnets). Two different sets of experiments were conducted.

A) Static experiments: To validate the analytical model formulation and results
B) Rotary experiments: To validate FE model formulation and results

Further, in the set of rotary experiments, different excitations were used to validate parts of the model. These include PM excitation without stator excitation; PM excitation with stator excitation; only stator excitation without PM excitation. It was deduced that both FE and analytical models can be used for predicting eddy current losses in case of open slot machines (which is generally the case for large machines with preformed coils). In case of semi-closed slot machine, the losses are very low and require very sensitive torque measurements in order to use power balance method. The 3d effects, measurement inaccuracies and ambiguity in calculation of stator iron losses are the important contributors to the difference in modeling results and experimental results.

Trend Analysis

Since FE method is more accurate, it was used to calculate eddy current losses for 44 useful slot-pole combinations spanning over whole useful range of winding factors and slots/pole/phase. From this analysis, useful trends were established and also some assumptions regarding modeling were verified.

From the perspective of eddy current losses, the most useful combinations lie within the range of slots/pole/phase ranging from 0.35 to 0.5. The 9-8 and 12-10 slot-pole combinations have high winding factor and low eddy current losses. The 3-2 slot pole combination had lowest losses but has also lowest winding factor.

In Conclusion

Concentrated windings have potential to lower cost of PM generators for wind turbines by utilizing winding automation processes known for this topology. The use of concentrated winding poses a challenge of keeping the additional eddy current losses in solid conducting parts of the machine to a minimum. The slot-pole combination plays a very vital role in generation and induction of eddy current losses. Therefore a suitable slot-pole combination at an early design stage promises a good electromagnetic design. In order to analyze the eddy current losses in various slot-pole combinations, an analytical model was formulated and verified with FE analysis as well as experiments. Analytical method is recommended for shortlisting useful slot-pole combinations and FE method being more accurate is recommended for actual loss calculation. Both the FE and Analytical models were compared against experimental results and the discrepancies were documented. Further research on more accurate experiments performed on a larger number of machines together with 3d FE modeling of eddy current losses is recommended.

Samenvatting

Eddy current loss modeling for design of PM generators for wind turbines

Proefschrift

van Anoop Jassal

Achtergrond

De voornaamste motivatie voor dit proefschrift komt voort uit de fabricage-ervaringen van een 2 MW direct aangedreven permanent-magneetgenerator voor windturbines. Het referentieontwerp heeft een verdeelde wikkeling in de stator en een interne rotor met permanente magneten aan het oppervlak. Het bleek dat een aanzienlijk deel van de kosten voor zo een generator in het fabricageproces van de verdeelde wikkelingen zitten. Het gebruik van geconcentreerde wikkelingen kan de wikkelkosten en daarmee de totaalkosten verlagen. Een tweede motivatie komt voort uit de trend om windturbines in grote offshore windparken te plaatsen. Deze windparken vereisen lichtere, goedkopere en efficiëntere generatoren die betrouwbaarder en modulair zijn om de totale kosten te verlagen.

Echter, het gebruik van geconcentreerde wikkelingen leidt dat extra verliezen in de massieve geleidende delen van de rotor ten gevolge van wervelstromen geïnduceerd door harmonischen in de stator-mmk. De wervelstroomverliezen moeten geanalyseerd worden zo dat geconcentreerde wikkelingen veilig kunnen worden toegepast in de generator.

Hoofddoel

Dit proefschrift richt zich op het modelleren, analyseren en valideren van de wervelstroomverliesmodellen geschikt voor PM-generatoren voor windturbines. De modelleringsmethode is een mengvorm tussen analytische methodes en eindige-elementenmethodes. Een vereenvoudigd generiek model wordt opgesteld om wervelstroomverliezen in een vroeg ontwerpstadium te voorspellen. Echter, door vereenvoudigende aannames is de analytische methode eerder een kwalitatieve dan een kwantitatieve analyse. De veelbelovendste topologieën volgens het analytische model worden in detail geanalyseerd met de

eindige-elementenmethode. Zowel de analytische methode als de eindige-elementenmethode moeten gevalideerd/geverifieerd worden waarvoor experimenten gedaan worden ter vergelijking. Ontwerprichtlijnen worden daarna opgesteld.

Literatuuronderzoek

Een gedetailleerd literatuuronderzoek naar de ontwikkeling van methodes voor wervelstroomverliesberekeningen in roterende elektrische machines is uitgevoerd. Het idee van dit onderzoek is het beantwoorden van basale vragen, namelijk

- Welk soort werk is reeds gedaan op het gebied van wervelstroomverliesberekeningen?

- Welke onderzoeksgebieden in roterende elektrische machines zijn uitgebreid beschreven en op welke gebieden kunnen we bijdragen?

Dit onderzoek vat nuttige bijdragen van eminente wetenschappers samen en brengt verscheidene trends naar voren op het gebied van methodes voor wervelstroomverliesberekeningen.

Modelleren van wervelstroomverliezen

Twee modelleringsmethodes worden gebruikt om wervelstroomverliezen te bepalen.

A) Analytische modellen
B) Eindige-elementenmodellen (FE)

Het analytische model is gebaseerd op vereenvoudigende aannames die vaak gebruikt worden in literatuur. De maxwellvergelijkingen worden opgelost naar de magnetische vectorpotentiaal op een vereenvoudigde geometrie met geschikte randvoorwaarden. De geïnduceerde stroomdichtheid wordt berekend uit de vectorpotentiaal waarna de wervelstroomverliezen worden berekend met de geïnduceerde stroomdichtheid. De invoer voor het model is afgeleid uit de Fourieranalyse van de lineaire stroomdichtheid in de stator (die groefloos verondersteld wordt). Het nut van het analytische model is een snelle kwalitatieve vergelijking van de wervelstroomverliezen voor verschillende mogelijke combinaties van groeven en polen. Dure software is niet nodig voor het oplossen van het analytische model, wat een voordeel is.

FE-modellering wordt in 2 dimensies gedaan met COMSOL software versie 3.5a. Het FE-model bevat alle geometrische effecten en niet-lineaire materiaaleigenschappen, behalve 3d-effecten. Dit kan geldig zijn voor machines met een lange axiale lengte en een korte poolsteek (wat in het algemeen het geval is voor grote direct aangedreven generatoren). Een groot aantal nuttige groef-poolcombinaties over het gehele bereik aan groeven per pool per fase zijn geanalyseerd en trends voor de wervelstroomverliezen zijn afgeleid. Aannames gebruikt in de analytische modellen zijn geverifieerd met FE-analyses. Hieruit bleek dat analytische modellen de wervelstroomverliezen overschatten wanneer een harmonische van lagere orde de verliezen veroorzaakt. De veronderstelling dat verliezen door vertanding min of meer gelijk blijven bij een zelfde geometrie van de statorgroeven is bevestigd. Dit betekent dat de wervelstroomverliestrend voor verschillende groef-poolcombinaties bepaald wordt door de verliezen geïnduceerd door statorstromen.

Experimentele Analyse

De experimentele analyse dient ter validatie van zowel de analytische als de FE-modellen. De experimenten zijn uitgevoerd met twee 9 kW PM-machines, een met open groeven en een met half gesloten groeven. Het vermogensbalansprincipe wordt gebruikt voor de bepaling van de gecombineerde rotorverliezen (rotorjuk en magneten). Twee verschillende sets proeven zijn uitgevoerd.

A) Statische proeven, voor de validatie van het analytische model en resultaten
B) Draaiende proeven, voor de validatie van het FE-model en resultaten

Verder zijn bij de draaiende proeven verschillende stimuli gebruikt om gedeelten van het model te valideren. Deze omvatten gemagnetiseerde magneten zonder statorstromen; gemagnetiseerde magneten met statorstromen; statorstromen zonder gemagnetiseerde magneten. Het is bepaald dat zowel de FE als de analytische modellen gebruikt kunnen worden voor het voorspellen van de wervelstroomverliezen voor machines met open groeven (wat in het algemeen het geval is voor grote machines met vormspoelen). In de machine met half gesloten groeven zijn de verliezen zeer laag en is een zeer gevoelige koppelmeting nodig om het vermogensbalansprincipe te kunnen gebruiken. De 3d-effecten, meetonzekerheden en ambiguïteit in de berekening van de ijzerverliezen zijn de belangrijkste oorzaken voor verschillen tussen de gemodelleerde resultaten en experimentele resultaten.

Trendanalyse

Omdat de FE-methode accurater is, is deze gebruikt voor de berekening van de wervelstroomverliezen voor 44 realistische groef-poolcombinaties uit het bruikbare bereik van wikkelfactoren en groeven per pool per fase. Met deze analyse zijn nuttige trends bepaald en enkele modelaannames geverifieerd.
Qua wervelstroomverliezen liggen de nuttigste combinaties tussen de 0.35 en 0.5 groeven per pool per fase. De 9-8 en 12-10 combinaties hebben een hoge wikkelfactor en lage wervelstroomverliezen. De 3-2 combinatie heeft de laagste verliezen maar ook de laagste wikkelfactor.

In Conclusie

Geconcentreerde wikkelingen hebben potentie om de kosten van PM-generatoren voor windturbines te verlagen door gebruik van automatische wikkelprocessen. Het gebruik van geconcentreerde wikkelingen vormt een uitdaging door de bijkomende wervelstroomverliezen in de geleidende delen van de machine. De groef-poolcombinatie speelt een sleutelrol in het opwekken en induceren van wervelstroomverliezen. In een vroeg stadium een geschikte groef-poolcombinatie selecteren belooft een goed elektromagnetisch ontwerp. Om de wervelstroomverliezen te analyseren voor verschillende groef-poolcombinaties is een analytisch model opgesteld en geverifieerd met zowel FE-analyse als experimenten. De analytische methode wordt aanbevolen voor een eerste selectie van bruikbare groef-poolcombinaties en de accuratere FE-methode wordt aanbevolen voor de daadwerkelijke verliesberekening. Zowel de FE als de analytische modellen zijn vergeleken met experimentele resultaten en de verschillen zijn beschreven. Verder onderzoek naar accuratere experimenten met een groter aantal machines en 3d FE-modellering van wervelstroomverliezen wordt aanbevolen.

List of Publications

As Author:

Journal Publications

1. Jassal, A; Polinder, H; Ferreira, J.A., "Literature survey of eddy current loss analysis in rotating electrical machines", *Electric Power Applications*, IET, vol.6, no.9.pp. 743-752, Nov. 2012.
2. Jassal, A.; Polinder, H.; Damen M.E.C.; Versteegh, K.;, "Design Considerations for Permanent Magnet Direct Drive Generators for Wind turbines", *International Journal of Engineering and Technology (IJET)* Vol.4(3): pp. 253-257 ISSN: 1793-8244, 2012.

Conference Publications

1. Jassal, A.; Polinder, H.; Shrestha, G.; Versteegh, C.;, "Investigation of Slot Pole Combinations and Winding Arrangements for Minimizing Eddy Current Losses in Solid Back-Iron of Rotor for Radial Flux Permanent Magnet Machines", *Electrical Machines (ICEM), 2008 XVIII International Conference on* , 6-9 Sept. 2008.
2. Jassal, A.; Polinder, H.; Shrestha, G.; Versteegh, K.;, "Closed Slot Topology for Reduction of Cogging and Noise in Permanent Magnet Direct Drive Generator for Wind Turbines" *Proceedings of European Wind Energy Conference EWEC*, Marseille, France, 16-19 March 2009.
3. Jassal, A.; Polinder, H.; Lahaye, D.; Ferreira, J.A.; , "Comparison of analytical and Finite Element calculation of eddy-current losses in PM machines," *Electrical Machines (ICEM), 2010 XIX International Conference on* , vol., no., pp.1-7, 6-8 Sept. 2010.
4. Jassal, A.; Polinder, H.; Lahaye, D.; Ferreira, J.A.; , "Analytical and FE calculation of eddy-current losses in PM concentrated winding machines for wind turbines," *Electric Machines & Drives Conference (IEMDC), 2011 IEEE International* , vol., no., pp.717-722, 15-18 May 2011.

Talks and Seminar

1. Jassal, A.; Polinder, H.; "Cost Optimization of Permanent Magnet Direct Drive Generators", *Dutch Wind Workshops, October 2010.*
2. Jassal, A.; Polinder, H.; Kirschneck, M. "Generator Systems for Wind Turbines", *Workshop at International Quality and Productivity Center (IQPC),* 22-23 May, Bremen, Germany 2012.

Books/Chapters

1. Jassal, A.; Versteegh, K.; Polinder, H.; "Case study of the permanent magnet direct drive generator in the Zephyros wind turbine", *Chapter in Electrical drives for direct drive renewable energy systems, woodhouse publishing* ISBN 1845697839 and ISBN-13: 9781845697839, March 2013.

As Co-Author:

1. G.Shrestha; D.Bang; A.Jassal; H.Polinder; J.A.Ferreira;, "Energy Converters for Future Wind Turbines", *Proceedings of Global Wind EnergyConference (GWEC),* Beijing, China,28-30 Sept. 2008.
2. G.Shrestha; D.Bang; A.Jassal; H.Polinder; J.A.Ferreira;, "Investigation on the Possible Use of Magnetic Bearings in Large Direct Drive Wind Turbines", *Proceedings of European Wind Energy Conference EWEC*, Marseille, France ,16-19 March 2009.
3. Firmansyah, M.; Jassal, A.; Polinder, H.; Lahaye, D., "Eddy current loss calculation in rotor back iron for concentrated winding PM generator," *Electrical Machines (ICEM), 2012 XXth International Conference on* , pp.2666,2670, 2-5 Sept. 2012.
4. Imoru O.; Jassal A.; Polinder H.; Nieuwkoop E.; Tsado J.; and Jimoh A.A.; "An inductive power transfer through metal object" Proceedings of IEEE *International Future Energy Electronics Conference (IFEEC),* pp. 246-251, Nov. 3-6, 2013.
5. Liu D.; Jassal A.; Polinder H.; Ferreira J.A., "Validation of Eddy Current Loss Models for Permanent Magnet Machines with Fractional-Slot Concentrated Windings" Proceedings of IEEE *Electric Machines & Drives Conference (IEMDC),* pp.678-685, 12-15 May 2013.

Biography

Anoop Jassal was born in Punjab, India in 1983. He graduated from Punjab Engineering College, Chandigarh, India in 2003. After graduation, he worked at Vardhman Spinning and General Mills (VSGM) at Baddi, India as Electrical Engineer for three years.
He joined Delft University of Technology in 2006 for his MSc. Thereafter, in August 2008 he started working towards his PhD at Electrical Power Processing (EPP) group of Delft University of Technology. His area of research is permanent magnet direct drive generator design for wind turbines.
He worked part time at VWEC (now XEMC-Darwind), at Hilversum, Netherlands since August 2008 till July 2012. Since August 2012, he is working at GE Global Research at Munich, Germany as Research Engineer. His present work is focused on design of various electro-mechanical devices and large machines.

Anoop Jassal is geboren in Punjab, India in 1983. Hij is afgestudeerd aan het Punjab Engineering College, Chandigarh, India in 2003. Hierna werkte hij drie jaar bij Vardhman Spinning and General Mills (VSGM) in Baddi, India als Electrical Engineer.
In 2006 begon hij aan de technische universiteit Delft zijn MSc.-opleiding. Daarna, in augustus 2008, begon hij een promotietraject in de Electrical Power Processing-groep aan de technische universiteit Delft op het gebied van direct aangedreven permanent-magneetgeneratoren voor windturbines. Ook werkte hij parttime bij VWEC (nu XEMC-Darwind) in Hilversum tussen augustus 2008 en juli 2012. Sinds augustus 2012 werkt hij bij GE Global Research in München, Duitsland als Research Engineer. Hierbij richt hij zich op het ontwerp van uiteenlopende elektromechanische apparaten en grote machines.